SURFACE MODIFICATION OF POLYPROPYLENE PIPETTE TIPS FOR

IN-SITU SYNTHESIS OF MONOLITHIC MATERIALS AND ITS

APPLICATION IN THE ANALYSIS OF CANNABIS METABOLITE

IN HUMAN URINE

KESARA AR-SANORK

A Thesis Submitted in Partial Fulfillment of the Requirements for the

Degree of Doctor of Philosophy in Chemistry

Suranaree University of Technology

Academic Year 2023

การดัดแปลงพื้นผิวพอลิโพรพิลีนปิเปตทิปสำหรับการสังเคราะห์วัสดุโมโนลิธและการประยุกต์ใช้ในการวิเคราะห์เมตาบอไลท์ของกัญชาในปัสสาวะมนุษย์

นางสาวเกศรา อาษานอก

วิทยานิพนธ์นี้เป็นส่วนหนึ่งของการศึกษาตามหลักสูตรปริญญาวิทยาศาสตรดุษฎีบัณฑิต
สาขาวิชาเคมี
มหาวิทยาลัยเทคโนโลยีสุรนารี
ปีการศึกษา 2566

SURFACE MODIFICATION OF POLYPROPYLENE PIPETTE TIPS FOR IN-SITU SYNTHESIS OF MONOLITHIC MATERIALS AND ITS APPLICATION IN THE ANALYSIS OF CANNABIS METABOLITE IN HUMAN URINE

Suranaree University of Technology has approved this thesis submitted in partial fulfillment of the requirements for the Degree of Doctor of Philosophy

Thesis Examining Committee

_____

(Dr. Chanpen Karuwan)

Chairperson

_____

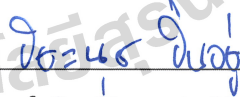(Asst. Prof. Dr. Patcharin Chaisuwan)

Member (Thesis Advisor)

_____

(Assoc. Prof. Dr. Sanchai Prayoonpokarach)
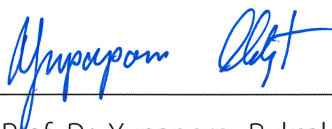
Member

_____

(Assoc. Prof. Dr. Kamonwad Ngamchuea)

Member

_____

(Asst. Prof. Dr. Piyanut Pinyu)

Member

_____

(Assoc. Prof. Dr. Yupaporn Ruksakulpiwat)

Vice Rector for Academic Affairs

and Quality Assurance

_____

(Prof. Dr. Santi Maensiri)

Dean of Institute of Science

เกศรา อาษานอก : การดัดแปลงพื้นผิวพอลิโพรพิลีนปิเปตทิปสำหรับการสังเคราะห์วัสดุโมโนลิธและการประยุกต์ใช้ในการวิเคราะห์เมตาบอไลท์ของกัญชาในปัสสาวะมนุษย์ (SURFACE MODIFICATION OF POLYPROPYLENE PIPETTE TIPS FOR IN-SITU SYNTHESIS OF MONOLITHIC MATERIALS AND ITS APPLICATION IN THE ANALYSIS OF CANNABIS METABOLITE IN HUMAN URINE). อาจารย์ที่ปรึกษา : ผู้ช่วยศาสตราจารย์ ดร.พัชรินทร์ ชัยสุวรรณ, 115 หน้า.

คำสำคัญ: วัสดุโมโนลิธ, การดัดแปลงพื้นผิว, การสกัดด้วยตัวดูดซับของแข็งขนาดเล็ก, กัญชา

โมโนลิธเป็นวัสดุที่กำลังได้รับความสนใจสำหรับการสกัดด้วยตัวดูดซับของแข็งขนาดเล็ก เนื่องจากสามารถปรับเปลี่ยนคุณสมบัติได้ทั้งทางเคมีและกายภาพ โมโนลิธในพอลิโพรพิลีนปิเปตทิปได้ถูกประดิษฐ์ขึ้น สำหรับใช้ในการสกัดสารด้วยตัวดูดซับของแข็งขนาดเล็ก เพื่อแก้ปัญหาการหลุดและการหดตัวของโมโนลิธในปิเปตทิป วิทยานิพนธ์นี้เสนอวิธีการดัดแปลงพื้นผิวของพอลิโพรพิลีนปิเปตทิปที่ใหม่และง่าย โดยใช้ 2,2-ไดเมทอกซี-2-ฟีนิลอะซีโตฟีโนน และการสร้างชั้นบางของ เอทิลีนไดเมทาคริเลท ก่อนการพอลิเมอร์ไรของโมโนลิธ ชนิดของมอนอเมอร์และตัวเชื่อมโยงพอลิเมอร์ที่มีผลต่อการหดตัวของโมโนลิธได้ถูกศึกษา นอกจากนี้ได้ทำการประเมินความจุของโมโนลิธที่สังเคราะห์ขึ้นในปิเปตทิปเทียบกับอุปกรณ์สกัดที่มีจำหน่ายเชิงพาณิชย์ชนิด C18 SPE คาร์ทริดจ์ การสกัดด้วยตัวดูดซับของแข็งโมโนลิธชนิดไม่มีขั้วในปิเปตทิปร่วมกับเซ็นเซอร์ขั้วไฟฟ้าพิมพ์กราฟีนได้ถูกพัฒนาขึ้นเพื่อวิเคราะห์ปริมาณ 11 นอร์-เดลต้า 9-เตตระไฮโดรแคนนาบินอล-9-คาร์บอกซิลิกแอสซิด ในปัสสาวะ เพื่อประยุกต์ใช้ในงานทางนิติเวช วิธีการที่พัฒนาขึ้นนี้ได้ตรวจสอบความใช้ได้ของวิธีและประยุกต์ใช้ในการวิเคราะห์ตัวอย่างปัสสาวะมนุษย์ โดยให้เปอร์เซ็นต์ความสามารถในการคืนกลับสูงในช่วง 85 ถึง 108 เปอร์เซ็นต์

สาขาวิชาเคมี   ลายมือชื่อนักศึกษา_____

ปีการศึกษา 2566   ลายมือชื่ออาจารย์ที่ปรึกษา_____

KESARA AR-SANORK : SURFACE MODIFICATION OF POLYPROPYLENE PIPETTE TIPS FOR IN-SITU SYNTHESIS OF MONOLITHIC MATERIALS AND ITS APPLICATION IN THE ANALYSIS OF CANNABIS METABOLITE IN HUMAN URINE. THESIS ADVISOR : ASST. PROF. PATCHARIN CHAISUWAN, Ph.D. 115 PP.

Keyword: Monolithic materials, Surface modification, Micro-solid phase extraction, Cannabis

Monolithic materials are gaining interest in micro-solid phase extraction (μ-SPE) due to their tunable chemical and physical properties. Monolith in polypropylene (PP) pipette tip has been invented for μ-SPE. In order to overcome the problems from detachment and shrinkage of the monoliths, this thesis introduces a new and simple surface modification method for PP pipette tips using 2,2-dimethoxy-2-phenylacetophenone and forming a linking thin layer of ethylene dimethacrylate before monolith polymerization. The effects of type of monomers and crosslinker content on monolith shrinkage were examined. Dynamic breakthrough capacities of the fabricated in pipette tip monoliths were evaluated and compared with those of commercial C18 SPE cartridges. Micro-solid phase extraction using nonpolar monolithic in pipette tip coupled with screen-printed graphene electrode sensor was developed for the determination of urinary 11-Nor-Δ^9-tetrahydrocannabinol-9-carboxylic acid in forensic applications. The developed method was fully validated and successfully applied to analyze authentic human urines with high % recovery ranging from 85 - 108 %.

| School of Chemistry | Student's Signature_____ |
| Academic Year 2023 | Advisor's Signature_____ |

ACKNOWLEDGEMENTS

CONTENTS

CONTENES (Continued)

CONTENES (Continued)

CONTENES (Continued)

CONTENES (Continued)

LIST OF TABLES

LIST OF TABLES (Continued)

LIST OF FIGURES

LIST OF FIGURES (Continued)

LIST OF FIGURES (Continued)

LIST OF FIGURES (Continued)

LIST OF FIGURES (Continued)

LIST OF ABBREVIATIONS

5-HIAA	5-Hydroxyindoleacetic acid
AA	Acrylic acid
AC	Activated charcoal
ACN	Acetonitrile
AIBN	Azobisisobutyronitrile
BJH	Barrett-joyner-halenda
BMA	Butyl methacrylate
BPA	Bisphenol A
CBD	Cannabidiol
CBN	Cannabinol
COC	Cyclic olefin copolymer
CV	Cyclic voltammetry
DMPAP	Dimethoxy-2-phenylacetophenone
DPX	Disposable pipette extraction
EDA	Ethylene diacrylate
EDMA	Ethylene dimethacrylate
FT-IR	Fourier transform infrared microscope spectrophotometry
GC	Gas chromatography
GMA	Glycidyl methacrylate
HCl	Hydrochloric acid
HEMA	2-hydroxythylmethacrylate
IT monolithic μ-SPE	In pipette tip based monolithic μ-SPE

LIST OF ABBREVIATIONS (Continued)

IUPAC	International Union of Pure and Applied Chemists
K	Partition coefficient
LC	Liquid chromatography
LLE	Liquid-liquid extraction
LMA	Lauryl methacrylate
LOD	Limit of detection
LOQ	Limit of quantitation
MAA	Methacrylic acid
MeOH	Methanol
MIP	Molecularly imprinted polymers
MMA	Methyl methacrylate
MS	Mass spectrometry
NaOH	Sodium hydroxide
PC	Polycarbonate
PDMS	Polydimethylsiloxane
PEDAS	Pentaerythritol diacrylate monostearate
PMMA	Poly(methyl methacrylate)
PP	Polypropylene
SEM	Scanning electron microscope
SMA	Stearyl methacrylate
SPE	Solid-phase extraction
SPGE	Screen-printed graphene electrode
SWGTOX	Scientific Working Group for Forensic Toxicology
SWV	Square wave voltammetry

LIST OF ABBREVIATIONS (Continued)

TEOS	Tetraethyl orthosilicate
THC	$\Delta 9$- tetrahydrocannabinol
THC-COOH	$\Delta 9$-tetrahydrocannabinol-9- carboxylic acid
THC-COOH-Glu	$\Delta 9$-tetrahydrocannabinol-11-oic acid glucuronide
THC-OH	11- hydroxy-$\Delta 9$-tetrahydrocannabinol
TMOS	Tetramethyl orthosilicate
WAX-S	Weak anion exchange sorbent with salt
μ-SPE	Micro-solid-phase extraction
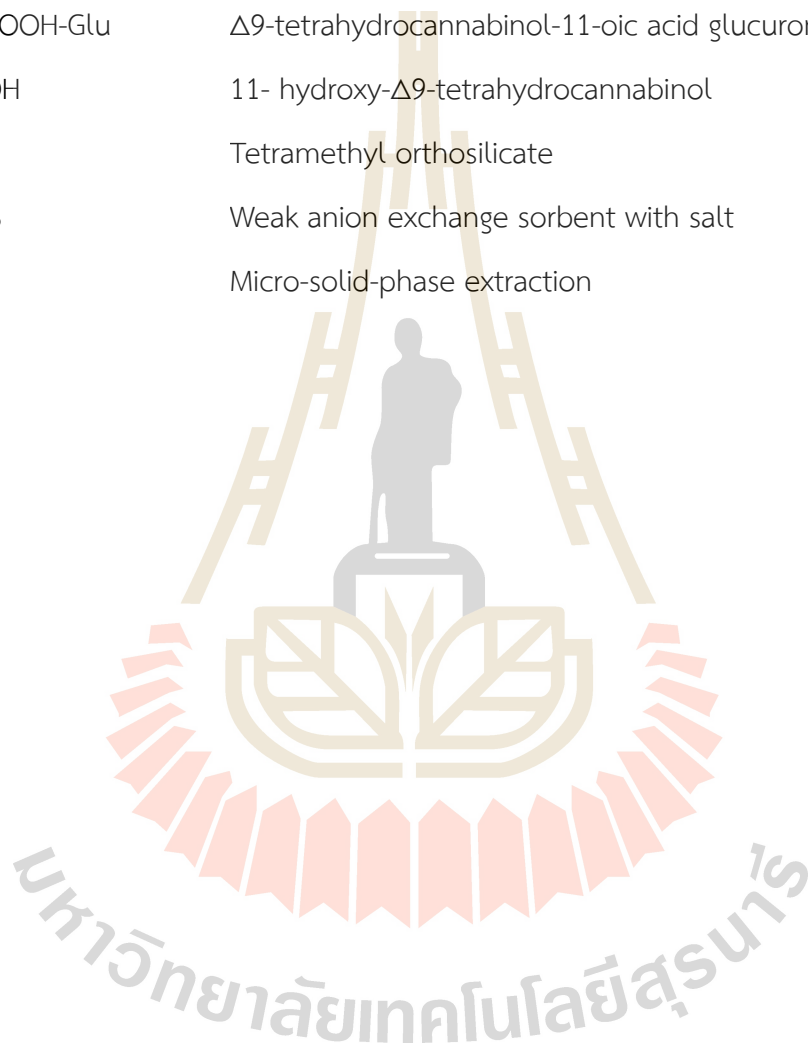
CHAPTER I

INTRODUCTION

In this chapter, the basics and principles involving the research work are introduced, which include four main topics: monoliths, solid-phase extraction, electrochemical detection, and cannabis. The first topic is the introduction of monolithic materials. In this section, characteristics, properties, type, and preparation of monolith are presented. The second topic focuses on principles, procedures, and miniaturization of the solid-phase extraction method. The third part involves principle of electrochemical detection and introduction of screen-printed electrode based electrochemical detection. The last part introduces an understanding cannabis and necessity for the development of an analysis method for identification of cannabis user.

1.1 Monoliths

Monolith is a Greek word which derived from the combination of the words "mono" and "lithos" which mean "single" and "stone". A monolith generally refers to a column or a single block of stone. However, a monolith is defined as a single piece of a porous material in separation science (Hefnawy et al., 2023).

The concept of the monolith or monolithic material was first introduced for chromatographic separation in 1967 by Kubin et al. (Kubín, Špaček, and Chromeček, 1967). The monolith composed of 2-hydroxyethyl methacrylate and ethylene dimethacrylate (EDMA), was used for size-exclusion chromatography to separate high molecular weight polysaccharides (Kubín et al., 1967).

Monoliths are high-permeability materials consisting of macropore and mesopore, providing high surface area with low flow resistance. This allows fast operations with relatively high efficiency. The material can be easily prepared in an appropriate mold, without need of frits, packing or special skills. Due to their advantages, monoliths are widely used for both chromatographic separation and solid-phase extraction (SPE). In this chapter, we introduce an overview of monolithic material, with a special focus on their SPE applications.

1.1.1 Characteristics of monoliths

1.1.1.1 Structure of monoliths

Unlike conventional particle-based material, monoliths are continuous single rod of porous material. SEM images of the continuous and particle-based materials are shown in **Figure 1.1**.
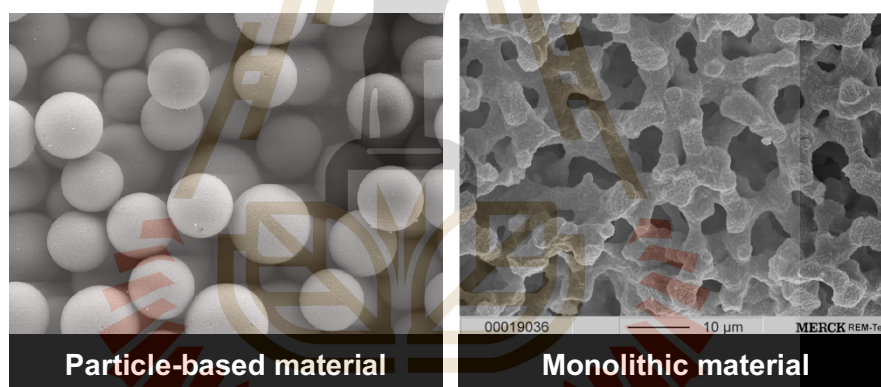
Figure 1.1 SEM images of particles and monolithic based materials.

The porous monoliths are commonly characterized by a bimodal pore size distribution consisting of two types of pores: macropores and mesopores. SEM images of the pore structures are shown in **Figure 1.2**. According to the International Union of Pure and Applied Chemists (IUPAC), mesopores are defined within a size range of 2-50 nm, while macropores are >50 nm (Rouquerol et al., 1994). Macropores or through pores facilitate solvent flow, providing high permeability and encourage good mechanical stability of the monolith structure. Meanwhile, mesopores contribute significantly to increasing of surface area.
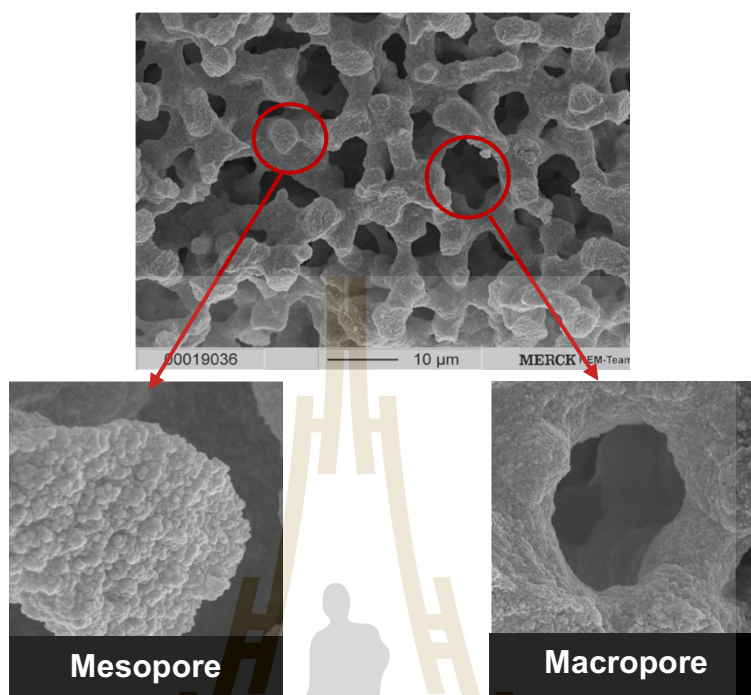
Figure 1.2 SEM images of a structure of monolithic material with macropores and mesopores.

1.1.1.2 Permeability

Permeability is one of the dominant properties of monoliths which refer to the ability of a liquid (usually a solvent) to flow through the pores in the material. Permeability is directly related to porosity which is controlled by the average size of the pores. It is one of the significant factors leading to the observation of high back pressure during liquid flow. In chromatographic applications, high permeability is preferred to facilitate high flow rate with low back pressure.

1.1.1.3 Mass transfer kinetic

Mass transfer is one of the important parameters for the adsorption mechanism. Mass transfer refers to the movement of molecules or analytes within and through the porous structure of the monolith. High mass transfer is expected in chromatography to ensures that analytes or target molecules can quickly and effectively interact with the active sites or binding sites within the materials. Compared to conventional particles-based materials, porous monoliths enable better contact

between the analyte and the active sites on the material surface, resulting in improved mass transfer properties. Comparison of solvent diffusion pathway occurred in particles-based and monolithic materials are illustrated in **Figure 1.3**.
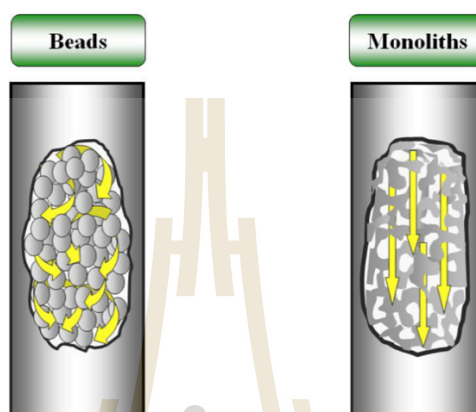
Figure 1.3 Diffusion of a solvent through particles-based pack material (left) and monolithic material (right) (Arrua, Strumia, and Alvarez Igarzabal, 2009).

1.1.2 Type and preparation of monoliths

Monoliths are typically classified based on the chemical composition of the materials used in their preparation. This classification generally distinguishes into two main categories: (i) organic monoliths and (ii) inorganic monoliths.

1.1.2.1 Organic monoliths

Organic monoliths are the original concept of monolithic structures, often referred to as polymer-based monoliths. The initiation of organic monoliths was pioneered by Hjerten et al. in 1989 (Hjertén, Liao, and Zhang, 1989). Organic monoliths can be prepared *in situ* using a simple and straightforward molding process through co-polymerization reactions of organic-based monomers such as methacrylate, acrylamide and styrene. The organic monoliths exhibit unique characteristics, including high permeability, porosity, and the ability to function effectively across a broad pH range. These polymers display flexibility in tolerating extreme pH variations, ranging from 1 to 14 (Gusev, Huang, and Horváth, 1999).

Typically, the polymerization solution is produced from a homogeneous mixture of functional monomer, crosslinker, porogenic solvent and

initiator. The polymerization process is then initiated by either heating or UV radiation, resulting in the formation of a single porous polymer structure. Schematic diagram of the preparation is indicated in **Figure1.4**.
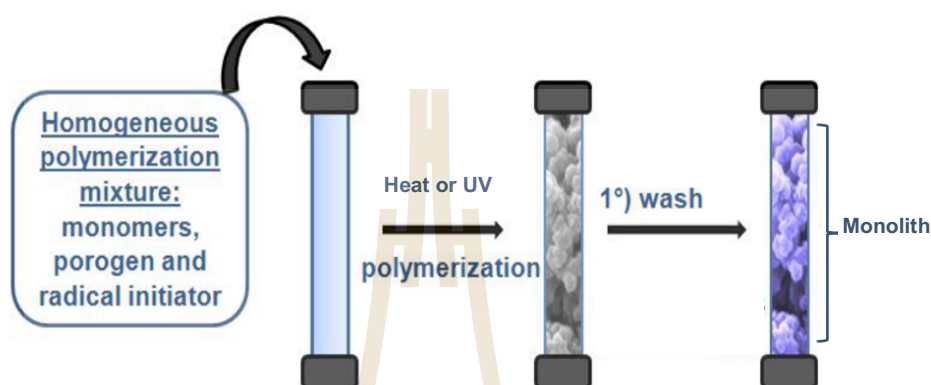
Figure 1.4 Schematic diagram for preparation of polymer-based monolith (adapted from (Arrua et al., 2009) .

1.1.2.1.1 Polymerization composition

- **Functional monomers**

Functional monomers are a critical component in the synthesis of monolithic materials. The monomers play a significant role in determining the surface chemical properties and functionalities of the monoliths. Methacrylate-based monomers are the most functional monomers widely used for the preparation of organic monoliths. Methacrylates generally exhibit non-polar to moderate polar properties due to the presence of carbonyl and ester bonds. However, their functionality has been derivatized to include numerous varieties of functional groups, including (i) hydrophobic groups achieved by incorporating alkyl chain lengths such as butyl methacrylate (BMA, C4), lauryl methacrylate (LMA, C12), stearyl methacrylate (SMA, C18)), or benzyl methacrylate; (ii) hydrophilic groups such as acrylic acid (AA), methacrylic acid (MAA), methyl methacrylate (MMA), or 2-hydroxythylmethacrylate (HEMA); and (iii) surface-charged groups, including anion, cation, and zwitterionic

monomers. Chemical structures of common methacrylate functional monomers are shown in **Figure 1.5**.
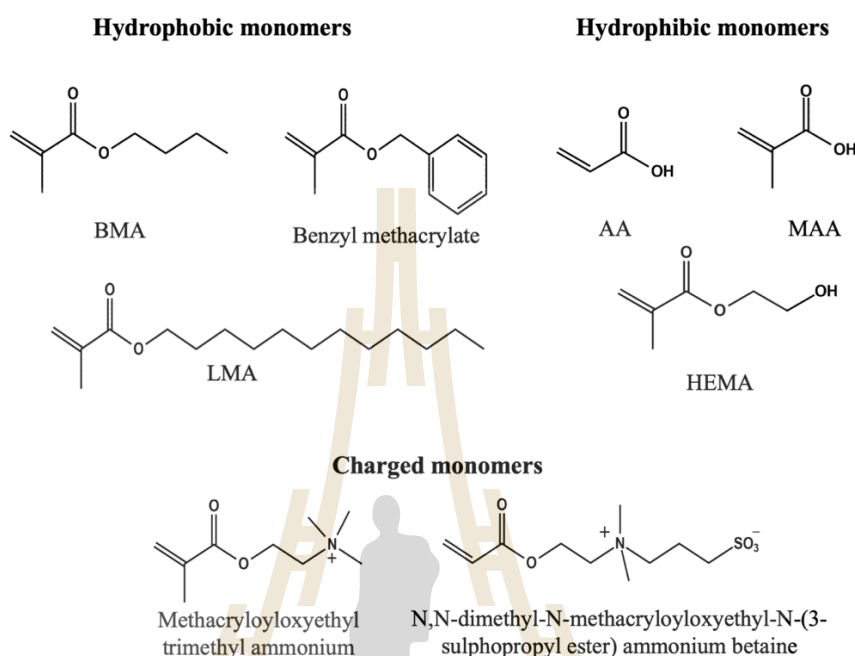
Figure 1.5 Representative chemical structures of methacrylate-based functional monomers for the synthesis of organic monoliths.

- Crosslinkers

Crosslinkers or crosslinking monomers are essential components for creating a three-dimensional network that provides mechanical stability, controls size and porosity. The degree of crosslinking affects the size and distribution of pores within the material. Common crosslinkers used in monolith synthesis include divinylbenzene, EDMA, N,N'-methylenebis(acrylamide) (the chemical structures are shown in **Figure 1.6**). The selection of crosslinker depends on the desired properties of the monolith such as its porosity, rigidity, and compatibility with specific applications.

| Divinylbenzene | EDMA | N,N'-methylenebis(acrylamide) |
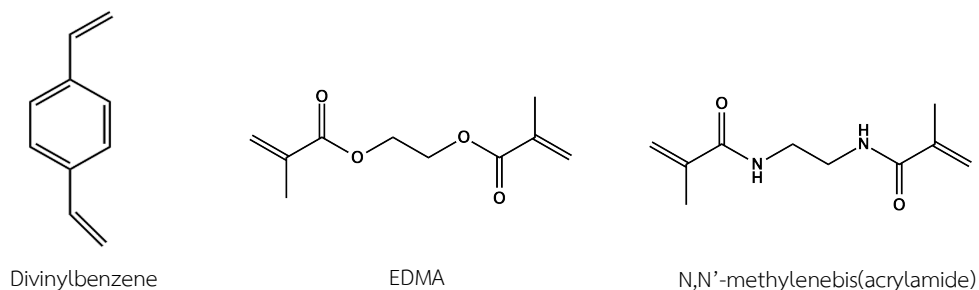
Figure 1.6 Example chemical structures of crosslinking monomers.

- **Porogenic solvent**

Porogenic solvent, also known as a porogen, is a solvent used to dissolve all components to achieve a homogeneous pre-polymerization solution. Additionally, porogenic solvents play a crucial role in creating and defining the pores or cavities within the monoliths. During polymerization, the porogens act as temporary templates or spaces, assisting in the maintenance of the desired pore structure. After the removal of these solvents, the monolith preserves its porosity, enabling control pore size, pore distribution and overall porosity.

- **Initiator**

Generally, an initiator is used to initiate the polymerization process by creation of free radicals that can react with monomers. These free radicals initiate the formation of covalent bonds between monomers, leading to the growth of the polymer chain. Initiator can be categorized into two main types, which are used based on the preferred polymerization methods. 2,2-Dimethoxy-2-phenylacetophenone (DMPAP) and azobisisobutyronitrile (AIBN) are common initiators used for photo and thermal polymerization methods, respectively (see **Figure 1.7**).
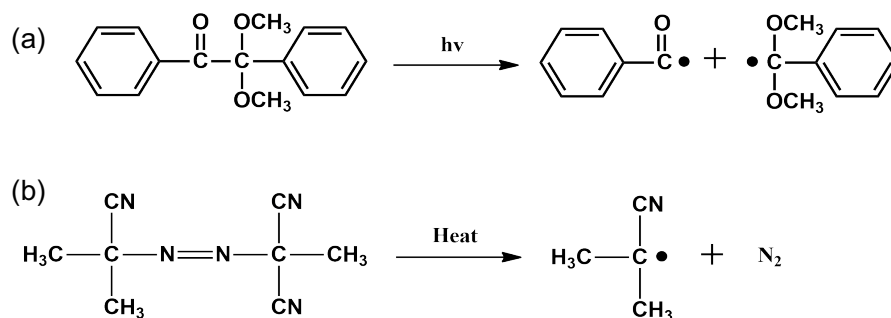
Figure 1.7 Free radical generations from (a) DMPAP and (b) AIBN.

1.1.2.2 Inorganic monoliths

Inorganic monoliths are one type of monolith categories, differ from their organic-based monoliths in both synthesis methods and precursors. The synthesis of inorganic monoliths typically relies on the sol-gel method, with common precursors including silica, metal-organic frameworks, or zirconia. Among these, silica is frequently chosen for the preparation of inorganic monoliths, leading to their classification as silica-based monoliths. Precursors such as tetraethyl orthosilicate (TEOS) or tetramethyl orthosilicate (TMOS) are commonly employed for the synthesis, undergoing hydrolysis and condensation reactions to form a gel-like structure. These monoliths exhibit a relatively high surface area (200-400 g/m^2) (Gama, Rocha, and Bottoli, 2019). However, the inorganic monoliths have limited tolerance, operating effectively within a narrow pH range between 2-8, and may face challenges related to dissolution and the breaking of silica linkages.

1.2 Solid-phase extraction

Solid-phase extraction (SPE) stands out as one of the most effective sample preparation methods available. This versatile technique allows for purification, sample matrix removal, and analyte pre-concentration to be successfully performed in a single process. When compared to conventional liquid-liquid extraction (LLE), SPE emerges as a more powerful method due to its ability to extract a wider range of chemical compounds. On the other hand, LLE is hindered by limitations in extracting polar compounds, and it is known for being time-consuming and labor-intensive.

Furthermore, LLE has a tendency for emulsion formation and requires large amounts of potentially hazardous and flammable organic solvents, thus posing safety and environmental concerns (Buszewski and Szultka, 2012; Płotka-Wasylka, Szczepań́ska, de la Guardia, and Namiesnik, 2015). Consequently, SPE methods have been widely developed and applied across various applications.

1.2.1 Principles and concepts of SPE

SPE is based on the adsorption of the analyte(s) on the solid phase (sorbent). The ability of an analyte to adsorb onto the solid sorbent is determined by the partition coefficient. The partition coefficient (K) is defined as the ratio of analyte concentration distributed between the two phases, solid and liquid, at equilibrium. The partition coefficient is represented by equation (1).

$$Partition\ coefficieny\ (K) = \frac{Concentration\ of\ analyte\ in\ solid\ phase}{Concentration\ of\ analyte\ in\ liquid\ phase} \qquad (1)$$

Analytes with high K values can strongly retain or adsorb onto the solid sorbent, whereas relatively low K values indicate weaker adsorption onto the adsorbent. This leads to varying adsorption capabilities for each analyte or matrices on the adsorbent.

1.2.2 Procedure of solid-phase extraction

In order to achieve pre-concentration and sample matrix removal, the procedure of SPE typically involves four key steps, which are conditioning, sample loading, washing, and eluting. Schematic diagrams of the four steps SPE are demonstrated in **Figure 1.8**.
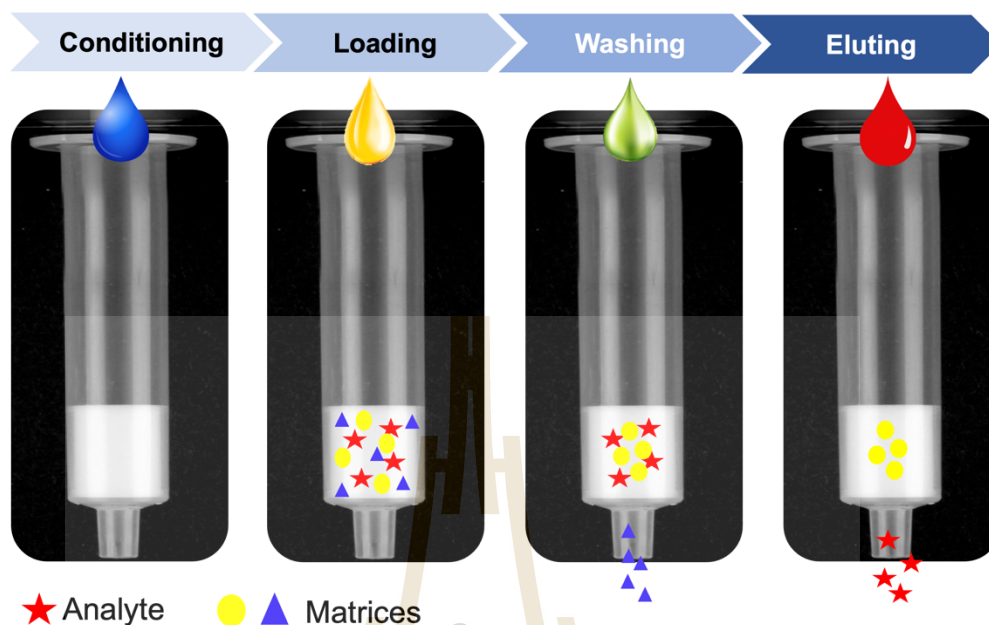
Figure 1.8 Schematic diagrams of solid-phase extraction procedures.

1.2.2.1 Conditioning

Conditioning is a crucial step essential for activating the functional groups on the surface of the sorbent before performing the extraction. During this step, a solvent with the appropriate polarity that matches the surface functional groups is applied through the solid sorbent. The selection of an appropriate solvent plays a critical role in ensuring the effective activation of solid sorbent, as illustrated in **Figure 1.9**.
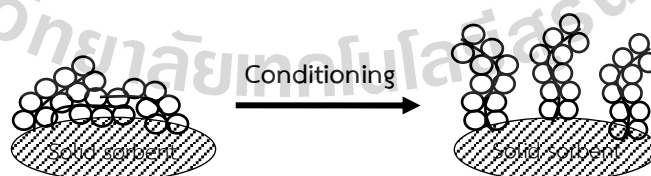
Figure 1.9 Activation of surface functional groups of solid sorbent (Ar-sanork, 2018).

1.2.2.2 Sample loading

After the conditioning step, the sorbent is ready to adsorb target compounds. The sample, which contain the analytes of interest along with unwanted matrix components, is introduced through the conditioned solid sorbent. Analytes are retained on the sorbent via adsorption mechanism (**Figure 1.10**). During the loading, sample matrix components may also be adsorbed on the sorbent which require washing step to clean up.
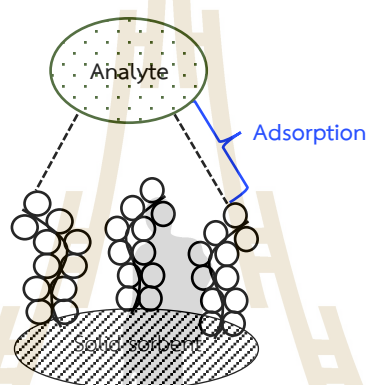
Figure 1.10 Adsorption of target analyte on the activated sorbent (Ar-sanork, 2018).

1.2.2.3 Washing

After the sample loading, unwanted matrix components are removed during the washing step. An appropriate washing solvent is used to eliminate adsorbed matrix compounds. The effective washing solvent should possess the capability to remove the matrix to the greatest extent possible while maintaining the retention of the target analyte on the sorbent, ensuring a high extraction efficiency. Matrices with relatively low K values are desorbed in this step, leading to sample cleanup.

1.2.2.4 Eluting

The final step is elution, which is important for achieving analyte pre-concentration or enrichment. Successful pre-concentration can be attained by utilizing a small volume of the appropriate solvent to completely desorb the target analyte from the sorbent. Furthermore, selective enrichment can be achieved by applying an

appropriate solvent composition to only elute the target analyte and prevent the co-elution of stronger adsorbed matrices.

1.2.3 Miniaturization of solid-phase extraction

SPE cartridges is a widely used format for performing extraction. Typically, an SPE cartridge is assembled by packing of particles-based sorbents in varying amounts within a high-density polypropylene (PP) syringe between two frits. Schematic construction of the SPE cartridge is illustrated in **Figure 1.11**. The amount of sorbent varies from milligram to several gram, depending on the applicable sample type and volume (ranging from 500 μL to 50 mL) (Badawy, El-Nouby, Kimani, Lim, and Rabea, 2022). This variation is necessary to achieve high extraction efficiency. The flow of the sample through the cartridge can be achieved by applying either positive pressure (applying pressure at the top of the cartridge) or negative pressure (using vacuum pump and chamber).
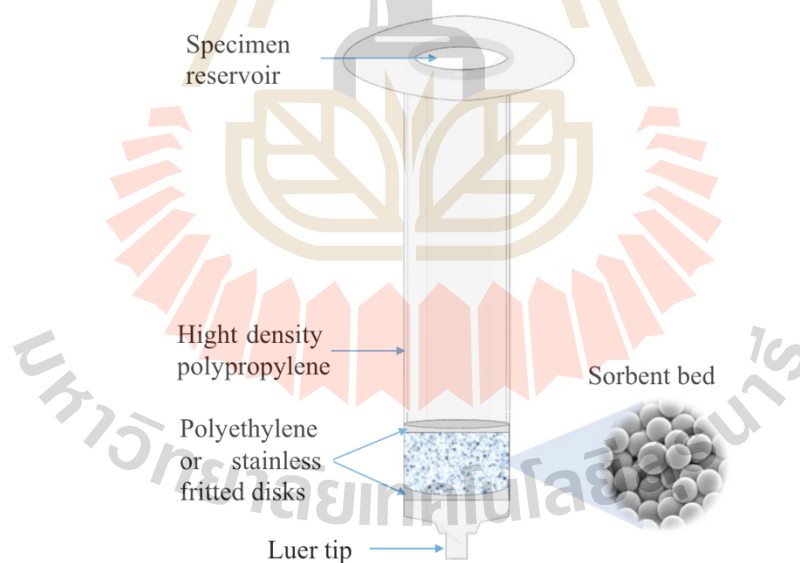
Figure 1.11 Schematic construction of SPE cartridge (Badawy et al., 2022).

However, smaller SPE platforms (typically SPE cartridges containing 100 mg of sorbent in a 1 mL syringe) are required for rapid extraction and sensitivity enhancement

by reducing the elution volume, especially when dealing with a limited amount of biological samples.

      Miniaturization of conventional SPE method also call micro-SPE (μ-SPE) is therefore developed to eliminate the limitations. Several designs of miniaturized SPE have been developed such as microextraction by packed sorbent, spin column, stir bar sorptive extraction, fiber solid-phase microextraction, magnetic SPE and in pipette tip μ-SPE (see **Figure 1.12**)
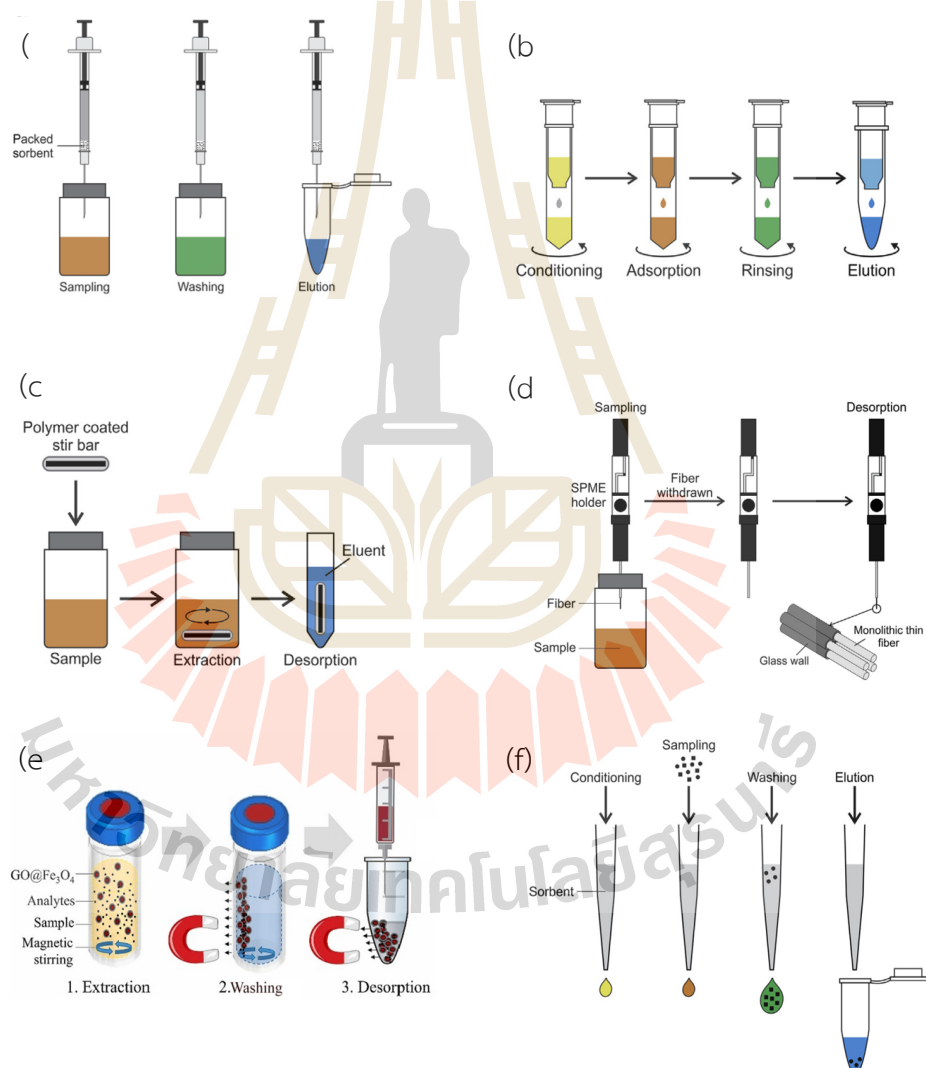
Figure 1.12 Miniaturization of SPE platforms: (a) microextraction by packed sorbent, (b) spin column, (c) stir bar sorptive extraction, (d) fiber solid-phase microextraction, (e) magnetic SPE, and (f) in pipette tip μ-SPE (Akamine, Vargas Medina, and Lanças, 2021; Gama et al., 2019).

Among these, in pipette tip based monolithic μ-SPE (IT monolithic μ-SPE) is a popular μ-SPE design due to its compact, portable, and low-cost system. Recently, IT monolithic μ-SPE has been fabricated through the *in situ* synthesis of monolithic material in the PP pipette tips (schematic diagram of IT monolithic μ-SPE is shown in **Figure 1.13**).
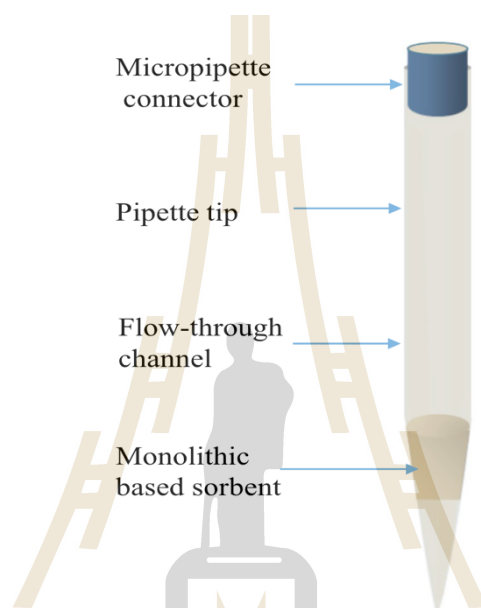
Figure 1.13 Schematic diagram of IT monolithic μ-SPE device (Badawy et al., 2022).

However, the preparation of monoliths in pipette tips presents challenges, as detachment of the monolith from the pipette tip and the presence of void spaces between the monolith and the tip wall are frequently observed, resulting in a loss of both preparation success rate and extraction efficiency. Pipette tip is polypropylene-based material which is hydrophobic and chemically inert, making direct attachment of the monolith to the PP pipette tip wall unachievable. Surface modification of the PP pipette tip is a key strategy to improve monolith attachment to the tip wall.

Reported surface modification approaches for polymeric substrates have been proposed, including instrumental and chemical methods. Instrumental methods such as flame treatment (Williams, Abel, Grant, Hrachova, and Watts, 2015), plasma treatment (Yaman, Özdoğan, Seventekin, and Ayhan, 2009), and low-pressure glow discharge (Chiper and Borcia, 2013; Choi, Rybkin, Titov, Shikova, and Ageeva, 2006) have

been utilized for polymeric surface modification to enhance the functionality of the materials. However, these methods have limitations, such as the requirement of flat-shaped substrates, making them unsuitable for cone-shaped pipette tips. Additionally, high-cost, complexity, and low-reproducibility are the disadvantages of the techniques.

In chemical treatment, a photo-induced grafting approach has been employed for surface modification of PP tips (Altun, Hjelmström, Abdel-Rehim, and Blomberg, 2007; Alwael et al., 2011; Fresco-Cala, Mompó-Roselló, Simó-Alfonso, Cárdenas, and Manuel Herrero-Martínez, 2018; Hu et al., 2004; Iacono, Connolly, and Heise, 2016; Krenkova and Foret, 2013; Sorribes-Soriano, Valencia, Esteve-Turrillas, Armenta, and Herrero-Martínez, 2019; Hongxia Wang, Zhang, Lv, Svec, and Tan, 2014). The approach involved functionalizing the tip wall by generating free radicals on the PP surface using a hydrogen abstraction initiator before grafting a linking polymer onto the radical surface.

However, the reported methods available for PP pipette tip modification are still limited. Proposing an alternative surface modification method for improving monolith attachment in the PP pipette tips is therefore essential.

1.3 Electrochemical detection

1.3.1 Principle of electrochemical detection

Electrochemical techniques are general analytical methods that rely on the measurement of electrical quantities, such as potential, current or charge, to provide information into chemical processes occurring at electrode surfaces. These techniques are widely recognized as powerful tools and find extensive applications, including clinical diagnostics, food safety, and environmental monitoring.

The electrochemical cell plays a central role in electrochemical technique. Generally, an electrochemical cell comprises two primary electrodes: the working electrode and the counter electrode, with the present of an electrolyte. In certain instances, a reference electrode may also be included alongside the working and counter electrodes. When the electrochemical cell is connected to an external circuit, it establishes a pathway for electric current (electrons) throughout the circuit. Within the cell, the electrolyte facilitates the flow of either electrons or ions. The chemical

reactions occurring within the cell facilitate the conversion of chemical energy into electrical energy. Consequently, the generated electrical energy completes the electrical circuit.

Electrodes are fundamental components of electrochemical technique. A common setup for electrochemical analysis is the three-electrode system, consisting of three different electrodes (see **Figure 1.14**), including:

(i) **Working electrode** is the important electrode where the electrochemical reaction of interest occurs. Working electrode serve as the site where analyte undergo oxidation or reduction. Platinum, gold, glassy, carbon graphene, and various modified surfaces were commonly used as the working electrode.

(ii) **Reference electrode** is employed as a reference point to measure the electrochemical potential of the working electrode. Reference electrode should be stable and well-defined potential against which the potential of the working electrode is compared. Reference electrode provides constant and known potential, ensuring accurate and reproducible measurements by maintaining a fixed reference point. Common reference electrodes include the silver/silver chloride (Ag/AgCl) electrode, saturated calomel electrode, and the standard hydrogen electrode.

(iii) **Counter electrode** (also known as the auxiliary electrode), is used to complete the electrical circuit within the electrochemical cell and allow the flow of current between the working electrode and reference electrode. Counter electrode balances the flow of electrons or ions generated at the working electrode. Counter electrode is typically made from an inert conductive material such as platinum.
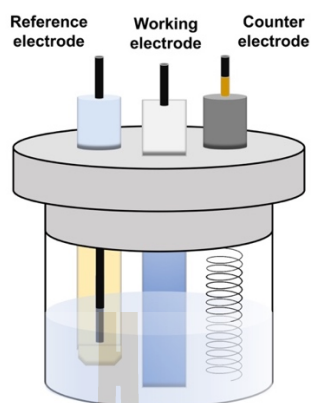
Figure 1.14 Schematic illustration of three-electrode system in electrochemical technique (Eom et al., 2022).

1.3.2 Screen-printed electrode-based electrochemical detection

Screen-printed electrodes have emerged as a primary branch of electrochemical detection, offering rapid, sensitive, and precise performance similar to traditional manufacturing methods but with the added advantages of being more cost-effective, simpler, and requiring smaller sample and reagent volumes.

Screen-printed electrodes typically comprise an electrochemical cell consisting of three electrodes: working electrode, reference electrode, and counter electrode. The design of a screen-printed electrode is illustrated in **Figure 1.15**, where three electrodes are printed on the same solid substate which normally are plastic, ceramic or textile.
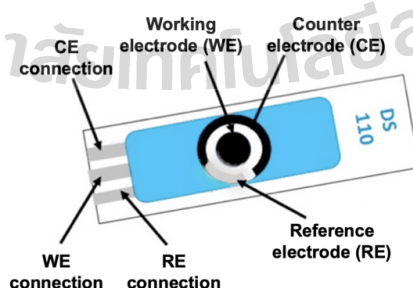
Figure 1.15 Common schematic design of a screen-printed electrode (Paimard, Ghasali, and Baeza, 2023).

1.4 Cannabis

Cannabis, also known as marijuana or hemp, is a tropical plant that predominantly grows in the regions of Eastern and Central Asia (Antunes, Barroso, and Gallardo, 2023). According to the United Nations Office of Drugs and Crime (UNODC) report, more than 192.2 million people between the ages of 15 and 64 have consumed cannabis (Crime, 2021). As a result, *cannabis* is the most widely used illicit drug globally.

The *cannabis* plant can produce more than 60 different compounds, collectively referred to as cannabinoids. Among these cannabinoids, Δ^9-tetrahydrocannabinol (THC), cannabidiol (CBD), and cannabinol (CBN) are the most prominent compounds (Klimuntowski, Alam, Singh, and Howlader, 2020). THC is the psychoactive substance responsible for including euphoria, sleepiness, temporal distortions, and hallucination (Wanklyn et al., 2016). In contrast, CBD and CBN are non-psychoactive but exerts neuroprotective, analgesic, sedative, and anti-inflammatory effects.

Cannabis remains a subject of controversy worldwide, as it has been identified as a primary contributing factor to incidents of driving under the influence of drugs (DUID) (Teixeira et al., 2007). A trauma center in the USA reported that approximately 60 % of patients involved in motor vehicle accidents tested positive for *cannabis* (Antunes et al., 2023). Despite changes in legislation, such as legalization or decriminalization in several countries, such as the USA, Canada, and Portugal (Rosendo et al., 2022), public health concerns, such as negative mental and respiratory health outcomes, an increased likelihood of problematic use, and occupational safety risks are still need to be considered. Therefore, the development of methods or protocols to identify and control cannabis consumption is crucial, not only due to its legal status but also because of its associated side effects.

Cannabis is commonly consumed through two routes which are inhalation (smoke and vapor and oral administration). In *cannabis* users, the psychoactive substance, THC is primarily metabolized in the liver through oxidation to form 11-hydroxy-Δ^9-tetrahydrocannabinol (THC-OH). Further oxidation of THC-OH continues, resulting in the production of an inactive metabolite, Δ^9-tetrahydrocannabinol-9-

carboxylic acid (THC-COOH). The addition of glucuronic acid improves the solubility of THC-COOH, presenting it in its conjugated form as Δ^9-tetrahydrocannabinol-11-oic acid glucuronide (THC-COOH-Glu). This conjugation facilitates its excretion in urine (Klimuntowski et al., 2020). The ratio of excreted THC-COOH-Glu/THC-COOH in the urine sample was reported to be between 1.3 to 4.5 (Weinmann, Vogt, Goerke, Müller, and Bromberger, 2000). Therefore, THC-COOH and THC-COOH-Glu are the predominant compounds excreted in urine. The metabolic pathway of THC in the liver is summarized in **Figure 1.16** and the molecular structures of THC, THC-OH, THC-COOH, and THC-COOH-Glu are presented in **Table 1.1**.
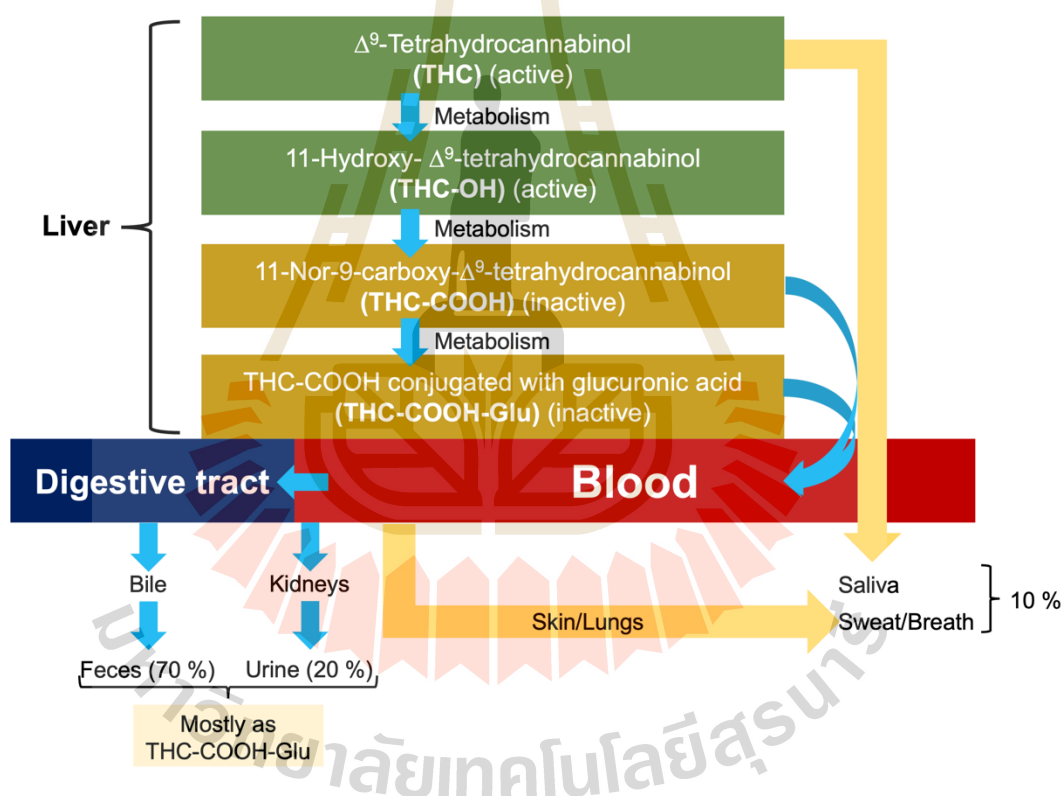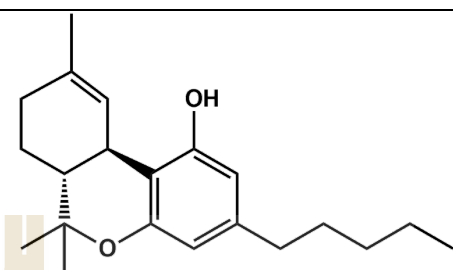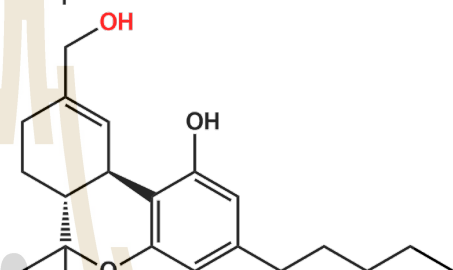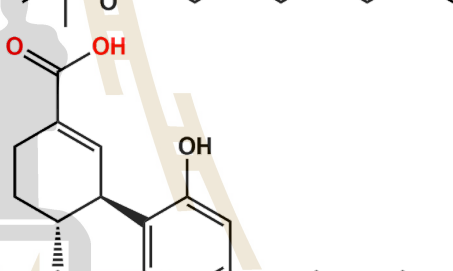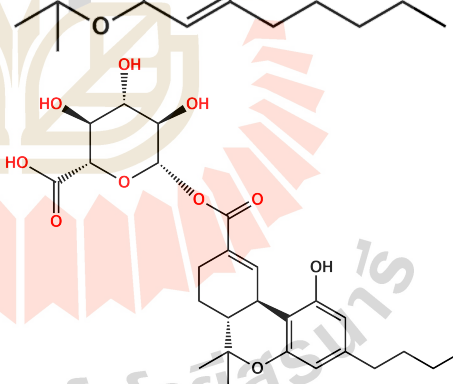
Figure 1.16 Metabolic pathway of THC in the liver (modified from (Klimuntowski et al., 2020).

Table 1.1 Molecular structures of THC, THC-OH, THC-COOH, and THC-COOH-Glu.

Cannabinoid	Structure
THC	
THC-OH	
THC-COOH	
THC-COOH-Glu	

In order to identify *cannabis* consumption, various sample matrices can be utilized, such as blood, plasma, oral fluid, breath, and urine. Different sample matrices can provide distinct information regarding consumption patterns, such as timing and amount (Nicolaou, Christodoulou, Stavrou, and Kapnissi-Christodoulou, 2021). Among the available options, urine has emerged as a prevalent choice due to its non-invasive collection process, ease of use, and extended detection window (Karschner, Swortwood-Gates, and Huestis, 2020).

Urinary THC-COOH is therefore widely used as evidence or biomarker for identification of cannabis intake. Notably, a defined positive cutoff concentration for THC-COOH, is set at 50 ng mL^{-1} for screening and 15 ng mL^{-1} for confirming in cases involving illegal cannabis intake, emphasizes the need for an accurate and reliable method for the determination of urinary THC-COOH to successfully identify cannabis consumption.

1.5 Research objectives

The objectives of this thesis are as follows:

1.5.1 To develop a new PP pipette tip surface modification method for anchoring of monolithic sorbents with the tip wall.

1.5.2 To develop a μ-SPE method using the fabricated in pipette tip monolith for THC-COOH extraction in human urine samples.

1.5.3 To couple the μ-SPE method with electrochemical sensor using screen printed electrode for rapid and simple determination of urinary THC-COOH in forensic applications.
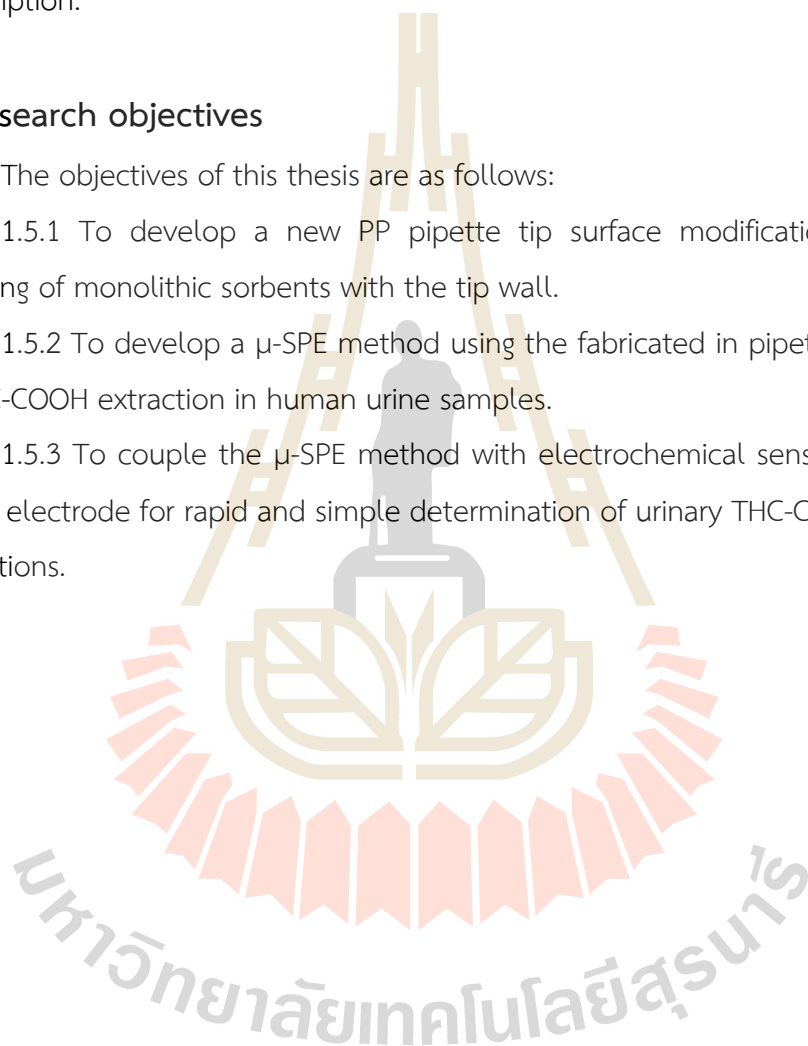
CHAPTER II

LITERATURE REVIEW

This chapter provides an overview of previous works related to the research objectives. Firstly, surface modification methods for anchoring of monolithic materials are reviewed to survey and gain an understanding of the reported works currently available. Additionally, to overcome the remaining research objectives, the review of analysis methods reported for the determination of THC-COOH is explored.

2.1 Surface modification methods for *in situ* synthesis of monoliths on polymeric housing

Due to the wide range of benefits offered by polymeric materials, such as flexibility, chemical and biocompatibility, cost-effectiveness, ease of manufacturing and reduced risk of breakage, they are suitable as housings for modern sample preparation techniques, including μ-SPE method.

IT monolithic μ-SPE combines the advantages of monolithic materials and polymeric PP pipette tips. It allows simple operations to perform extractions with good efficiency, making it widely used for μ-SPE applications. The development of IT monolithic μ-SPE methods has been widely proposed. However, fabricating monoliths in polymeric housings is challenging, as detachment and void space of the monoliths are the main problems during *in situ* synthesis. Therefore, surface modification is necessary to improve the polymeric surface functionalities prior to anchoring the preferred monoliths.

In silica-based housings (glass), monoliths can be directly bonded through silanization reaction using a primer of 3-tri((methoxysilyl)propyl) methacrylate. For the polymeric housing, two different chemical methods, including photografting and thin layer creation, have been reported for the modification of the polymeric housing surface to anchor monolithic materials.

2.1.1 Photografting approach

Photografting is a photochemical reaction method that involves the use of ultraviolet (UV) irradiation, a hydrogen-abstracting photoinitiator, and reactive monomer(s), typically vinyl monomers, to graft onto the surface of the material (B. Rånby, Yang, and Tretinnikov, 1999). The photografting approach was first pioneered for polyacrylamide and natural rubber by Oster and Shibata in 1957 (Oster and Shibata, 1957)

In 1992, Rånby et al. first proposed the photografting method using a hydrogen-abstracting photoinitiator, benzophenone (Bengt Rånby, 1992). The benzophenone-based photografting methods were continuously published by Rånby and the group from 1992 to 1999 (B. Rånby et al., 1999; Bengt Rånby, 1992, 1992; Yang and Rånby, 1996), prior to explaining the mechanism of the process in 1999 (B. Rånby et al., 1999). The grafting method was carried out using the hydrogen abstracting photoinitiator named benzophenone. The grafting procedure was commonly performed in two steps: (i) the creation of a initiator surface of benzophenone and (ii) the grafting of a polymerizable chains. A schematic diagram of the photografting method is demonstrated in **Figure 2.1**.
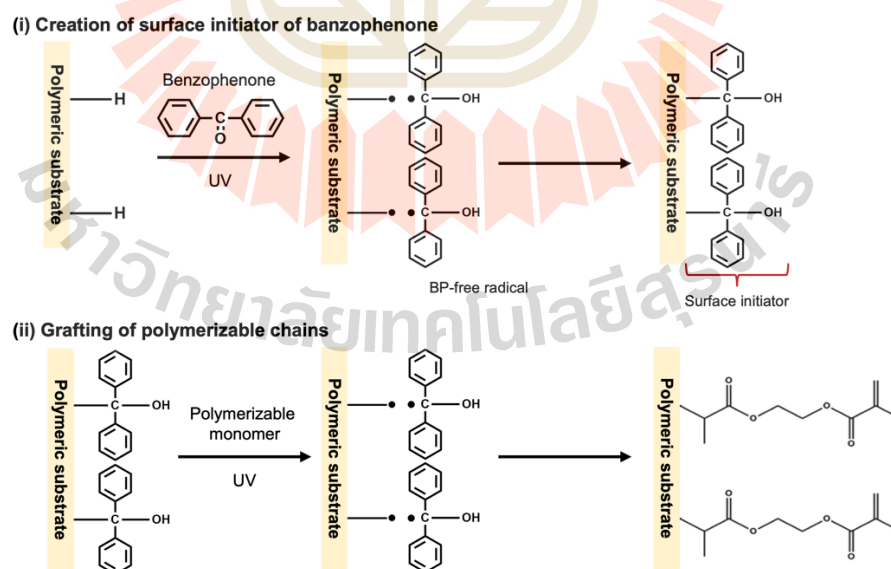
Figure 2.1 Schematic diagram of the photografting method using benzophenone of polymeric substrate (Ma, Davis, and Bowman, 2000).

To generate the initiator surface, a benzophenone solution was introduced to the housing before exposing it to UV light (see **Figure 2.1(i)).** The carbonyl groups on benzophenone were excited to the triplet state by UV irradiation. The excited molecule then abstracted a hydrogen atom from the substrate surface to generate free radicals on the surface. This radical surface could recombine with the benzophenone radicals, leading to covalent bonding between the initiator and the surface, resulting in the initiator surface. In the second step, the radicals were later regenerated by exposure to UV light. Polymerizable monomers were then grafted onto the surface via a polymerization reaction initiated by the surface radicals (see **Figure 2.1(ii))** (Castell, Wouters, de With, Fischer, and Huijs, 2004; Ma et al., 2000; B. Rånby et al., 1999). These polymerization groups can be further polymerized with the desired monolithic polymer, allowing anchoring via covalent bonds between the grafting layer and monolithic material.

The benzophenone-based photografting method was applied for various polymeric materials such as polycarbonate (PC), poly(methyl methacrylate) (PMMA), cyclic olefin copolymer (COC), polydimethylsiloxane (PDMS), and polypropylene (PP), as reported by Rohr and his group (Rohr, Ogletree, Svec, and Fréchet, 2003).

In 2003, the photografting method using benzophenone for modifying COC channels and PP pipette tips walls in a microfluidic chip to anchor monolithic material was first proposed by Stachowiak et al. (Stachowiak et al., 2003). The initiator surface was generated by using a benzophenone solution and exposed to UV light. Monovinyl monomer, MMA, and divinyl monomer, ethylene diacrylate (EDA), were grafted onto the prepared tips by UV irradiation for 3 min. The grafted housings were then used for anchoring monolith (BMA-co-EDMA). The residual double bonds of MMA and EDA on the modified surface formed covalent bonds with the growing monolithic network. The successful attachment between the monolith and tip wall was confirmed through scanning electron microscope (SEM) imaging. As shown in **Figure 2.2**, without the grating method (**Figure 2.2(a)**), void space can be observed due to the lack of anchoring between the monolith and tip wall. Meanwhile, the void space was eliminated when the tip was grafted with the MMA and EDA as shown in **Figure 2.2**

(b). These results demonstrate the successful use of photografting to eliminate the void space of the synthesized monolith within the tips.
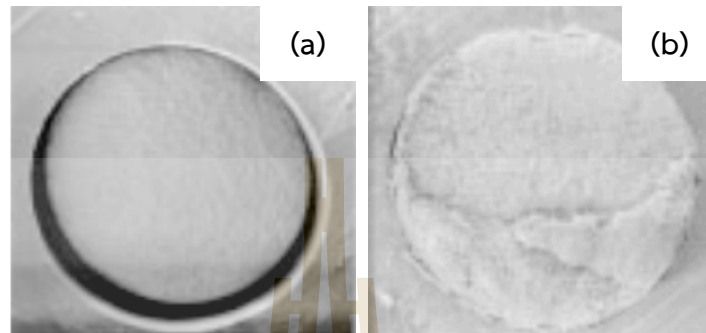
Figure 2.2 SEM images of porous polymer monoliths inside PP tips (a) without surface modification and (b) with surface modification using photografting method with MMA-co-EDMA monomers (Stachowiak et al., 2003).

The benzophenone-based photografting method was extensively developed and applied for the modification of PP housings, prior to anchoring monolithic materials. The reported photografting method are summarized in **Table 2.1**.

Table 2.1 Photografting methods using benzophenone reported for PP housings.

Housing material	Monolith	Grafting procedure		Analyte/Sample	Reference
		Grafting monomer	Time (min)		
PP tip	BMA-co-EDMA	MMA and EDA (1:1 w/w)	12	-	(Stachowiak et al., 2003)
PP tip (550 µL)	BMA-co-EDMA	MMA and EDMA (1:1 w/w)	10	Ropivacine / Plasma	(Altun et al., 2007)
PP tip (20 µL)	Functionalized GMA-co-EDMA	15 % (w/w) EDMA/MeOH	-	Glycoproteins / E.coli cell lysate	(Alwael et al., 2011)
PP tip (200 µL)	Nanoparticle-modified monolithic	MMA and EDMA (1:1 w/w)	-	Phosphopeptides	(Krenkova and Foret, 2013)
PP syringe	GMA, BMA, and LMA-co-EDMA	15 % (w/w) EDMA/MeOH	6	Metal ion / Water	(Hongxia Wang et al., 2014)
PP tubing (i.d.2mm)	GMA-co-EDMA	5 % (w/w) EDMA/MeOH	30	-	(Iacono et al., 2016)
PP-spin column	GMA-co-EDMA with oxidized single-walled carbon nanohorns	15 % (w/w) EDMA/MeOH	20	Nonsteroidal anti-inflammatory drugs / Urine	(Fresco-Cala, Cárdenas, and Herrero-Martínez, 2017)
PP tip (200 µL)	MWCNTs- GMA-co-EDMA	15 % (w/w) EDMA/MeOH	60	Antidepressants / Urine	(Fresco-Cala et al., 2018)
PP tip (200 µL)	MAA-co-EDMA	15 % (w/w) EDMA/MeOH	20	Abuse drugs / Oral fluids	(Sorribes-Soriano et al., 2019)

GMA=Glycidyl methacrylate, MeOH=Methanol, MWCNTs=Multi-wall carbon nanotubes

As summarized in **Table 2.1**, the divinyl monomer, EDMA (the chemical structure shown in **Figure 2.3**), was the most popularly used as a grafting monomer for PP surface modification.
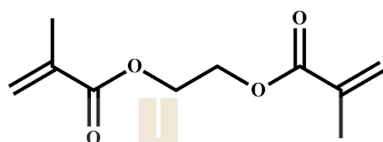
Figure 2.3 Chemical structure of EDMA.

SEM images, as shown in Figure 2.4, clearly indicated good attachment of the modified gold nanoparticles-monolith within the modified PP pipette tip (**Figure 2.4(a) and (c)**). Meanwhile, void space between the PP tip surface and a piece of monolith could be observed in an unmodified PP tip (see **Figure 2.4(b) and (d)**) (Altun et al., 2007).
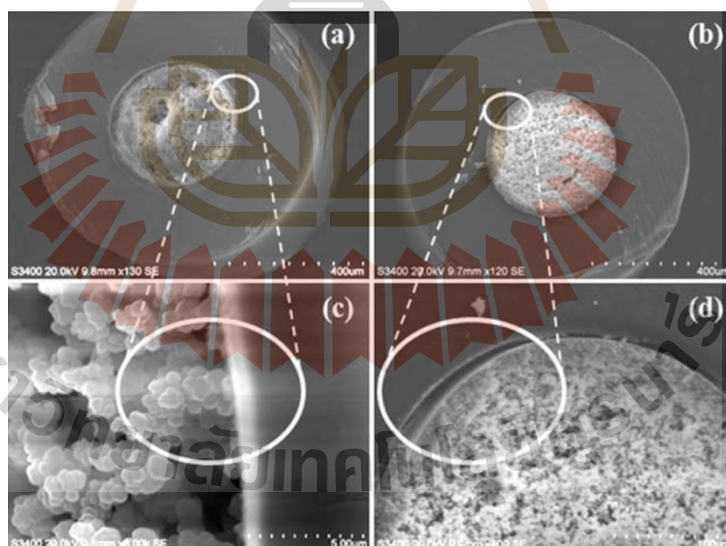
Figure 2.4 SEM images of monoliths formed inside the modified PP pipette tip (a) and (c) and the unmodified PP pipette tip (b) and (d) (Altun et al., 2007).

Good retentions of the iron oxide nanoparticles-modified monoliths were also illustrated in the photographs, as shown in **Figure 2.5**. A piece of the modified

monolith was well-attached in the modified PP pipette tip, ready for the enrichment of phosphopeptides (Krenkova and Foret, 2013).
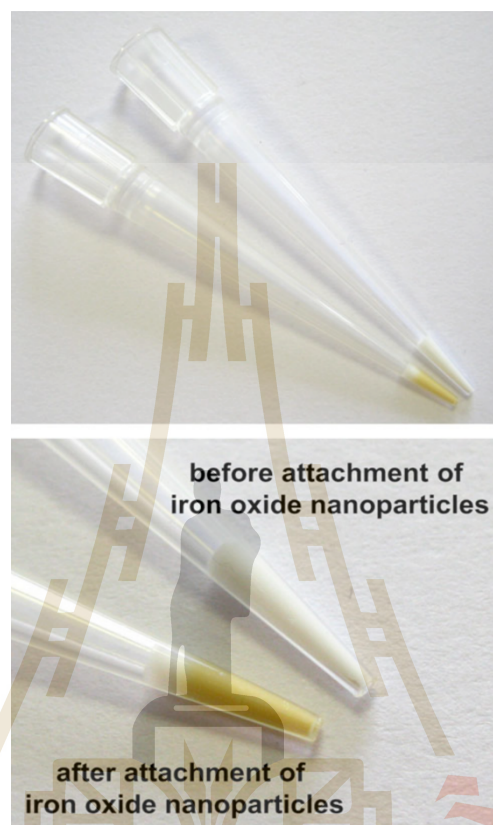
Figure 2.5 Photographs of iron oxide nanoparticles-modified monolith synthesized in the modified PP pipette tip by photografting method (Krenkova and Foret, 2013).

In 2016, Iacono et al. published a method for the fabrication of a GMA-co-EDMA monolith in a 2.0 mm i.d. PP tubing (Iacono et al., 2016). Without surface modification, the monolith slipped out of the tube when external pressure was applied using a syringe pump, as shown in **Figure 2.6(a)**. To improve the attachment of the monolith in the PP tube, the photografting method was carried out. The method consisted of two sequential steps: (i) grafting benzophenone and (ii) grafting the linking layer, EDMA, on the PP tubing (see **Figure 2.6(b)**).
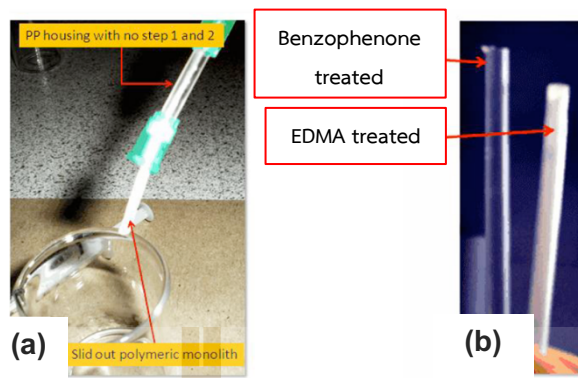
Figure 2.6 Photograph of (a) Slipped out of GME-EDMA monolith from the unmodified PP-tubing and (b) PP-tubing after treatment with benzophenone and EDMA (Iacono et al., 2016).

Successful grafting of the EDMA polymer on the PP tubing surface was investigated by SEM technique. Longitudinal cross-section and a close-up of PP tubing grafted with EDMA are demonstrated in **Figure 2.7(a) and (b)**, clearly presenting plaques of grafted EDMA polymer on the tubing surface. A comparison between the preparation of monolith in the unmodified and modified PP tubing confirmed the achievement of grafting; void space could be observed only in the tubing without surface modification (**Figure 2.7(c) and (d)**). A large void space was clearly invisible when the photografting was applied. Good attachment and lack of void space were observed (see **Figure 2.7(e) and (f)**).
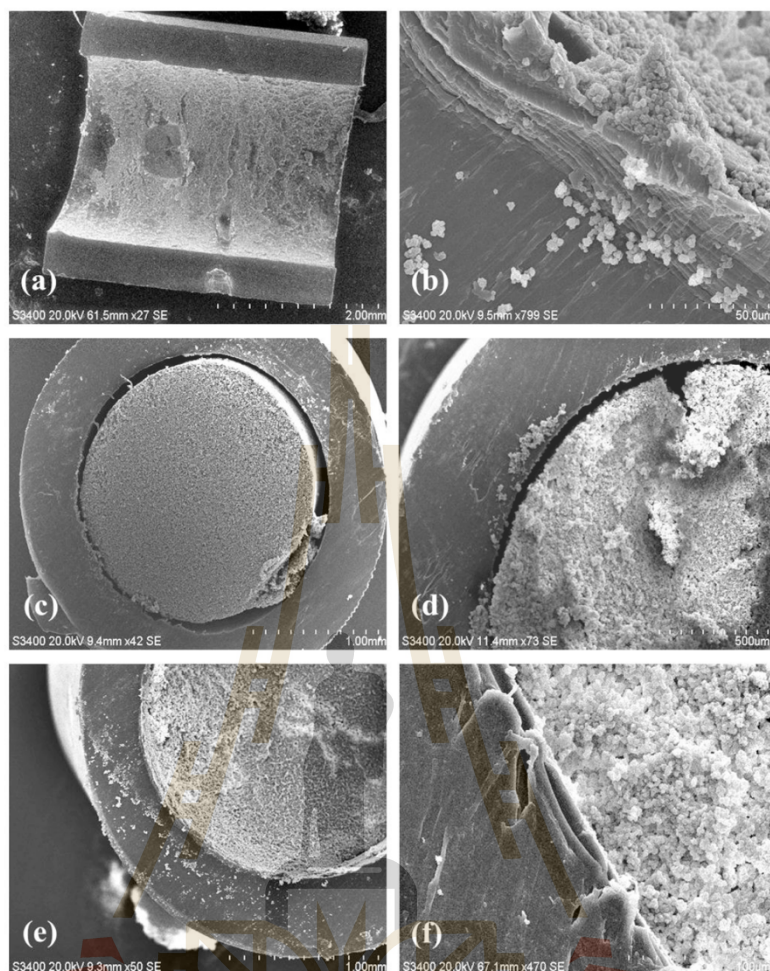
Figure 2.7 SEM images of (a) a cross-section of EDMA grafted PP-tubing surface, (b) EDMA clusters grafted on the wall, (c) and (d) GMA-co-EDMA monolith synthesized in unmodified PP-tubing, and (e) and (f) GMA-co-EDMA monolith synthesized in modified PP tubing (Iacono et al., 2016).

Currently, the photografting method based on hydrogen abstraction and vinyl monomers grafting is still reported for anchoring of monoliths in the polymeric housing. However, low repeatability of the process is a significant concern, as the method is related to the generation of free radicals, which are extremely sensitive and unstable.

2.1.2 Thin layer creation approach

Another approach to polymeric surface modification is the creation of a linking polymer as a thin layer on the surface substrate. In 2012, Burke and their group proposed the thin layer creation method for modifying PDMS walls prior to anchoring

monoliths in a microfluidic platform (Burke and Smela, 2012). Unlike the photografting method, in this approach, a surface initiator was generated using a non-hydrogen abstracting initiator, 2,2-dimethoxy-2-phenyl-acetophenone (DMPAP), before the formation of the linking thin layer.

In order to generate a surface initiator of DMPAP, a solution of DMPAP dissolved in acetone was flushed through the PDMS channels. The DMPAP penetrated into the PDMS materials prior to the local polymerization of the linking monomers, MMA and EDA. Since the DMPAP had penetrated into the PDMS, the linking thin layer polymer initiated only within the PDMS (**Figure 2.8**).
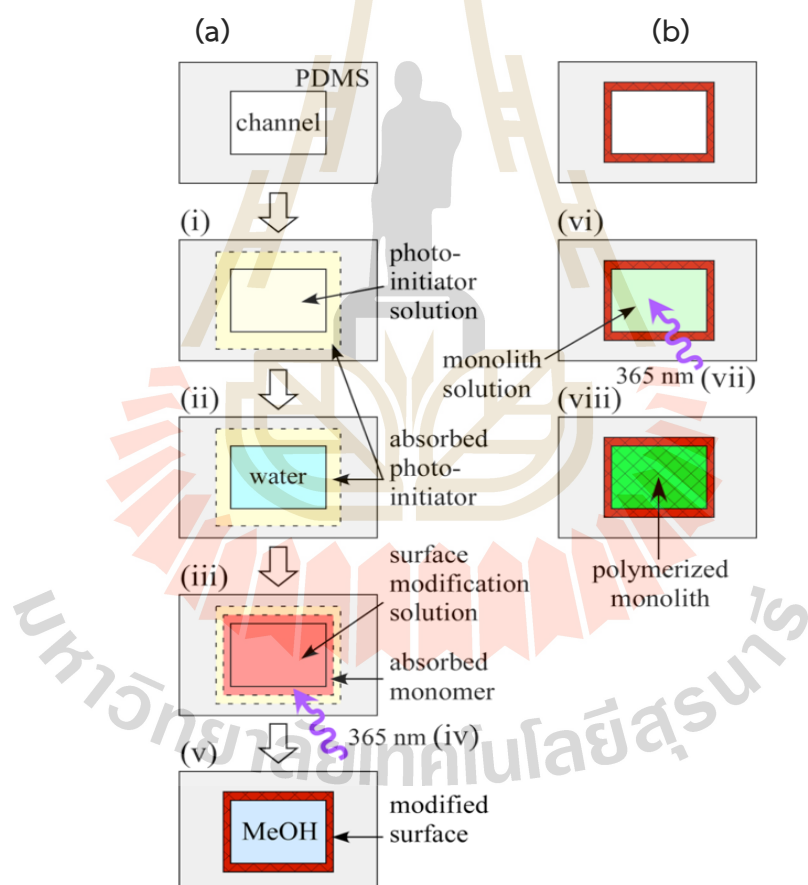
Figure 2.8 Schematic diagrams of (a) surface modification based on the thin-layer creation method and (b) *in situ* synthesis of monolith in the modified microchannels.

SEM images demonstrated the smooth surface of an unmodified empty microchannel (**Figure 2.9(a)**). The gap between the monolith and the PDMS wall observed in **Figure 2.9(b)** resulted from the shrinkage of the monolithic material. However, after modification with the proposed method, a thin layer of linking polymer was obtained (see **Figure 2.9(c)**). Since DMPAP was adsorbed into the PDMS, the linking polymer of MMA and EDA was initiated only within the PDMS. Good attachment of the monolith to the PDMS substrate was achieved. There was no gab between the monolith and the PDMS wall, as illustrated in **Figure 2.9(d)**. In this work, the anchoring of the monolith onto the PDMS wall was predicted to entangle with the modified layer but not from covalent bonds.
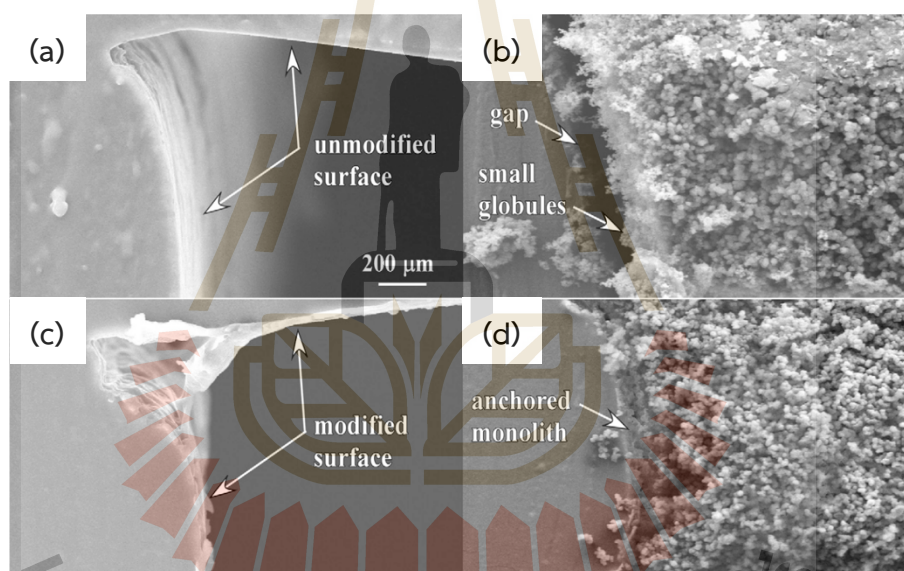
Figure 2.9 SEM images of (a) unmodified PDMS microchannel, (b) monolith formed in the unmodified PDMA microchannel, (c) modified PDMS microchannel and (d) monolith formed in the modified PDMS microchannel (Iacono et al., 2016).

Although the thin layer creation approach is more convenient for the modification of polymeric housing, the method has only been proposed for PDMS material. Surface modification methods for PP pipette tips are still in their infancy and remain limited.

2.2 Analytical methods for determination of THC-COOH

Due to the side effects and the legal status of cannabis, the identification and quantification of cannabis consumption are essential. Various analytical methods have been developed for the analysis of a marker of cannabis use, THC-COOH, including chromatographic immunoassay, chromatographic techniques coupled with mass spectrometry and electrochemical methods.

2.2.1 Chromatographic immunoassay for screening of urinary THC-COOH

Chromatographic immunoassay strip test is a common method widely used for screening of THC-COOH in urine to identify cannabis users, especially for workplace or roadside screening (Moore et al., 2006; Agius et al., 2012). THC-COOH screening protocol using the strip test is simple, fast, and cheap, the collected urine samples can be directly analyzed by dropping on the testing area, the analysis could be observed by naked eyes within a few minutes. However, false positive results are often found in complex sample analysis. The screening results need to be confirmed by high selective and sensitive methods, gas chromatography (GC) or liquid chromatography (LC) coupled with mass spectrometry.

2.2.2 Electrochemical detection

A rapid and sensitive method, electrochemical detection was reported for detection of cannabinoids including THC and its metabolites.

Recently, Renaud-Young and group proposed electrochemical detection method for THC and its metabolites (THC-OH and THC-COOH) using carbon paper electrode (Renaud-Young et al., 2019). The electrochemical method was first developed for detection of THC by immersion of the carbon paper electrode in the THC dissolved in borate buffer saline pH 10. Oxidation peak of THC was observed at +0.25 to +0.30 V vs SCE, reasoning from an oxidation mechanism of phenol on the THC structure as shown in **Figure 2.10**.
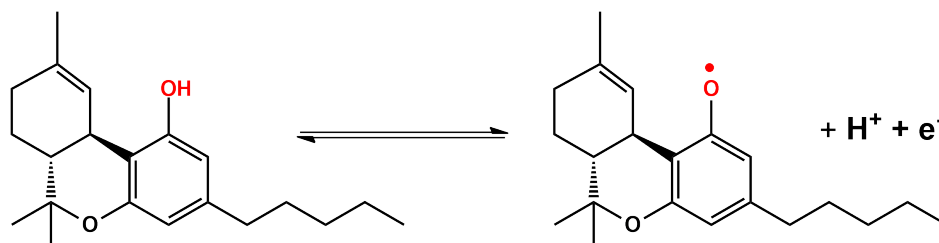
Figure 2.10 Oxidation reaction of phenol group on THC.

The detection method was then applied to THC-COOH. Similar to THC, THC-COOH exhibited an oxidation peak at +0.26 to +0.32 V vs SCE, resulted from the similarities structural between THC and THC-COOH (see **Figure 1.16**). A limit of detection of 2.75 ng mL^{-1} was achieved by the square-wave voltammetry analysis mode. The developed method was only used to analyze THC in saliva samples. The application for analyzing THC-COOH was not performed on real samples.

Even though electrochemical detection is fast, sensitive, and cost-effective, there have been limited developments in method for analyzing THC-COOH.

2.2.3 Chromatographic techniques coupled with mass spectrometry

Chromatographic separation techniques, such as GC and LC coupled with mass spectrometry (MS) or tandem mass spectrometry (MS/MS), are powerful analytical methods known for their high selectivity and sensitivity. Consequently, GC-MS, GC-MS/MS, and LC-MS/MS are the most commonly utilized methods for the analysis of THC-COOH in various samples. The analytical performance of reported methods using GC-MS, GC-MS/MS, and LC-MS/MS are summarized in **Table 2.2**.

Table 2.2 Summarization of analytical performances of reported methods for the analysis of THC-COOH.

Sample	Sample preparation	Conc. range (ng/mL)	LOD (ng/mL)	Recovery (%)	Ref
LC-MS/MS					
Urine	Dilution 10 times	25 - 8000	25	90	(Young and Victoria Zhang, 2022)
Blood	LLE	2 - 160	2	105	(del Mar Ramirez Fernandez, De Boeck, Wood, Lopez-Rivadulla, and Samyn, 2008)
Urine	Commercial C18 tips	6 - 250	2	71 - 75	(Montesano et al., 2014)
Urine	DPX (WAX-S)	1 - 500	1	86-89	(Sempio, Scheidweiler, Barnes, and Huestis, 2018)
Urine	MIP-SPE	5 - 170	1	12 - 15	(Sartore, Vargas Medina, Costa, Lanças, and Santos-Neto, 2020)
Saliva/ urine	SPE (Mixed C8 and SAX sorbent)	2 - 2000	0.5	83 - 96	(Teixeira et al., 2007)
Urine	DPX (WAX-S)	0.5 - 100	0.5	69 - 74	(Andersson, Scheidweiler, Sempio, Barnes, and Huestis, 2016)
Blood	DPX (WAX-S)	0.5 - 100	0.3	71	(Andersson et al., 2016)
Serum/ saliva/ urine	Automated SPE (Strata X-C µElution Plate)	-	0.2	-	(Bach, Fleischer, Wijayawardena, and Thurow, 2022)
Urine	In-tube SPME (C8, 18)	10 - 16	-	-	(Morisue Sartore, Costa, Lanças, and Santos-Neto, 2022)

Table 2.2 Summarization of analytical performances of reported methods for the analysis of THC-COOH (Continued).

Sample	Sample preparation	Conc. range (ng/mL)	LOD (ng/mL)	Recovery (%)	Ref
GC-MS					
Blood	LLE	50 - 1500	40	80	(Álvarez-Freire, Valeiras-Fernández, Cabarcos-Fernández, Bermejo-Barrera, and Tabernero-Duque, 2023)
Urine	Monolithic silica spin column	10 - 1000	5	95 - 103	(Namera and Saito, 2013)
Urine	Microextraction by packed sorbent (MEPS)	10 - 400	5	26 - 85	(Rosendo et al., 2022)
Urine	DPX (RP divinyl benzene)	-	3.4	57	(Ellison, Brewer, and Morgan, 2009)
Blood/ urine	Automated on-line SPE (C18)	3 - 200	1	79	(Frei, Frauchiger, Scheurer, and Mercer-Chalmers-Bender, 2022)
Urine	MIP-SPE	2 - 150	1	75	(Nestić, Babić, Pavlović, and Sutlović, 2013)
Urine	LLE	1 - 100	0.5	-	(Chericoni, Battistini, Dugheri, Pacenti, and Giusiani, 2011)
Serum	Automated LLE	up to 350	0.3	101 - 121	(Purschke, Heinl, Lerch, Erdmann, and Veit, 2016)

LOD=Limit of detection, SAX=Strong anion exchange; MIP=Molecularly imprinted polymer; SPME=solid phase micro extraction; WAX-S=Weak anion exchange with salt.

The determination of THC-COOH could be performed in various samples, including blood, serum, oral fluid and urine (see **Table 2.2**). Among these, urine is the most popular matrix samples for identifying cannabis consuming due to its wide detection window (concentration range from 120 ng mL^{-1} to 3380 ng mL^{-1} (Álvarez-Freire et al., 2023)), non-invasiveness, and ease of collection. LODs in the range of ng/mL level were achieved which were sufficient for urinary THC-COOH analysis (the cutoff concertation of THC-COOH was 50 ng/mL for screening and 15 ng/mL for confirming.

Although the analysis was performed using highly selective and sensitive methods, effective extraction methods for sample preparation were still required.

2.3 Sample preparation methods for THC-COOH

Sample preparation methods are a crucial step for the analysis of THC-COOH in complex biological samples. The sample preparations were primarily aimed at matrices removal and analyte pre-concentration. Extraction methods, including SPE and LLE, are among the most widely used sample preparation steps, as shown in **Table 2.2**. Compared to sample preparation through simple dilution, extraction strategies resulted in better LOD. Dilution alone provided an LOD of 25 ng/mL (Young and Victoria Zhang, 2022), whereas the LODs were lower when extraction methods were employed (see **Table 2.2**).

2.3.1 Liquid-liquid extraction

Liquid-liquid extraction or LLE is a classical sample preparation method that is simple and easily performed. The extraction can be carried out using basic equipment, typically including a separatory funnel, solvent, and collection vessel. From the literature, it is evident that LLE was still used for the THC-COOH analysis, but it was not widely adopted. Since, it is well known that its extraction efficiency is lower when compared to the SPE method. Low sensitivity was observed when GC-MS was coupled with LLE, resulting in an LOD of 40 ng mL^{-1} (Álvarez-Freire et al., 2023) (see **Table 2.2**).

2.3.2 Solid-phase extraction

Solid-phase extraction or SPE is one of the most powerful sample preparation methods. Interference removal and analyte pre-concentration can be achieved through 4 consecutive SPE steps: conditioning, sample loading, washing and elution. The SPE method offered high efficiency with relatively low LOD (see **Table 2.2**). The LOD could be down to lower than 1 ng mL^{-1}. The extraction efficiency is affected not only by the SPE condition optimization but also by the selecting sorbent types and functional groups, which play a role in adsorbing the target analyte via adsorption. Several functional groups and types of sorbent materials have been employed for THC-COOH extraction with different SPE designs.

2.3.2.1 Packed sorbent SPE or µ-SPE

SPE cartridges served as common housing for packing solid sorbents. Various sorbent materials, such as C18 particle-based sorbents (Frei et al., 2022), mixed-mode sorbents combining non-polar C18 and strong anion exchange (Bond Elut Certify II®) (Teixeira et al., 2007), and mixed sorbent of reversed-phase and strong cation exchange like sulfonic acid (Strata-X-C®) (Frei et al., 2022), were packed between two frits to retain the sorbents in the cartridges.

Home-made sorbents were also prepared for the extraction of THC-COOH. Molecularly imprinted polymers (MIPs) was synthesized by synthesizing functional monomer, crosslinker, and template of MMA, EDMA, and THC-OH, respectively, via thermal polymerization for selective extraction of THC, THC-OH, and THC-COOH (Nestić et al., 2013). However, only a slight improvement in recovery was observed when using MIP materials. Recoveries of 74 - 76 % were achieved for MIP materials, while non-MIP materials provided recoveries in the range of 64 - 67 %.

Commercial particles-based sorbent materials, including Luna C8, Luna C18, LiChroSorb RP-8, and LiChroSorb RP-18 were packed in 508 µm i.d. x 50 mm stainless-steel tube for in-tube solid phase micro extraction (in-tube SPME) (Morisue Sartore et al., 2022). In this work, the extraction required 250 µL of urine. Sample throughput was achieved for 3 samples per hour, and the in-tube SPME could be reusable over 150 times.

2.3.2.2 Disposable pipette extraction

Disposable pipette extraction (DPX) is widely used for the extraction of THC-COOH, as indicated in Table 2.2. Two different sorbents were employed for DPX which were weak anion exchange sorbent with salt (WAX-S) and divinyl benzene sorbent. Among these, DPX with WAX-S was the most widely method for THC-COOH extraction. The WAX sorbent was utilized for adsorbing the target analyte, while the salt was used to facilitate the salting-out process, aiding in the adsorption of the analyte onto the sorbent. The DPX was assembled with loose packing of the sorbent between two frits, allowing for the contact between the sample and the sorbent. It required slow aspiration and dispensing for several cycles.

In addition, divinyl benzene was also employed as sorbent for DPX sorbent. The reversed phase served as the main chromatographic mode for the extraction, which differed from the WAX-S method.

2.3.2.3 Commercial C18 tips

Commercial silica-based monolith with C18 functional group was ultilized for the extraction of THC-COOH in urine samples by Montesano et al (Montesano et al., 2014). Good recvoeries in the range of 80 - 82 % were observed.

CHAPTER III

MATERIALS AND METHODS

This chapter presents information and details regarding the materials and methods employed in this thesis. The chemicals and reagents, instruments and equipment, preparation of solutions, and experiments are comprehensively explained.

3.1 Chemicals and reagents

The chemicals and reagents utilized in this thesis are listed in **Table 3.1**.

Table 3.1 Lists of chemicals and reagents.

Chemical	Supplier	Country
1-Decanol	Signa-Aldrich	USA
1-Pentanol	Signa-Aldrich	USA
1,4-Butadiol	Signa-Aldrich	USA
2,2-Dimethoxy-2-phenylacetophenone (DMPAP)	Signa-Aldrich	USA
5-Hydroxyindoleacetic acid (5-HIAA)	Signa-Aldrich	USA
Acetonitrile (ACN)	Signa-Aldrich	USA
Activated charcoal (AC)	RCI-Labscan	Thailand
Bisphenol A (BPA)	Signa-Aldrich	USA
Butyl methacrylate (BMA)	Signa-Aldrich	USA
Disodium hydrogen phosphate	Signa-Aldrich	USA
Ethylene dimethacrylate (EDMA)	Signa-Aldrich	USA
Ethylene glycol	Signa-Aldrich	USA
Glycidyl methacrylate (GMA)	Signa-Aldrich	USA
Hydrochloric acid (HCl)	Signa-Aldrich	USA
Isoamyl alcohol	Signa-Aldrich	USA
Methacrylic acid (MAA)	Signa-Aldrich	USA

Table 3.1 Lists of chemicals and reagents (Continued).

Chemical	Supplier	Country
Methanol (MeOH)	RCI-Labscan	Thailand
Pentaerythritol diacrylate monostearate (PEDAS)	Signa-Aldrich	USA
phospheric acid	Carlo Erbo	USA
Potassium dihydrogen phosphate	Carlo Erbo	USA
Serotonin	Signa-Aldrich	USA
Sodium hydroxide (NaOH)	Signa-Aldrich	USA
Stearyl methacrylate (SMA)	Signa-Aldrich	USA
Toluene	Qrec	New Zealand
Δ^9-tetrahydrocannabinol-9-carboxylic acid (THC-COOH) (Certified reference material, 100 ng mL^{-1} in MeOH, 1 mL)	Signa-Aldrich	USA

*Purity of all chemicals and reagents was purchased in the analytical grade.

3.2 Instrumentations

The details for the instruments and equipment used are listed in the table below.

Table 3.2 Instruments and apparatus.

Instrument/Apparatus	Model	Supplier	Country
12 position SPE manifold	Chromabond®	Lubitech technology	USA
20-µL sample loop injector	Model 7725i Rheodyne™	Thermo Fisher Scientific	USA
Analytical balance	AB 104-S	Metter Toledo	USA
C18 SPE cartridge	Vertipak™ (C18, 50 mg)	Vertical®	Thailand
C18 SPE cartridge	SampliQ (C18, 500 mg)	Agilent	USA
C18 SPE cartridge	AccuBond II (C18, 500 mg)	Agilent	USA

Table 3.2 Instruments and apparatus (Continued).

Instrument/Apparatus	Model	Supplier	Country
Carbon and hydrogen analyzer	TruSpec Micro	LECO	USA
eDAQ data processing system	Model ET120	eDAQ	Australia
Fourier Transform Infrared Microscope Spectrophotometry (FT-IR)	TENSOR 27-Hyperrion	Bruker	USA
Hot air oven	Model UF 30	Memmert	Germany
HPLC column	BDS Hypersil™ C18 (150 mm x 4.6 mm, 5 μm)	Thermo Fisher Scientific	USA
HPLC pump	Model 515	Water	USA
Nitrogen adsorption-desorption analyzer	3 Flex instrument	Micromeritics	USA
pH meter	827 pH Lab	Metrohm	Natherlands
Polypropylene (PP) pipette tip	epT.I.P.S®	Eppendorf	Germany
Potentiostat	Autolab PGSTAT302N	Metrohm	Natherlands
Scanning electron microscopy (SEM)	Auriga®60 microscope	Zeiss	Germany
UV lamps	15 W	Osram	Germany
UV-visible detector	Model 785A	PerkinElmer	USA
Vacuum pump	ChemVal V300	Wiggens	China

3.3 Preparation of solutions and experiments for Part I: investigation of monolith shrinkage and surface modification of PP pipette tips for anchoring methacrylate monoliths and activated charcoal composite monoliths for µ-SPE

The method of solution preparation and experiment for Part I are descripted as follows:

3.3.1 Chemical preparation

3.3.1.1 Preparation of buffer solutions

20 mM phosphate buffer pH 2.0 and 7.0 were prepared by dissolving 123 µL of phosphoric acid and 0.2772 g of potassium dihydrogen phosphate in DI water. Subsequently, 1 M NaOH was added to adjust the pH, and the volume was made up to 100.00 mL in volumetric flasks.

3.3.1.2 Preparation of standard BPA, 5-HIAA, and serotonin

Stock standard solutions of BPA, 5-HIAA, and serotonin at a concentration of 1000 ug mL^{-1} were prepared by weighing 0.0100 g of the pure standard BPA, 5-HIAA, and serotonin. The volume was then made up to 10.00 mL with MeOH in volumetric flasks.

Working solutions of BPA, 5-HIAA, and serotonin were prepared by diluting the prepared stock solutions with DI water for BPA and serotonin and 20 mM phosphate buffer at pH 2.0 for 5-HIAA.

3.3.1.3 Preparation of pre-polymerization solutions of methacrylate monoliths and AC composite monoliths

The compositions of the synthesis of SMA-co-EDMA, BMA-co-EDMA, MAA-co-EDMA, GMA-co-EDMA, and PEDAS-co-EDMA monoliths were adopted from previous works (Ar-sanork et al., 2021; Jiang, Smith, David Ferguson, and Robert Taylor, 2007; Ohyama, Horiguchi, Kishikawa, and Kuroda, 2011; Okanda and El Rassi, 2005; Tian et al., 2008). The pre-polymerization solutions consisted of functional monomers (SMA, BMA, GMA, MAA, and PEDAS), crosslinking monomer (EDMA), porogenic solvent, and photoinitiator (DMPAP) (chemical structures of SMA, BMA, MAA, GMA, and PEDAS monomer are shown in **Figure 3.1**). The optimum ratio of functional monomer to

porogenic solvent was adopted from our previous work at 18 : 82 % (w/w) (Ar-sanork et al., 2021).
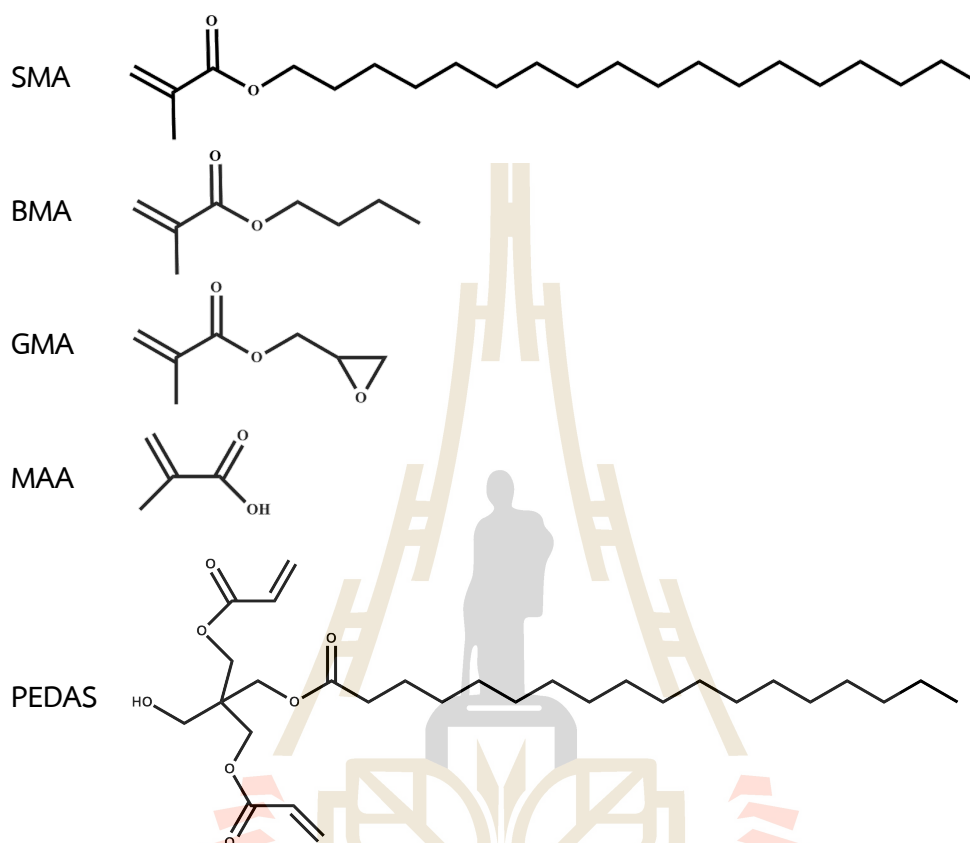
Figure 3.1 Chemical structures of SMA, BMA, GMA, MAA, and PEDAS monomers.

The influence of the EDMA crosslinker on shrinkage was examined for various monomer to EDMA ratios, including 10 : 90, 50 : 50, and 60 : 40 w/w. The compositions and weights are detailed in **Table 3.3**. The monomer, crosslinker, porogens and initiator were accurately weighed in cleaned glass vials. Subsequently, the mixtures were vortexed at room temperature, with the exception of the PEDAS-co-EDMA monolith, which was heated at 60 °C.

For the AC composite monolith, the AC powder was dispersed and homogenized within the pre-polymerization solutions of SMA-EDMA to attain an AC powder content of 1 % w/w.

Table 3.3 Weight of monomers, porogens, and initiator for preparation of pre-polymerization solutions.

	% w/w EDMA*	Weight (g) Monomer (18 % w/w)			Weight (g) Porogenic solvent (82 % w/w)			Initiator
					Formulation I			
		MAA	EDMA	-	Toluene	1-Decanol	-	DMPAP
MAA-co-EDMA	90	0.0182	0.1624	-	0.0990	0.7219	-	0.0022
(Ar-sanork et al.,	50	0.0911	0.0910	-	0.1000	0.7230	-	0.0024
2021)	40	0.1111	0.0770	-	0.0998	0.7215	-	0.0026
					Formulation II			
		PEDAS	EDMA	-	Ethylene glycol	1-Pentanol	Water	DMPAP
PEDAS-co-EDMA	90	0.0186	0.1820	-	0.1299	0.7096	0.0350	0.0025
(Okanda and El	50	0.0906	0.0950	-	0.1349	0.6971	0.0401	0.0025
Rassi, 2005)	40	0.1113	0.0765	-	0.1356	0.6605	0.0330	0.0024
					Formulation III			
		GMA	EDMA	-	1,4-Butadiol	1-Pentanol	-	DMPAP
GMA-co-EDMA	90	0.0266	0.1804	-	0.3436	0.4110	-	0.0020
(Jiang et al., 2007)	50	0.0900	0.0900	-	0.1656	0.2064	-	0.0022
	40	0.1108	0.0765	-	0.3391	0.4060	-	0.0024
					Formulation IV			
		BMA	EDMA	-	1,4-Butadiol	1-Pentanol	Water	DMPAP
BMA-co-EDMA	90	0.0190	0.1700	-	0.2532	0.4532	0.1085	0.0020
(Tian et al., 2008)	50	0.1002	0.1000	-	0.2460	0.4674	0.1102	0.0025
	40	0.0200	0.1700	-	0.2560	0.4564	0.1072	0.0021
					Formulation V			
		SMA	EDMA	-	Isoamyl alcohol	1,4-Butadiol	-	DMPAP
SMA-co-EDMA	90	0.0180	0.1620	-	0.6560	0.1640	-	0.0024
(Ohyama et al.,	50	0.0910	0.1002	-	0.6568	0.2004	-	0.0028
2011)	40	0.1322	0.0552	-	0.6536	0.1688	-	0.0024
		SMA	EDMA	AC	Isoamyl alcohol	1,4-Butadiol	-	DMPAP
AC-SMA-co-EDMA	90	0.0180	0.1620	0.0019	0.6560	0.1640	-	0.0024

**% EDMA in total monomer.

3.3.2 Experiments

The experiments for the first part included surface characterization, the surface modification procedure, *in situ* synthesis of monoliths in PP pipette tips, evaluation of dynamic breakthrough capacities of BPA, 5-HIAA, and serotonin, and HPLC-UV analysis.

3.3.2.1 Surface characterizations

To investigate the formation of the linking thin layer of EDMA on the PP inner tip wall, the morphology and attachment of the monoliths in the PP tips were investigated by SEM technique. SEM experiment was carried out at an acceleration voltage of 3 kV. Cross sectional cut of the synthesized IT monoliths was performed approximately 4 mm from the narrow tip end. Subsequently, the samples were mounted on a brass stub using silver paint and subjected to gold sputtering for 5 min.

To investigate the adsorption of DMPAP on the inner tip wall, the DMPAP-treated and untreated PP tips were cut into 2 mm x 2 mm pieces. The examination was performed using the FT-IR technique in attenuated total reflectance (ATR) mode, in the wavenumber of 400 - 4000 cm^{-1}, with a resolution of 4 cm^{-1} and scan time of 64 scans.

Surface area and average pore size diameter assessments for the materials were conducted through a nitrogen adsorption-desorption isotherm at 393 K. The samples were heated for 3 hours under vacuum to eliminate any adsorbed components. The surface area was calculated using the Brunauer-Emmett-Teller (BET) equation for P/P_0 ranging from 0.05 to 0.2. Average pore size was derived from the desorption part of the isotherm using the Barrett-Joyner-Halenda (BJH) equation.

The carbon and hydrogen contents of the synthesized monoliths were determined by precisely weighing approximately 0.2003 - 0.2008 g of the materials in aluminum cups. Subsequently, the samples were introduced into the loading head of the elemental analyzer and heated at 950 °C for 10 min.

3.3.2.2 Surface modification procedure

The schematic diagram for the PP pipette tip surface modification is illustrated in **Figure 3.2**. The PP pipette tips was initially rinsed with MeOH. After drying, the narrow ends were securely sealed with Parafilm®. A 40 µL solution containing 15

% (w/w) DMPAP in MeOH was introduced into the sealed PP tips and allowed to remain for 10 min to facilitate DMPAP adsorption, thereby creating the initiator surface on the PP tips (see **Figure 3.2, step I**). Subsequently, the DMPAP solution was removed, and the tips were subjected to drying in an oven at 40 °C for 5 min.

In the second step, a linking thin layer of EDMA was established. The treated-DMPAP tips were filled with 40 μL of methanolic EDMA solution. The concentrations of EDMA were optimized. To initiate the polymerization of the EDMA, the tips were exposed to UV light at 365 nm for 5 min. Pressure was then applied to the top of the tip using a micro pipettor to remove excess solid EDMA, leaving behind a layer of EDMA on the inner surface of the tips (see **Figure 3.2, step II**). The modified PP tips were subsequently stored at room temperature until use.
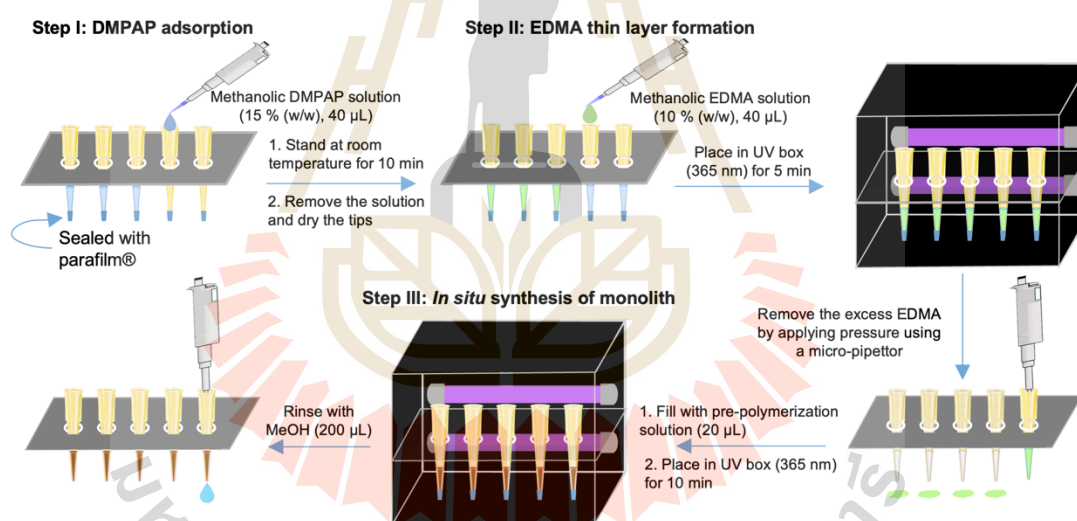
Figure 3.2 Schematic diagram of PP pipette tip surface modification and *in situ* synthesis of monoliths.

3.3.2.3 *In situ* synthesis of monoliths in PP pipette tips

The methacrylate monoliths and AC composite monoliths were *in situ* synthesized through photo-polymerization in both unmodified and modified PP tips. A 40 μL of pre-polymerization solution was accurately pipetted into the 200 μL and 1 mL modified PP pipette tips, which were sealed at the narrow end with Parafilm®,

while 200 μL of the pre-polymerization solution was used for the 5 mL modified tips. The tops of the tips were sealed with Parafilm® and exposed to UV light at 365 nm for 10 min to initiate the polymerization reaction of the monoliths. After the polymerization, the monoliths were rinsed with 200 μL MeOH to eliminate unreacted components, and the monoliths in pipette tips were then stored at room temperature until use (see **Figure 3.2, step III**).

For the synthesis in the unmodified tips, the bare PP tips were cleaned with MeOH, dried, and their tip ends were sealed with Parafilm® before the *in situ* synthesis of the monoliths.

3.3.2.4 Mechanical strength test

To assess mechanical strength of the monolith in pipette tips, MeOH was manually flowed through the monolith by using a micro-pipettor.

The success rate of the preparation of the fabricated IT monoliths was determined by assessing whether the monoliths allowed MeOH to flow through with a micro-pipettor and exhibited no detachment during the process.

3.3.2.5 Evaluation of dynamic breakthrough capacity of BPA, 5-HIAA, and serotonin

The extraction performances of the synthesized methacrylate monoliths and AC composite monolith were assessed through dynamic breakthrough capacity. Five methacrylate monoliths with a monomer : EDMA ratio of 10 : 90 w/w and AC composite monolith containing 1 % w/w AC in the pre-polymerization of SMA : EDMA at 10 : 90 w/w were used to evaluate breakthrough capacity. The monoliths were initially conditioned with 200 μL MeOH, followed by 20 μL of DI water. Subsequently, the monoliths were loaded with standard working solutions of BPA, 5-HIAA, and serotonin.

The standard solutions of 500 μL 5-HIAA (10 μg mL^{-1} in 20 mM PB pH 2.0), 500 μL serotonin (10 μg mL^{-1} in DI water), or 1.25 mL of BPA (200 μg mL^{-1} in DI water), were sequentially loaded onto the monoliths or composite monolith until achieving the breakthrough of the compounds. Following each loading, the eluates were analyzed using the HPLC-UV method.

3.3.2.6 HPLC-UV analysis

The chromatographic conditions were carried out under isocratic conditions. The optimum mobile phases were determined as 50 : 50 (v/v) ACN : H_2O for BPA, and 10 : 90 (v/v) MeOH : 20 mM phosphate buffer pH 7.0 for serotonin and 5-HIAA. The separations were performed at a flow rate of 1 mL min^{-1}, 20 µL injection volume, and absorbance detection at 210 nm.

3.4 Preparation of solutions and experiment for Part II: development of an ultra-sensitive and high-throughput analytical method using IT monolithic µ-SPE coupled with screen-printed graphene electrode sensor for the determination of urinary THC-COOH in forensic application

The preparation methods and experiment performing for Part II are described as follow.

3.4.1 Chemical preparation

3.3.4.1 Preparation of standard THC-COOH solution

The stock solution of THC-COOH, obtained from the certified reference material at a concentration of 100 µg mL^{-1} in MeOH. The stock was used to prepare working solutions by direct dilution the stock solution in an appropriate solution.

3.3.4.2 Preparation of buffer solutions

Solutions of 20 mM phosphate buffer pH 2.0, 7.0, and 10.0 were prepared by dissolving 123 µL of phosphoric acid, 0.2772 g of potassium dihydrogen phosphate, and 0.2839 g disodium phosphate in DI water. Adjustments to pH were made by adding 1 M NaOH or 1 M HCl, followed by making up the volume to 100.00 mL in volumetric flasks.

20 mM acetate buffer pH 5.0 was prepared by dissolving 116 µL glacial acetic acid in DI water before adjusting the pH with 1 M NaOH. The volume was then made up to 100.00 mL with DI water in volumetric flask.

3.4.2 Experiments

3.4.2.1 Fabrication of IT monolithic μ-SPE

1 mL PP pipette tips were modified as followed the PP surface modification method developed in the first part. The modified PP tips were used for synthesis of a SMA-co-EDMA monolith. The pre-polymerization solution, consisting of 0.0549 g SMA, 0.1266 g EDMA, 0.6563 g isoamyl alcohol, 0.1644 g 1,4-butadiol and 0.0020 g DMPAP was prepared in a cleaned glass vial and homogeneously mixed. A 40 μL of the pre-polymerization solution was accurately pipetted into the modified PP tip, which was sealed at the end with parafilm®. To prevent solvent evaporation, the top of the tip was sealed with Parafilm®. Polymerization was carried out by UV irradiation, keeping the tip in the UV box at 365 nm for 10 min. After the polymerization, the remaining reagents were washed with 400 μL MeOH and kept dry until use.

3.4.2.2 Optimization of IT monolithic μ-SPE for the extraction of THC-COOH

To achieve a highly-selective and sensitive analysis method for THC-COOH, μ-SPE conditions were systematically investigated. The IT monolith was conditioned with 200 μL MeOH and 20 μL water to activate the functional surface. A 2.00 mL of standard solution of THC-COOH or urine sample was loaded to adsorb the target analyte. A 400 μL of washing solvent was applied to remove adsorbed interferences. Finally, eluting solvent was introduced to desorb the THC-COOH. The eluate was subjected to the HPLC-UV method. To obtain a suitable μ-SPE condition, sample loading pH, ACN concentration of washing solvent, ACN concentration and volume of eluting solvent were optimized. The procedure for the IT monolithic μ-SPE is shown in **Figure 3.3**.
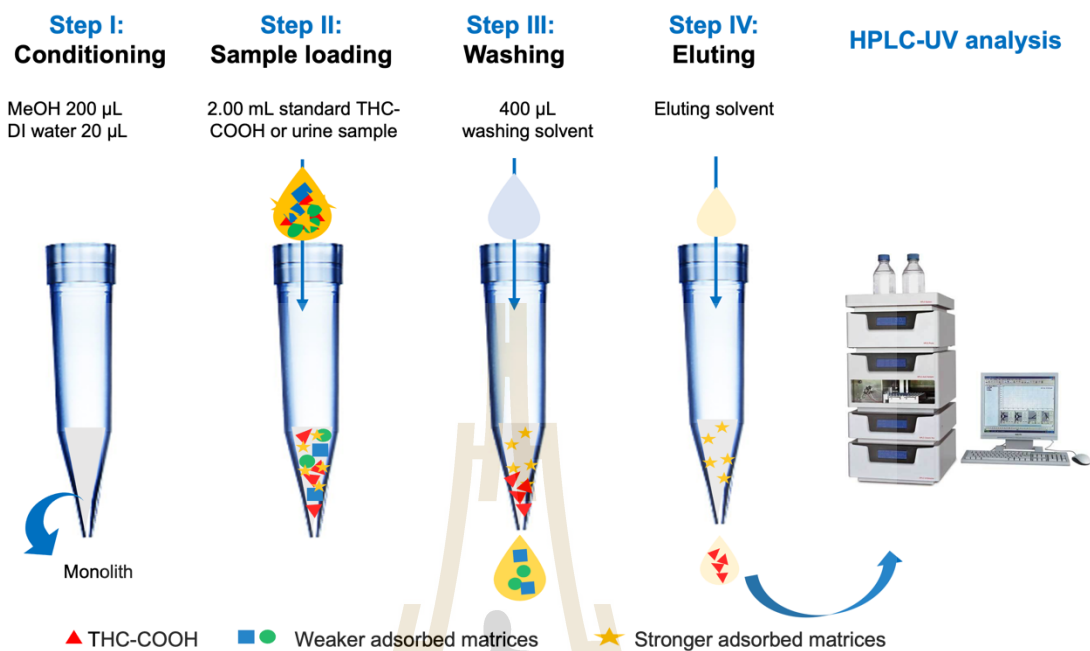
Figure 3.3 The optimization of IT monolithic μ-SPE condition.

3.4.2.3 HPLC-UV analysis

The separation was performed on C18 column with the optimum mobile phase of 60 : 40 (v/v) ACN : 20 mM acetate buffer pH 5.0. The separation condition was carried out at flow rate of 1 mL min^{-1}, injection volume of 20 μL, and absorbance detection at 210 nm.

3.4.2.4 Optimization of screen-printed graphene electrode sensor method for the detection of THC-COOH

The screen-printed graphene electrode (SPGE) was connected to the potentiostat via an electrical connector. For the measurement, 45 μL of the sample solution was directly dropped onto the sensing area before running the cyclic voltammetry (CV) or square wave voltammetry (SVW). CV measurements were conducted by applying voltage between -0.4 and +0.6 V at a scan rate of 50 mV s^{-1} to study THC-COOH electrochemical behavior. Meanwhile, SWV was utilized for highly sensitive quantitative determination of THC-COOH with a potential range between -0.4 to +0.6 V. The SVW parameters, including step potential, amplitude, and frequency were optimized.

3.4.2.5 Operation of parallel IT monolithic μ-SPE coupled with SPGE sensor for the determination of THC-COOH in human urine samples.

The determination of THC-COOH in human urine samples were conducted using a parallel IT monolithic μ-SPE coupled with SPGE sensor. A parallel IT monolithic μ-SPE system was assembled using 12-positions SPE manifold with a vacuum pump, as shown in **Figure 3.4**.
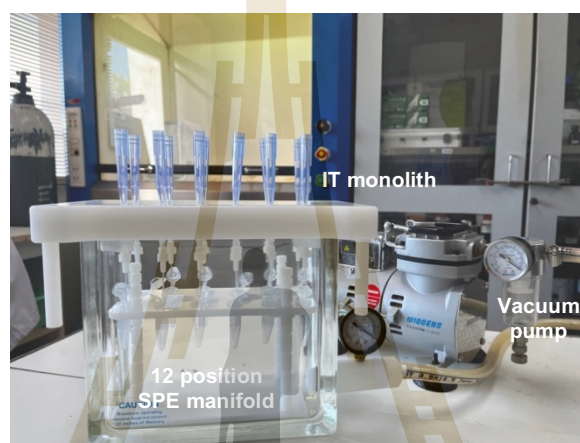
Figure 3.4 A parallel IT monolithic μ-SPE system comprising the fabricated IT monoliths, 12 positions SPE manifold and vacuum pump.

Twelve samples were simultaneously extracted by manually loading samples at the top of the IT monoliths using a micro-pipettor. Simultaneously, the μ-SPE was performed by applying negative pressure using a vacuum pump. Optimal washing and elution conditions were applied to achieve cleanup and pre-concentration.

For the detection, the extracted samples were completely dried by purging with N_2 gas before reconstitution with an appropriated supporting electrolyte. A 100 μL aliquot of the supporting electrolyte was added into the vial and then vortexed for 30 s to ensure complete dissolution. A 45 μL aliquot of reconstituted sample was dropped into the sensing area of SPGE for the analysis.

3.4.2.6 Method validation

Method validation was carried out following the Scientific Working Group for Forensic Toxicology (SWGTOX) guidelines (SWGTOX, 2013), encompassing linearity, accuracy, precision, specificity, selectivity, matrix effect, limit of detection (LOD), limit of quantitation (LOQ), as well as pre-concentration factor and % extraction efficiency.

3.4.2.6.1 Linearity, LOD, and LOQ

A calibration curve was established from five concentration levels: 10, 25, 50, 125, and 250 ng mL^{-1}. Linearity was assessed using the correlation coefficient (r^2).

LOD and LOQ were defined as concentrations that corresponding to a signal-to-noise ratio (peak height/noise signal) of 3 and 10, respectively.

3.4.2.6.2 Selectivity and specificity

Selectivity was examined by analyzing pooled negative blank urine samples (n=10 samples), while specificity was evaluated through the analysis of three urine samples containing positive drugs. The samples are listed in **Table 3.4**.

Table 3.4 List of positive abused drugs in urine samples screening by immunoassay strip test.

Sample	Screened drug				
	THC-COOH	MET	MDMA	K	Mitra
Sample-1[a]	-	-	-	-	-
Sample-2	-	+	+	+	+
Sample-3	+	-	-	-	-
Sample-4	+	-	-	-	-

[a]Pooled negative urine samples (n=10); MET: Methamphetamine; MDMA: 3,4-Methyl enedioxy methamphetamine; K: Ketamine; Mitra: Mirtazapine.

3.4.2.6.3 Accuracy

Accuracy was determined through % recovery of spiked samples at three concentration levels: 25, 50, and 125 ng mL^{-1}. % Recovery was calculated using the formular:

$$\text{Recovery (\%)} = \left(\frac{C_{\text{spiked sample}} - C_{\text{non-spiked sample}}}{C_{\text{standard added}}}\right) \times 100$$

Where $C_{\text{spiked sample}}$ is the concentration of THC-COOH from the spiked urine sample, $C_{\text{non-spiked sample}}$ is the concentration of THC-COOH from the non-spiked urine sample, and $C_{\text{standard added}}$ is the concentration of added THC-COOH.

3.4.2.5.4 Precision

Method precision was investigated by determining THC-COOH concentration at three levels: 25, 50, and 125 ng mL^{-1} in five-replicate analyses. Precision was expressed as the % coefficient of variance (% CV) using the formular:

$$CV\ (\%) = \frac{Standard\ diviation\ of\ determined\ concentration}{average\ of\ determined\ concentration} \times 100$$

3.4.2.6.5 Reusability

Reusability was assessed by repeating the extraction of 125 ng mL^{-1} standard THC-COOH under the optimum conditions for 10 times, and the results were reported in terms of % RSD.

3.4.2.6.6 Matrix effect

Matrix effect was evaluated by comparing the slope ratio of the target analyte constructed in DI water and matrix urine samples.

3.4.2.6.7 Pre-concentration factor and % extraction efficiency

The pre-concentration factor and % extraction efficiency were calculated using the following formular:

$$\text{Pre} - \text{concetration factor} = \frac{C_2}{C_1}$$

$$\% \text{ Extraction efficiency } = \left(\frac{C_2 V_2}{C_1 V_1}\right) \times 100$$

Where C_1 is the concentration of THC-COOH before extraction (ng mL^{-1}), C_2 is the concentration of THC-COOH after extraction (ng mL^{-1}), V_1 is the volume of the loading sample (mL) and V_2 is the volume of the eluting solvent (mL).

3.4.2.7 Human urine sample collection and pretreatment

Negative urine samples were collected from 10 healthy volunteers and pooled in disposable polypropylene tube. Three urine samples containing positive drugs were collected and screened for contained drugs by the Institute of Forensic Medicine, Thailand. Ethical approval of the use of human samples was obtained from the Institutional Review Board Committee-Police General Hospital, Thailand (IRB-PGH) (PGH-EC-05). The urine samples were stored in -20 °C util analysis.

Basic hydrolysis was performed to cleave THC-COOH-Glu to THC-COOH by adding KOH (10 M, 100 μL) to the urine sample (1000 μL). The mixture was vortexed for 30 s and incubated in a hot water bath at 60 °C for 15 min. After the incubation, the sample was cooled at room temperature before adjusting the pH by adding glacial acetic (160 μL) and making up the volume to 2.00 mL with 50 mM phosphoric acid (final sample pH was 2-3). The hydrolyzed urine sample was filtered through 0.22 μm nylon syringe filter before preforming the IT monolithic μ-SPE.

CHAPTER IV

RESULTS AND DISCUSSION

This thesis comprehensively investigated the fabrication of IT monolith and its μ-SPE application. This chapter consists of two main parts, the first part involves investigation of monolith shrinkage and surface modification of PP pipette tips for anchoring of methacrylate monoliths and activated charcoal composite monoliths. In the second part, the fabricated IT monolithic μ-SPE coupled with SPGE sensor was developed for the determination of THC-COOH in human urine samples. The developed method was fully validated according to the SWGTOX guidelines and applied for forensic applications.

4.1 Part I: Investigation of monolith shrinkage and surface modification of PP pipette tips for anchoring methacrylate and activated charcoal composite monoliths

PP pipette tips, polymeric housing for fabrication of monolithic-based μ-SPE. Provide advantages for on-site use, resistance to various solvents, cost-effectiveness, non-fragility, and transparency. Moreover, their conical shape facilitates monolith molding, making them suitable for *in situ* synthesis of monoliths in the tips. However, the preparation of the monolith in PP tips is challenging, as detachment and gap formation between the synthesized monoliths and the tip wall are frequently observed due to the shrinkage of the monoliths during the polymerization and drying process (Burke and Smela, 2012; Stachowiak et al., 2003). Basically, monolith shrinkage and detachment can be avoided by synthesizing the monoliths with a high degree of crosslinking. Nevertheless, this limits the composition adjustment, and the high crosslinking, resulting in low permeability and limited number of functional sites on the materials.

4.1.1 Investigation of methacrylate monoliths *in situ* synthesized in unmodified PP pipette tips

To gain a clear understanding of the factors affecting the shrinkage and detachment of the monoliths from PP pipette tips, the preparation of methacrylate monoliths in unmodified PP pipette tips were investigated.

The shrinkage and detachment of five different common methacrylate-based monoliths were examined. Five different methacrylate monoliths were *in situ* synthesized in unmodified PP tips through photo-assisted polymerization. Functional monomers, including SMA, BMA, GMA, PEDAS, and MAA were employed, and were co-polymerized with the common crosslinker, EDMA. Chemical structures of the five functional monomers are illustrated in **Figure 3.1**. Reversed-phase property was obtained from SMA-co-EDMA (C18) and BMA-co-EDMA (C4) monoliths. The GMA-co-EDMA monolith containing functional group of epoxy ring, allowed for further functionalization. Mixed mode interactions were observed with PEDAS-co-EDMA, which contained a hydrophobic chain of C17 and a hydrophilic -OH group (hydroxyl group). MAA-co-EDMA monolith presented weak acid group of -COOH (carboxyl group).

The effect of crosslinking monomer content, EDMA, was evaluated. The content of EDMA was varied by adjusting changing the ratio of functional monomer to EDMA, with ratios of 10 : 90, 50 : 50, and 40 : 60 % w/w.

At % EDMA of 90 % w/w, white rigid monoliths were successfully formed inside the PP tips, with % preparation success rate ranging from 40 - 100 % (**Table 4.1**). Photographs of the formed monoliths in unmodified tips are shown in **Figure 4.1.** Significant decrease in % success rate was observed when % EDMA was reduced to 50 and 40 % (w/w), as shown in **Table 4.1**. Detachment of the monoliths from PP tips occurred when % EDMA was decreased to 40 % w/w, resulting in a 0 % preparation success rate, except for the GMA-co-EDMA monolith, which still achieved a good preparation success rate of 80 %.
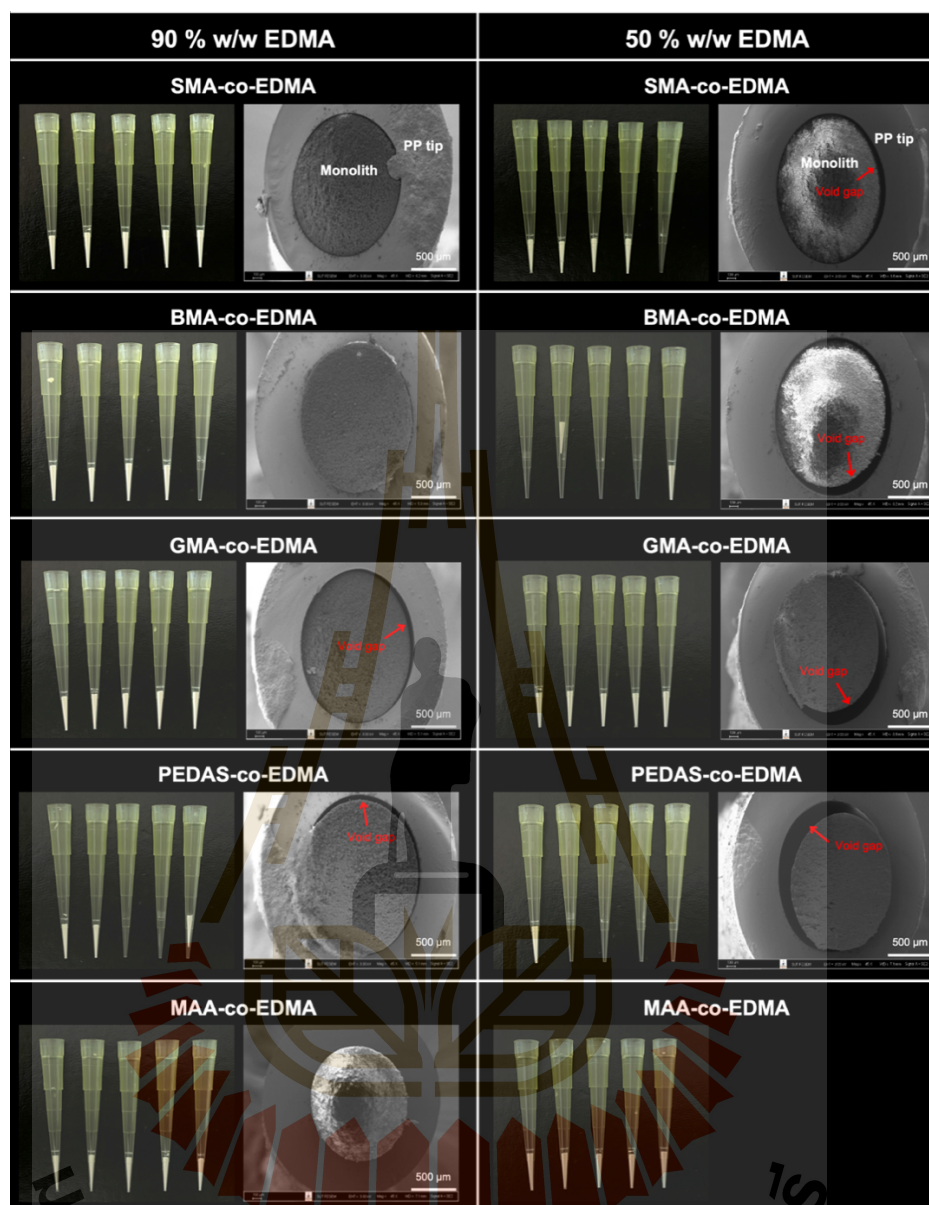
Figure 4.1 Representative photographs and SEM images at magnification of 45x of the synthesized methacrylate monoliths in unmodified PP tips at % EDMA of 90 % w/w and 50 % w/w. The MAA-co-EDMA monolith at 50 % w/w EDMA were not measured as they were not permeable.

Table 4.1 Percent of preparation success rate for synthesis of monoliths in unmodified and modified PP pipette tips with different % EDMA (n=40 tips).

Monolith	Success rate of IT monolith preparation (%)					
	Unmodified PP tip			Modified PP tip		
	% EDMA (w/w)*			% EDMA (w/w)*		
	90 %	50 %	40 %	90 %	50 %	40 %
MAA-co-EDMA	100	0	0	100	0	0
PEDAS-co-EDMA	40	20	0	100	100	100
GMA-co-EDMA	100	100	80	100	100	100
BMA-co-EDMA	80	10	0	100	100	100
SMA-co-EDMA	100	50	0	100	100	100
AC-SMA-co-EDMA	0	0	0	100	100	100

*% w/w EDMA in total monomer

SEM images were employed to observe morphology of the prepared monoliths in PP tips. The monoliths were fully formed inside the PP tips, with small gabs between the monolith and tip observed when % EDMA was 90 %. Large void spaces between the monolith and tip wall were observed when % EDMA was equal to or lower than 50 % w/w (see SEM images in **Figure 4.1**). It should be noted that the synthesized MAA-co-EDMA monolith at 50 % w/w EDMA were not measured using SEM as they were not permeable.

Interestingly, the GMA-co-EDMA monolith exhibited the most effective retention in the PP tips. This may be attributed to relatively weak intermolecular-forces between the polymer chains of the epoxy group, resulting in minimal shrinkage and detachment. Predicted intermolecular-force are illustrated in **Figure 4.2**. In contrast, detachment of the SMA-co-EDMA, BMA-co-EDMA, and PEDAS-co-EDMA monoliths was primarily influenced by the content of EDMA. When considering their structural properties, it is noteworthy that the hydrophobic groups of SMA (C18) and BMA (C4) contributed to strong inter-forces between the polymer chains through hydrophobic interactions (see **Figure 4.2**). Additionally, the PEDAS-co-EDMA monolith features both long hydrocarbon chain (C17) and -OH (hydroxyl group), contributing to strong

interactions among the functional groups through a combination of hydrophobic interactions (between C17 chains) and H-bonding (between -OH groups) (see **Figure 4.2**).
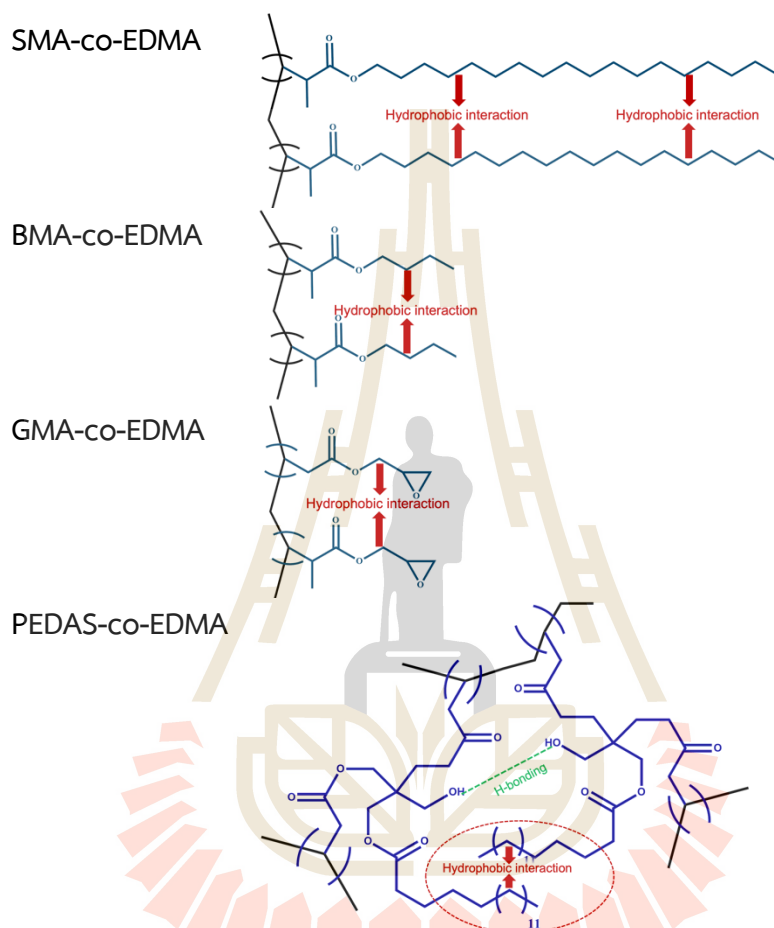
Figure 4.2 Predicted intermolecular-forces between the polymer chains in the synthesized monoliths.

The effect of the porogenic solvent on the detachment of the monoliths from PP tips was explored for the BMA-co-EDMA monolith. Various porogenic solvent systems (the recipes of the porogenic solvent are detailed in **Table 3.3**). The results revealed that the choice of porogens did not have a significant impact on the retention of the monoliths in the PP tips (data not shown).

These investigations can be summarized as follows: the appearance of the large void space and detachment of monoliths resulted from the phenomena of monolith

shrinkage, which is influenced by both degree of crosslinking and type of functional monomers employed. This void space is a risk to poor extraction efficiency, as IT monolithic µ-SPE is commonly performed using the dynamic adsorption method. The occurrence of void space allows sample/solvent bypass instead of percolating through the materials. To eliminate detachment and void space, performing surface modification prior to anchoring monolithic materials is therefore necessary.

4.1.2 PP pipette tip surface modification and *in situ* synthesis of methacrylate monoliths in modified PP pipette tips

This thesis proposed a novel, simple, and straightforward surface modification method for PP pipette tips to anchor monolithic material against the tip wall, thus eliminating monolith detachment and void space. The approach consisted of the following three steps:

- **Step I:** Creating an initiator surface by adsorption of a photoinitiator, DMPAP.
- **Step II:** Forming a polymeric linking thin layer of EDMA.
- **Step III:** Anchoring the monolithic material against the linking thin layer-modified PP tip wall.

Chemical process of the proposed PP tip surface modification method and anchoring of the monolith in the modified tip is illustrated in **Figure 4.3**.

Step I: Creating an initiator surface
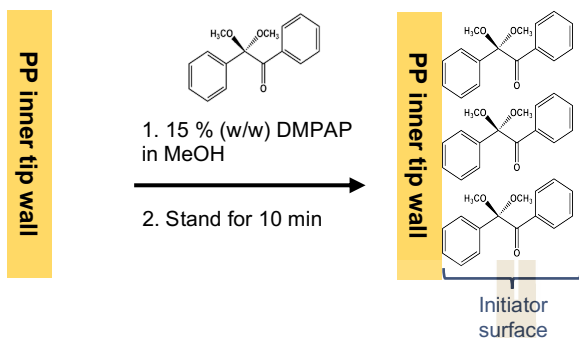
Step II: Forming a polymeric linking thin layer of EDMA
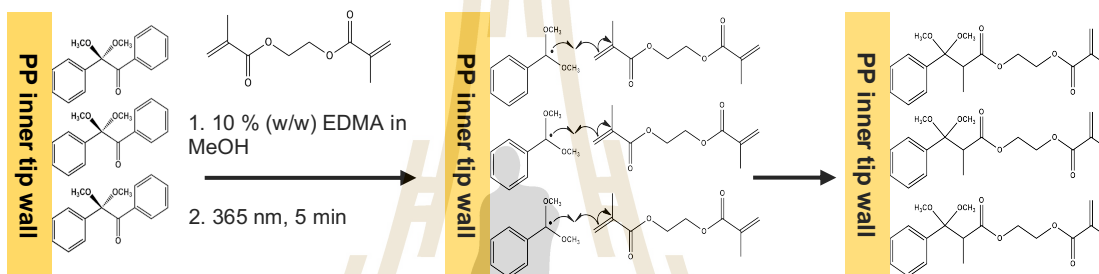
Step III: Anchoring of monolith with the linking thin layer-modified tip wall
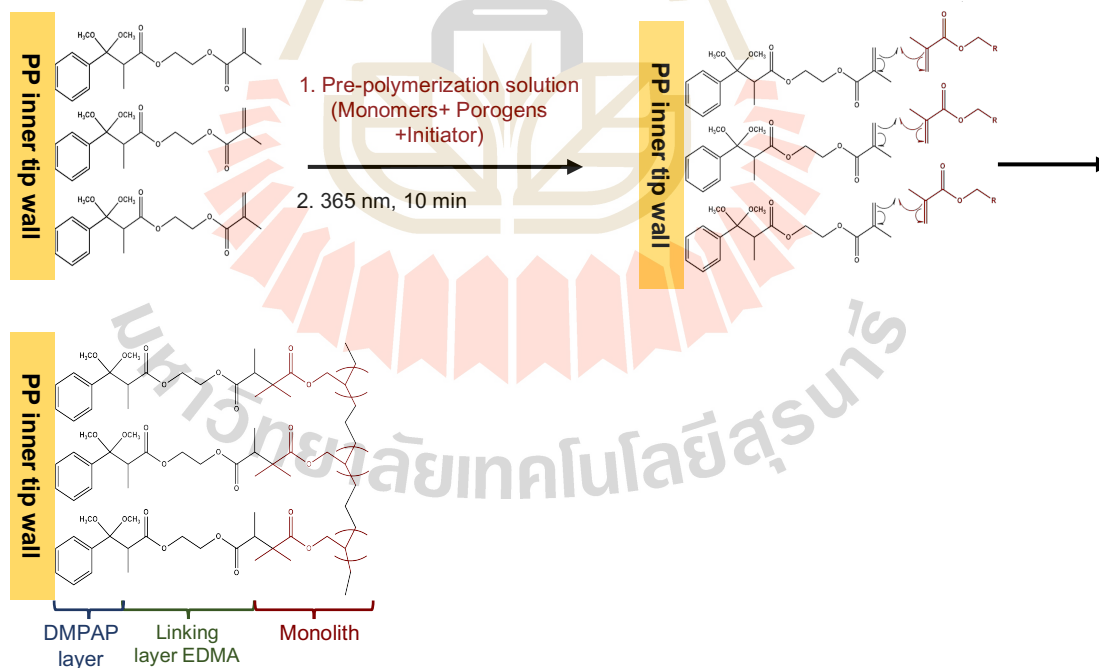
Figure 4.3 Chemical process of the proposed PP pipette tip surface modification method and anchoring of monolith in the modified tip.

Step I: Creating an initiator surface by adsorption of a photoinitiator, DMPAP.

DMPAP is a photoinitiator commonly used to initiate polymerization reactions by generating free radicals. The initiator surface of DMPAP was firstly created through the adsorption of 15 % (w/w) methanolic DMPAP on the PP tip wall for 10 min (see **Figure 4.3, step I**). The adsorption of DMPAP on the inner tip wall was investigated using FT-IR technique.

FT-IR spectra of untreated and DMPAP-treated PP tips are depicted in Figure 4.4, and absorption peaks are summarized in **Table 4.2**. The untreated PP tip indicated only the characteristic FT-IR peaks of PP-based material, as shown in **Figure 4.4(black line)** and **Table 4.2** (Gopanna, Mandapati, Thomas, Rajan, and Chavali, 2019). After treatment with 15 % (w/w) methanolic DMPAP for 10 min, the FI-IR spectrum demonstrated characteristic peaks of both the PP-based material and the adsorbed DMPAP, with adsorption peaks of aromatic rings, C-O, and C=O (carbonyl group) functional groups, confirming the successful adsorption of DMPAP on the PP tip wall (see **Figure 4.4(red line)** and **Table 4.2**) (Kaczmarek, Gałka, and Kowalonek, 2010).
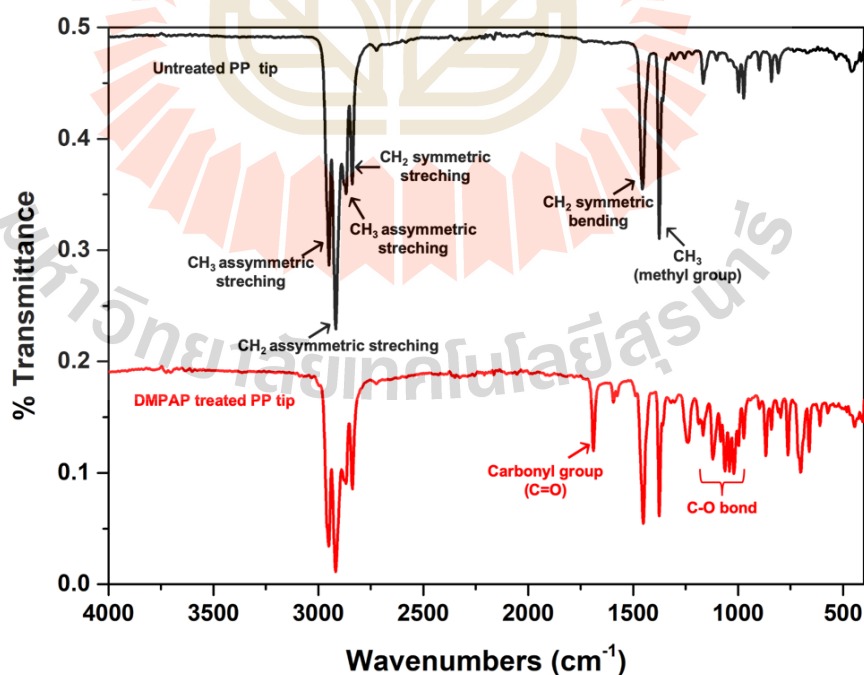
Figure 4.4 FT-IR spectrums of untreated and DMPAP treated-PP pipette tips.

Table 4.2 Characteristic FT-IR absorption peaks of untreated and DMPAP treated-PP pipette tips.

Characteristic peak	Wavenumber (cm^{-1})	Untreated PP tip	DMPAP treated PP tip
PP-based material characteristic peak			
-CH$_3$ asymmetric bending	2950	/	/
	2868	/	/
-CH$_2$ symmetric bending	1452	/	/
	2838	/	/
	2917	/	/
-CH$_3$ (methyl group)	1376	/	/
DMPAP characteristic peak			
Aromatic ring	1594	X	/
C-O	1000 - 1200	X	/
C=O	1690	X	/

Step II: Forming a polymeric linking thin layer of EDMA.

After achieving the initiator surface of DMPAP, a thin layer of linking polymer was subsequently formed on the DMPAP-treated PP tip wall. A divinyl monomer, EDMA, was selected and employed as a linking monomer to create the polymeric linking thin layer on the tip surface.

In this step, methanolic EDMA was introduced into the DMPAP-treated tip before being exposed to UV light at 365 nm for 5 min. During the irradiation, the coated DMPAP was excited and then cleaved, generating free radical surface (see **Figure 4.3, step II**). These generated free radicals then initiated the polymerization of the EDMA locally at the tip wall, resulting in the thin layer of linking polymer of EDMA on the PP tip wall (see **Figure 4.3, step II**).

The effect of EDMA concentration on the creation of the linking thin layer of EDMA was studied. Different methanolic EDMA concentrations of 10 %, 50 %, and 100 % w/w were varied. After the polymerization and removal of the excess solid polymer EDMA, turbid tips were observed when 10 % w/w EDMA in MeOH was used. The original

tips and modified PP tips with 10 % EDMA are shown in **Figure 4.5(a) and (b)**, respectively.
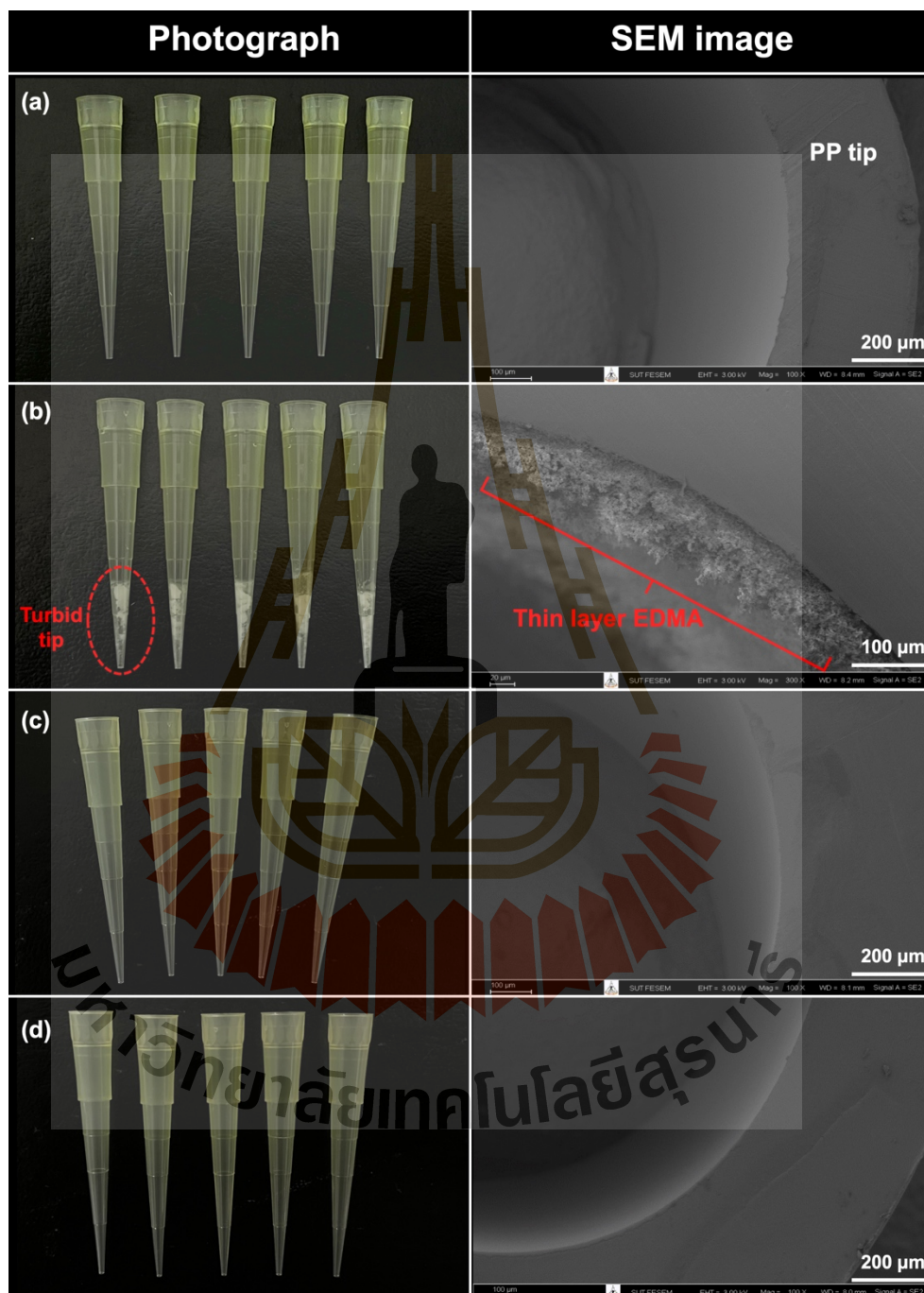
Figure 4.5 Photographs and SEM images of the original PP tip (a); and the modified PP pipette tips with 10 % (w/w) EDMA (b), 50 (w/w) EDMA (c), and 100 % (w/w) EDMA (d).

The formation of the polymeric thin layer of EDMA was confirmed by SEM images. The SEM image shown in **Figure 4.5(b)**, clearly demonstrates the attachment of the linking polymer of EDMA as a thin layer on the inner tip wall. However, when using 50 % and 100 % w/w EDMA, solid plug of EDMA polymer was obtained and detached from the tips.

Therefore, 10 % w/w EDMA in MeOH was selected as the optimum concentration for forming the linking polymeric thin layer of EDMA on the PP pipette tip.

Step III: Anchoring the monolithic materials against the linking thin layer-modified PP tip wall.

To evaluate the performance of the modified PP pipette tips, five common methacrylate monoliths (SMA, BMA, GMA, PEDAS, and MAA) were *in situ* synthesized in those modified tips. As shown in **Figure 4.6** (photographs), detachment of the five monoliths was completely eliminated, achieving 100 % preparation success rate (see **Table 4.1**). Excellent % preparation success rates were still achieved even when a low % crosslinker, EDMA of 50 % and 40 % w/w, were employed.

SEM images were used to investigate the void space and monolith shrinkage in the tips. As shown in **Figure 4.6**, SEM images demonstrated good attachment of the synthesized monoliths against the modified PP tip wall without void space and monolith shrinkage observed.
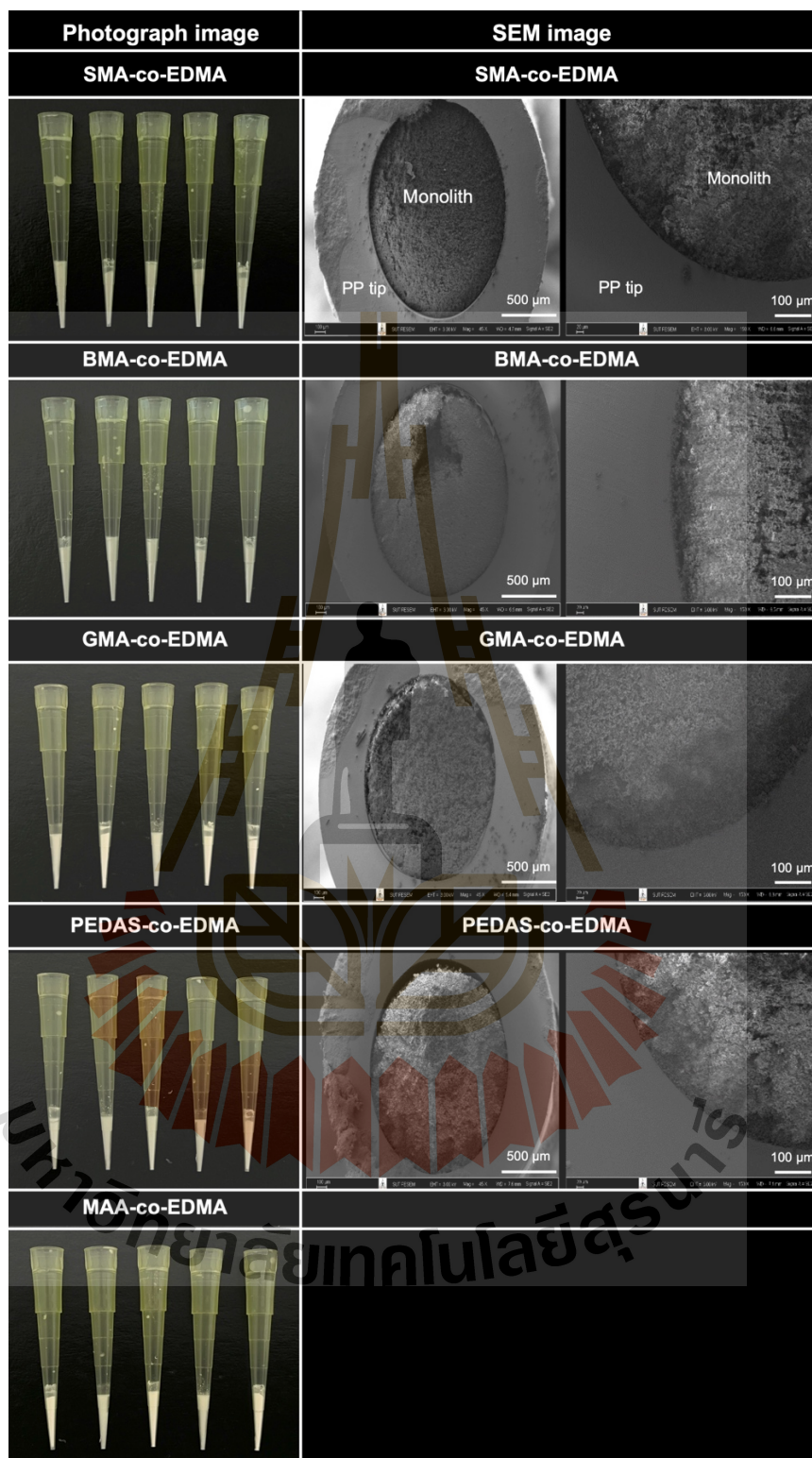
Figure 4.6 Representative photographs and SEM images at magnifications of 45x and 150x of the synthesized methacrylate monoliths with 50 % (w/w) EDMA in the modified PP pipette tips.

The elimination of monolith detachment, monolith shrinkage and void space can be attributed to two reasons: (i) the covalent bonding between the synthesized monoliths and the EDMA-modified surface of the PP tip wall. The polymerizable groups of EDMA (vinyl groups) were co-polymerized with the desired monolith, resulting in monolith anchoring (see **Figure 4.3, step III**), and (ii) the physical intertwining of the polymeric thin layer on the tip wall and a piece of the formed monolith.

The surface modification was successfully applied to all tip sizes commonly used in the laboratory. Representative BMA-co-EDMA monoliths synthesized in 200 µL, 1 mL, and 5 mL are shown in **Figure 4.7**.

Tip size: 5 mL 1 mL 200 µL

Figure 4.7 Photographs of representative fabricated BMA-co-EDMA monolith synthesized in 5 mL, 1 mL, and 200 µL modified-PP pipette tips.

Additionally, the mechanical strength of the IT monoliths was evaluated by drawing and dispensing MeOH through the monoliths using a micro-pipettor. The IT monoliths could withstand testing for at least 20 cycles without slipping out of the

materials, indicating the robustness of the IT monoliths and the efficiency of the proposed PP surface modification method.

4.1.3 Activated charcoal composite monoliths in modified pipette tips

Composite monolithic materials have been gaining significant attention to enhance their extraction efficiency and expand their applications. The extraction efficiency, selectivity, and capacity can be modified through the combination of monolithic-based materials with other solid materials, such as gold nanoparticles (Alwael et al., 2011), iron oxide nanoparticles (Krenkova and Foret, 2013), zeolite (Lirio, Fu, Lin, Hsu, and Huang, 2016), and AC (Huiqi Wang, Li, Niu, Ma, and Jia, 2015). The monoliths not only serve as a solid support but also facilitate the functionalization and dispersion of the composite materials. However, fabricating these composite monoliths in pipette tips for μ-SPE is complicated because the added material can reduce the adhesion between the monolith and the tip surface, resulting in detachment of the composite materials.

In this context, we applied the developed PP surface modification method to fabricate AC composite monoliths in pipette tip for μ-SPE. AC was employed with the aim of improving the functionality of the monolith. AC powder was added to the pre-polymerization solution of SMA-EDMA to create the AC-SMA-co-EDMA monolith. Without applying the surface modification, a 0 % preparation success rate was observed as the composite material completely detached from the tips (see **Table 4.1**). In contrast, the preparation success rate reached 100 % when our surface medication was applied prior to the composite monolith synthesis. Good attachment of the AC-SMA-co-EDMA could be observed, as illustrated in **Figure 4.8**.
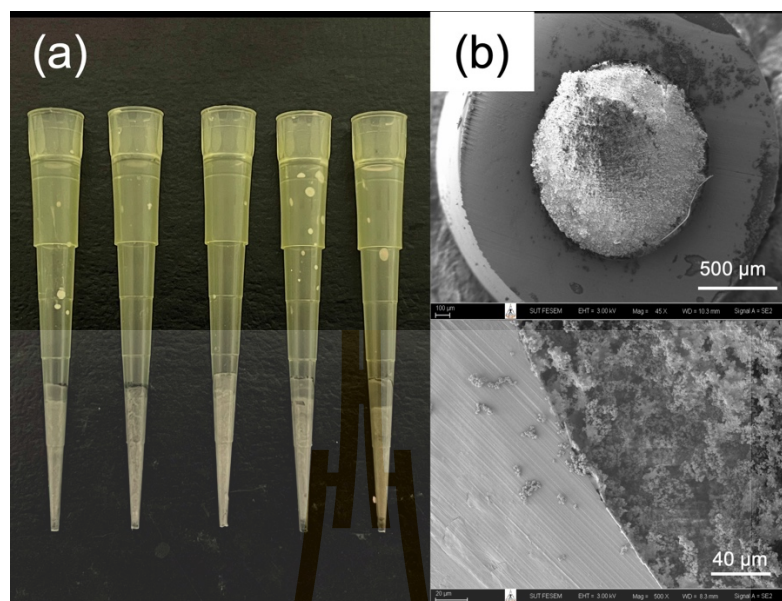
Figure 4.8 Representative (a) photographs and (b) SEM images (magnification of 45x (upper frame) and 150x (lower frame)) of the AC-SMA-co-EDMA synthesized in the modified PP pipette tips.

4.1.4 Characterization of the synthesized methacrylate monoliths and AC composite monoliths

By utilizing the proposed PP surface modification method, five different methacrylate monoliths and AC composite monoliths could be synthesized *in situ* in the PP pipette tips without detachment, void space, or shrinkage. In this section, physical properties, including morphology, surface area, pore volume, average pore diameter, carbon and hydrogen content of the synthesized methacrylate monoliths and AC composite monolith, were investigated.

The morphology of the synthesized monoliths was examined using SEM technique. SEM images, as shown in **Figure 4.9**, demonstrated the incorporation of microglubules leading to the formation of large clusters, resulting in a continuous monolithic structure. Due to the influence of the porogenic solvent, macropores could be clearly observed in the SEM images, contributed to the high permeability of the desired monoliths.
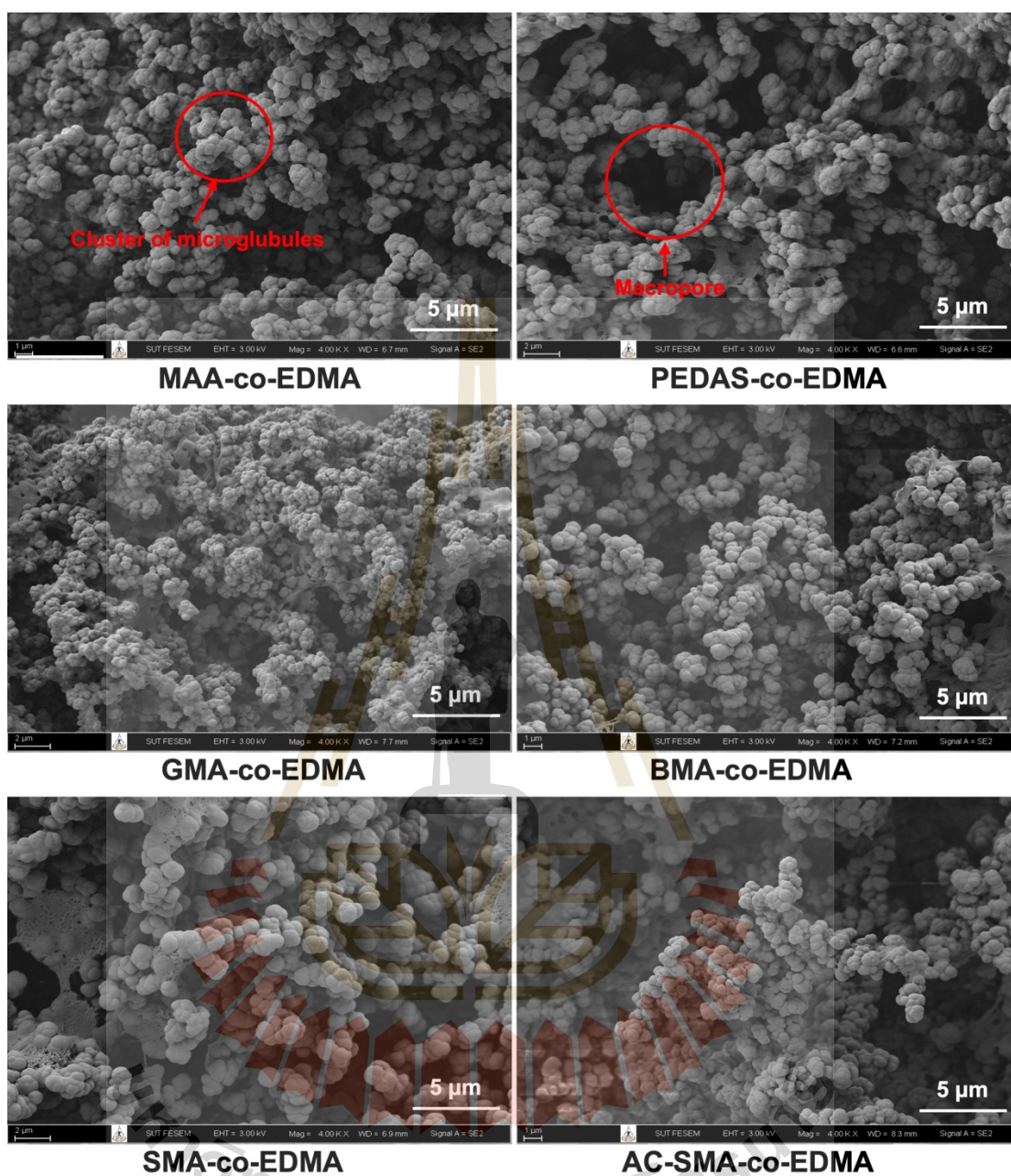
Figure 4.9 SEM images of five methacrylate monoliths (10 : 90 (w/w) functional monomer : EDMA) and AC composite monolith (1 % wt AC in pre-polymerization solution of SMA-EDMA (10 : 90 w/w)) *in situ* synthesized in the modified PP pipette tips.

The physical properties investigated are summarized in **Table 4.3**, indicating average pore diameters in the range of 29.5 to 46.3 nm, confirming the mesoporous

structure of the materials. The smallest microglublues were observed in the GMA-co-EDMA monolith, which also exhibited the smallest average pore diameter and the highest BET surface area and pore volume (see **Figure 4.9** and **Table 4.3**). Meanwhile, the other monoliths showed minor variations in their physical properties (see **Table 4.3**). Due to its favorable physical properties and the presence of the reactive functional group (epoxy ring), the GMA-co-EDMA monolith has been widely employed for further functionalization or modification.

Table 4.3 BET surface area, pore volume, average pore diameter, carbon and hydrogen content of the methacrylate monoliths and AC composite monolith.

Monolith	BET surface area (m^2/g)	Pore volume (cm^3/g)	Average pore diameter (nm)	C content (wt %)	H content (wt %)
MAA-co-EDMA*	10.4	0.034	33.9	35.2	9.6
PEDAS-co-EDMA*	7.9	0.057	46.0	34.7	6.9
GMA-co-EDMA*	35.7	0.179	29.5	39.8	6.7
BMA-co-EDMA*	10.0	0.063	46.3	34.8	6.8
SMA-co-EDMA*	11.7	0.124	41.9	36.5	10.4
AC-SMA-co-EDMA**	13.4	0.053	34.6	35.8	10.2

*The pre-polymerization composition was monomer : EDMA at 10 : 90 (w/w).
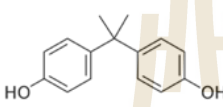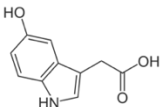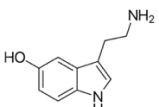
**The monolith containing 1 % wt of AC in the pre-polymerization of SMA : EDMA at 10 : 90 w/w.

4.1.5 Evaluation and comparison of dynamic breakthrough capacities of IT monolithic μ-SPEs and commercial SPE cartridges

Methacrylate monoliths have been commonly used for different chromatographic modes, such as reversed-phase, ion exchange, and hydrophilic interaction liquid chromatography (HILIC), as their chemical properties can be tailer-made by changing the functional monomer. In order to evaluate the capabilities of the fabricated methacrylate monoliths and composite monolith, dynamic breakthrough capacities were carried out. 5-HIAA, serotonin, and BPA were selected as

the tested model compounds. The structures of these compounds and breakthrough capacities are shown in **Table 4.4**.

Table 4.4 Breakthrough capacities of IT monolithic μ-SPEs and commercial SPE cartridges for the adsorption of BPA, 5-HIAA, and serotonin.

Type of SPE	Dynamic breakthrough capacity (mg per $g_{material}$ / mg per tip or cartridge)		
	BPA	5-HIAA	Serotonin
IT monolithic μ-SPE			
MAA-co-EDMA*	160.00 / 0.80	5.04 / 0.03	8.00 / 0.04
PEDAS-co-EDMA*	214.29 / 1.50	6.60 / 0.05	0.71 / 0.01
GMA-co-EDMA*	41.67 / 0.30	0.05 / 0.00	0.00 / 0.00
BMA-co-EDMA*	53.57 / 0.30	0.38 / 0.00	0.13 / 0.01
SMA-co-EDMA*	71.43 / 0.40	0.45 / 0.00	0.04 / 0.00
AC-SMA-co-EDMA**	232.14 / 1.30	7.50 / 0.04	0.00 / 0.00
Commercial SPE cartridge			
Vertipak™ C18	2.40 / 0.12	0.00 / 0.00	0.00 / 0.00
SampliQ C18	15.00 / 7.50	0.40 / 0.02	0.40 / 0.02
AccuBond II ODS-C18	11.00 / 5.50	0.40 / 0.02	0.40 / 0.02

*The pre-polymerization composition was monomer : EDMA at 10 : 90 (w/w).

**The monolith containing 1 % wt of AC in the pre-polymerization of SMA : EDMA at 10 : 90 w/w.

The capacities presented in **Table 4.4,** provided the great potential of the six monoliths for retaining the relatively low-polarity compound of BPA, confirming hydrophobic nature of the methacrylate monoliths.

Interestingly, higher retention of BPA was decreased from using the MAA-co-EDMA, PEDAS-co-EDMA, and AC-SMA-co-EDMA monoliths. When considering the structure of BPA and the surface functional groups of the monoliths, PEDAS-co-EDMA demonstrated a combination of hydrophobic characteristics due to the hydrocarbon chain (C17) and hydrophilic properties due to the hydroxyl group (-OH). MAA-co-EDMA

exhibited a weak acid with a carboxyl group (-COOH). These functional groups contributed to both hydrophobic interactions and H-bonding with BPA, thereby improving the adsorption capacities. Predicted interactions are illustrated in **Figure 4.10(a) and (b)**, respectively.
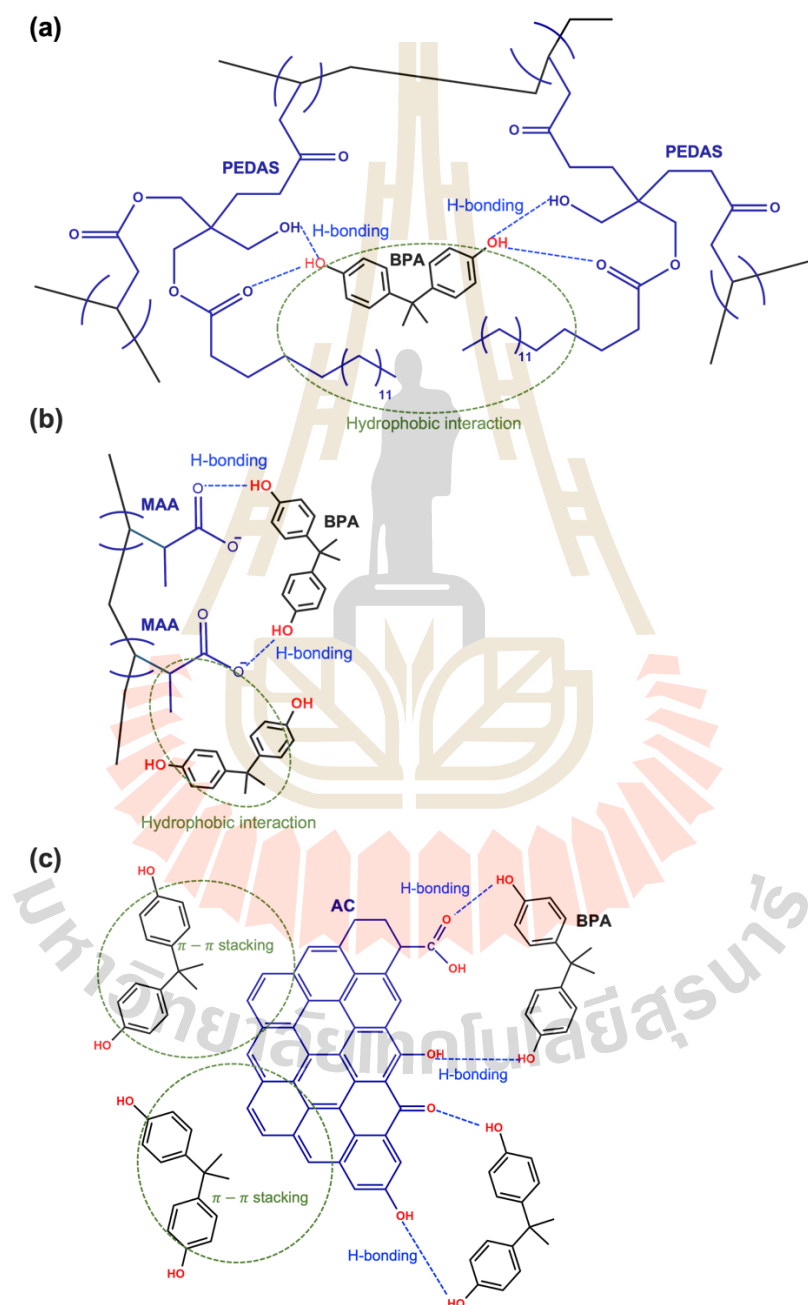
Figure 4.10 Predicted interactions between BPA and (a) PEDAS-co-EDMA, (b) MAA-co-EDMA, and (c) AC-SMA-EDMA monoliths.

Meanwhile, the AC-SMA-co-EDMA monolith contributed to hydrophobic interactions derived from π-π interactions involving the aromatic planar BPA and the planar sp$_2$-sheet of AC, as well as H-bonding, as depicted in **Figure 4.10(c)**.

As expected, poor retention for polar compounds, 5-HIAA and serotonin, was observed using the non-polar monoliths, GMA-co-EDMA, BMA-co-EDMA, and SMA-co-EDMA, as shown in **Table 4.4**. The presence of polar groups such as -COOH on the MAA-co-EDMA and -OH on the PEDAS-co-EDMA significantly enhanced the adsorption capacity of 5-HIAA. Moreover, the AC composite monolith exhibited the highest capacity for 5-HIAA. H-bonding and hydrophobic interactions were predicted as the main mechanisms for retaining 5-HIAA on the PEDAS-co-EDMA, MAA-co-EDMA, and AC-SMA-co-EDMA materials, as shown in **Figure 4.11**.
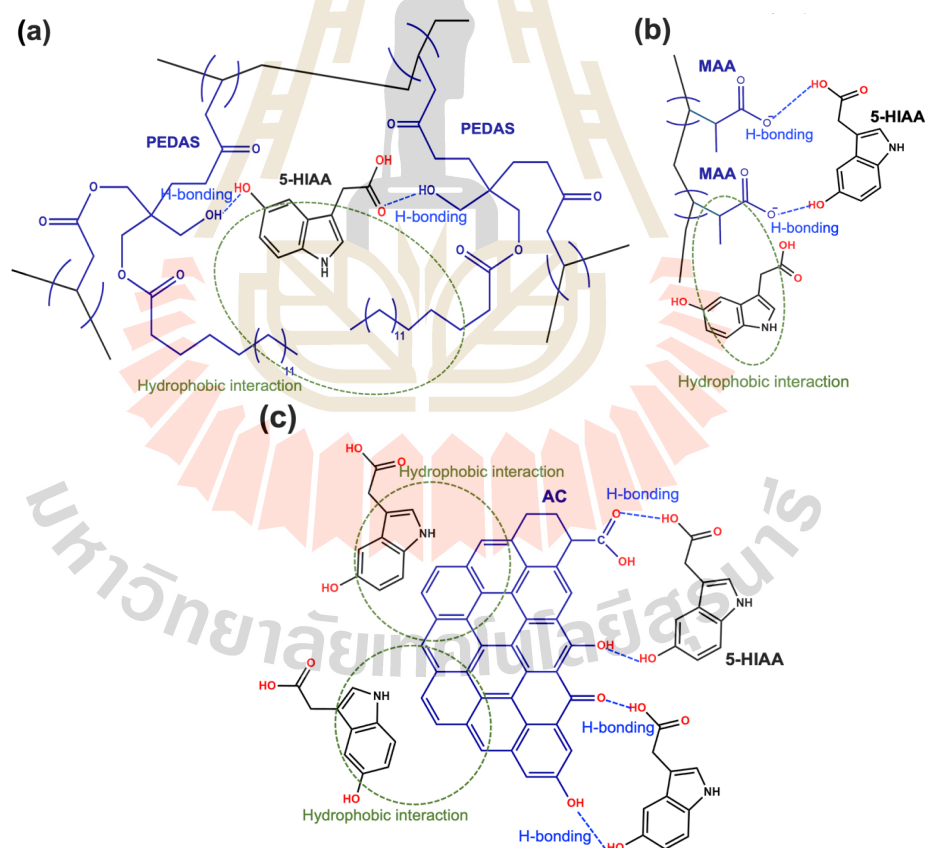
Figure 4.11 Predicted interactions between 5-HIAA and (a) PEDAS-co-EDMA, (b) MAA-co-EDMA, and (c) AC-SMA-EDMA monoliths.

Under neutral loading condition, the negatively charged monolith, MAA-co-EDMA, was the only sorbent capable of retaining the positively charged molecule, serotonin, via columbic interaction and H-bonding, as illustrated in **Figure 4.12**.
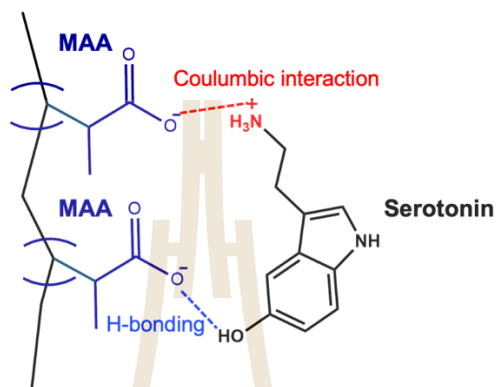
Figure 4.12 Predicted interactions between serotonin and MAA-co-EDMA monolith.

Three commercial packed C18 SPE cartridges from different manufacturers were also tested to compare their adsorption capacities with our IT monolithic μ-SPEs. These particle-based sorbents exhibited high adsorption capacity only for non-polar compound, BPA. However, it is important to note that the maximum capacity in mg per cartridge for commercial particle-based sorbents, such as SampliQ C18 and AccuBond II ODS-C18, is greater due to the larger quantity of sorbent contained within the cartridges. For applications involving samples with only small quantities of target compounds, the integrated monolith may be more suitable choice for the extraction.

4.2 Part II: IT monolithic µ-SPE coupled with screen-printed graphene electrode sensor for the determination of urinary THC-COOH in forensic applications

Urinary THC-COOH is commonly used as evident to identify cannabis consumption. Even though analytical methods are well established in laboratory-based techniques, miniaturized and portable THC-COOH sensor are not well developed. Complicated sample matrices and low analyte concentration are the main concerns for achieving an accurate and reliable method. Effective sample preparation is needed to enhance the selectivity and sensitivity of the analytical method.

In this part, an ultra-sensitive and high-throughput method was developed for the determination of urinary THC-COOH in forensic applications. A parallel IT monolithic µ-SPE was developed to cleanup and preconcentrate THC-COOH from human urine samples, prior to coupling with a simple and rapid SPGE sensor. Workflow of the developed method for the analysis of urinary THC-COOH is illustrated in **Figure 4.13**.
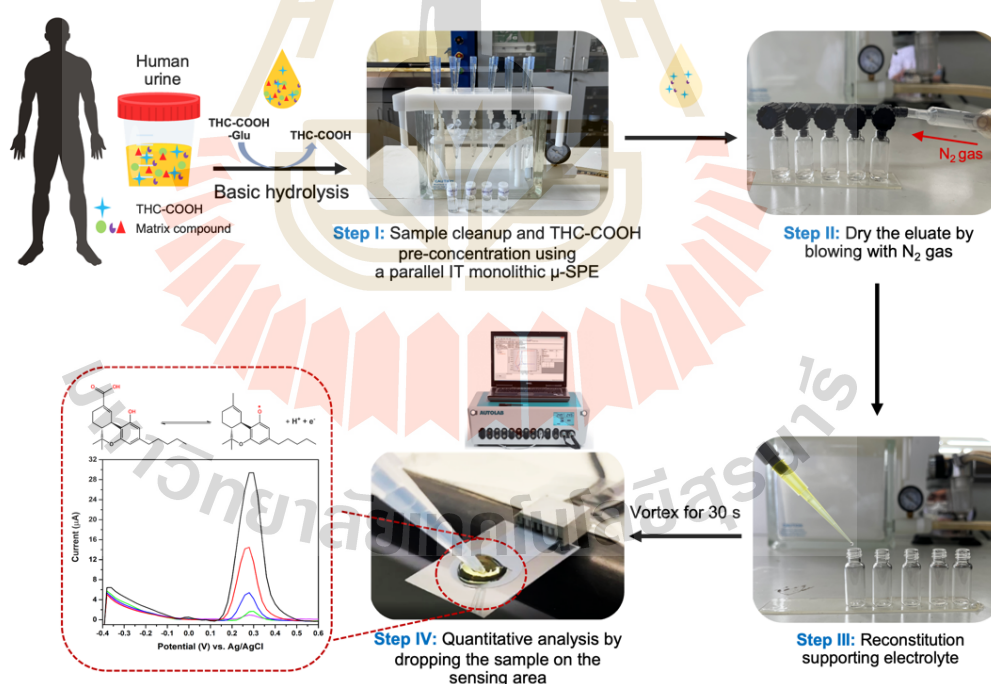
Figure 4.13 Workflow diagram of the parallel IT monolithic µ-SPE coupled with SPGE sensor for the determination of THC-COOH in human urine sample.

4.2.1 Fabrication and characterization of IT monoliths for μ-SPE

The IT monoliths were fabricated by adopting the method developed in the first part. In brief, the PP tip was modified with linking layer of EDMA prior to anchoring SMA-co-EDMA monolith. The SMA-co-EDMA monolith was *in situ* synthesized in the modified PP pipette tips through a photo-assisted co-polymerization of the C18-functional monomer SMA and the common crosslinking monomer EDMA. A schematic diagram for the fabrication of IT SMA-co-EDMA monolithic μ-SPE is illustrated in **Figure 4.14**.
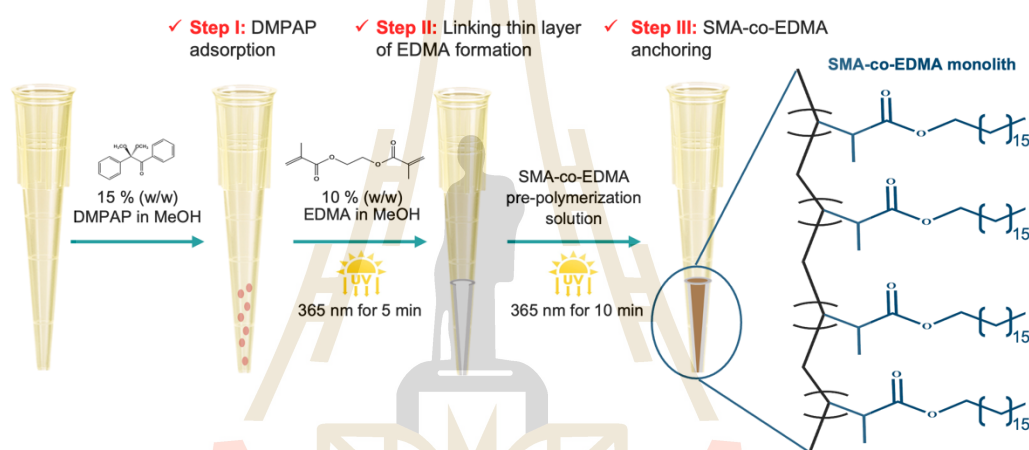
Figure 4.14 Schematic diagram of the fabricating IT SMA-co-EDMA monolithic μ-SPE.

The fabricated IT monoliths provided a rigid plug of monolithic material in the modified PP tips, as shown in **Figure 4.15(a)**. A preparation success rate of 100 % was achieved for the fabrication of 100 tips. The mechanical strength and permeability of the fabricated IT monoliths were preliminarily evaluated by flowing several volumes of MeOH (5 mL) using a 12-position vacuum SPE manifold (the apparatus is shown in **Figure 4.13, step** I). The solvent easily percolated through the monoliths without cracking, swelling, or detachment, demonstrating the robustness of the IT monoliths and their readiness for use.

The attachment of the synthesized SMA-co-EDMA monolith in the tip was observed by SEM image. As expected, good attachment of the monolithic material against the modified inner tip wall was observed, as shown in **Figure 4.15(b)**.
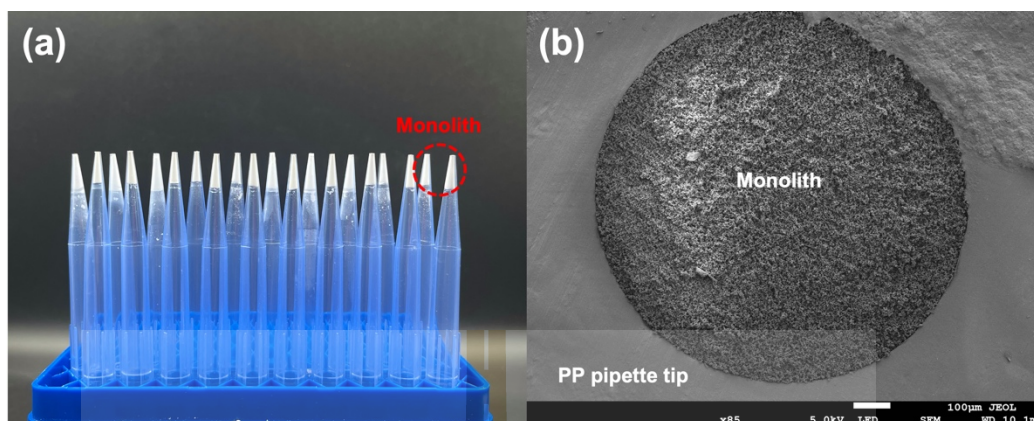
Figure 4.15 Representative (a) photograph and (b) SEM image of the SMA-co-EDMA monolith synthesized in modified PP pipette tips.

4.2.2 Characterization of the fabricated SPGEs

In this work, the SPGEs were produced by Graphene Sensor Laboratory, Graphene and Printed Electronics for Dual-Use Applications Research Division, National Science and Technology Development Agency (NSTDA). As depicted in **Figure 4.16(a)**, the SPGE was fabricated on the PET substrate, comprising working electrode (WE), counter electrode (CE), and reference electrode (RE) on the sensing area. The WE and CE were constructed by printing the graphene paste on the PET substrate. Meanwhile, the RE was created by printing Ag/AgCl paste.

Electrochemical performance of the fabricated SPGEs was preliminarily evaluated by observing cyclic voltammogram of a redox probe, $K_3[Fe(CN)_6]$ in 0.01 M phosphate buffer saline pH 7.4. As shown in **Figure 4.16(b)**, the cyclic voltammogram indicated well-defined anodic and cathodic peaks of the redox probe. This result demonstrates good electrochemical performance of the fabricated SPGE for use as a sensor for target molecule.
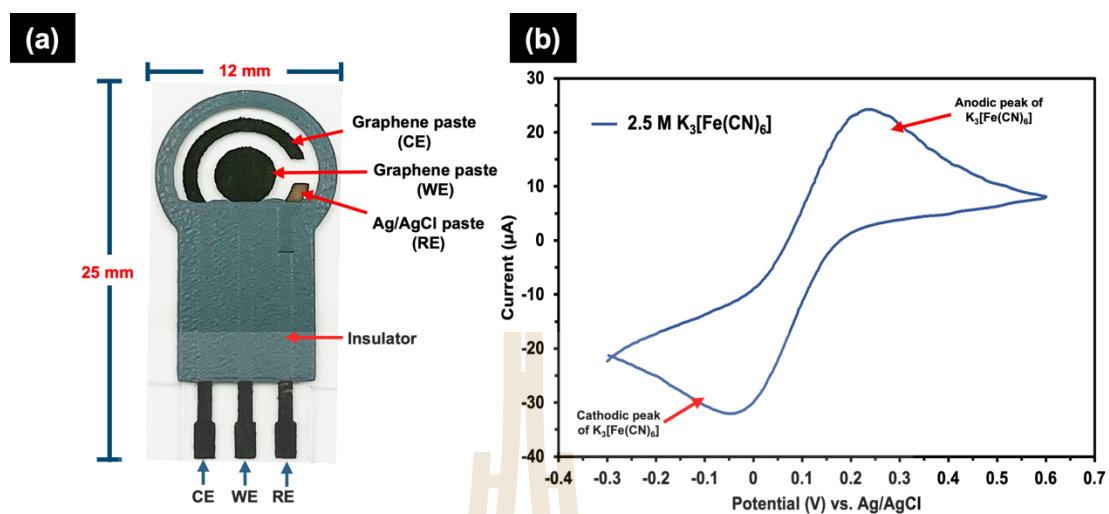
Figure 4.16 (a) Photograph and design of the fabricated SPGE and (b) cyclic voltammogram of 2.5 M K$_3$[Fe(CN)$_6$] in 0.01 M phosphate buffer saline pH 7.4 with a scan rate of 50 mV s^{-1}.

4.2.3 Optimization of IT monolithic μ-SPE for THC-COOH extraction

THC-COOH presents a hydrophobic-based structure with ionizable groups of phenolic group (pKa=9.30) and carboxylic group (pKa=4.87) (Apul et al., 2020) (see THC-COOH structure in **Table 1.1**). Anion-exchanger sorbent was reported for THC-COOH extraction via electrostatic interaction (Gasse, Pfeiffer, Köhler, and Schürenkamp, 2016; Stout, Horn, and Klette, 2001). However, this extraction method in ion exchange mode is probably interfered with by endogenous compounds in urine, such as organic acids, nucleosides, amino acids, and inorganic salts. Consequently, the reversed-phase sorbent is therefore selected for THC-COOH extraction, as it can effectively retain THC-COOH through hydrophobic interaction while weakly retaining highly polar matrices in urine. In this work, the reversed-phase monolith with the C18 functional group of SMA-co-EDMA was selected and employed as a solid sorbent for extracting THC-COOH. A schematic diagram for the μ-SPE procedure is illustrated in **Figure 4.17**.
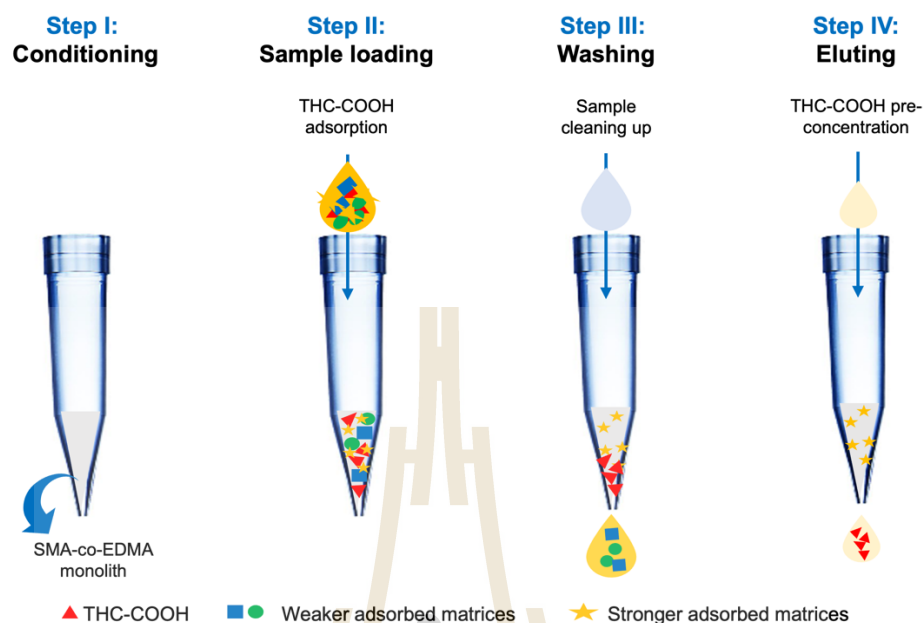
Figure 4.17 Selective IT monolithic μ-SPE procedure for extraction of THC-COOH.

In order to acquire an optimum μ-SPE condition, important parameters were investigated, including pH of sample, washing solvent and eluting solvent.

4.2.3.1 Effect of sample pH

Due to the presence of phenolic and carboxylic groups in THC-COOH structure, its polarity can be changed with the pH of the medium, which can affect the retention of THC-COOH on the sorbent. We therefore initially studied the effect of sample pH on % recovery of THC-COOH.

As expected, high % recovery was observed when the pH of the loading sample was equal to 7.0 or lower (see **Figure 4.18**). The % recovery significantly decreased when the pH was 10.0. At pH 10.0 as THC-COOH became deprotonated (pKa were 4.87 and 9.30 for carboxylic and phenolic groups, respectively), resulting in weaker retention on the C18, SMA-co-EDMA monolith. A sample pH of ≤7 was therefore recommended for the loading step.
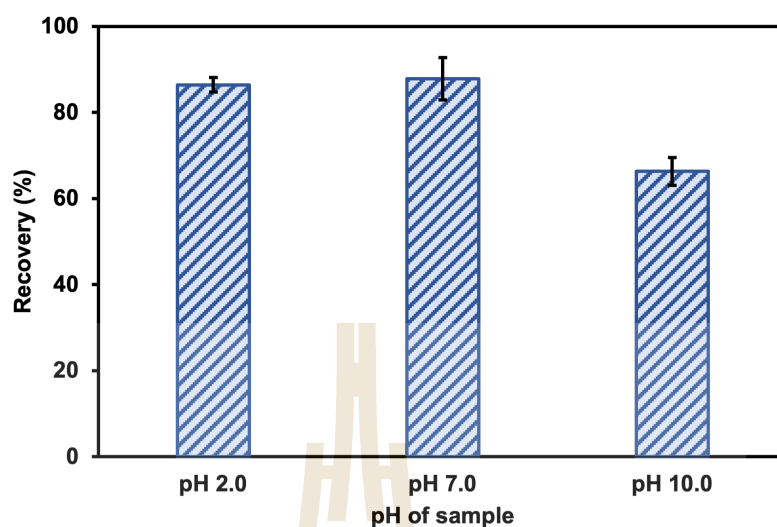
Figure 4.18 Effect of sample pH on recovery (%) of THC-COOH using the IT SMA-co-EDMA monolithic μ-SPE. IT monolith μ-SPE condition; Conditioning: 200 μL MeOH and 20 μL DI water, loading: 2.00 mL spiked urine sample containing 1 mg L^{-1} THC-COOH, washing: 400 μL, 15 % (v/v) ACN : 20 mM PB pH 2.0, eluting: 100 μL 70 % (v/v) ACN : 20 mM tris buffer pH 10.0. HPLC-UV analysis; C18-column, mobile phase: 60 : 40 (v/v) ACN : 20 mM AB pH 5.0, flow rate: 1 mL min^{-1}, wavelength: 210 nm, injection volume: 20 μL.

4.2.3.2 Effect of ACN concentration in washing solvent

After sample loading, washing step is required to remove matrices that probably adsorbed on the sorbent. In this step, the adsorbed target analyte, THC-COOH, must be retained on the sorbent, and only matrices that adsorbed weakly are desorbed by applying an appropriate solvent.

To retain THC-COOH on the monolith, the analyte would be maintained in its neutral form by using a buffer solution at pH lower than its pka, to facilitate strong hydrophobic interaction between THC-COOH and the C18-monolith. A mixture of ACN and phosphate buffer pH 2.0 (20 mM) was used as the washing solvent. In order to obtain an effective washing, concentrations of ACN were varied from 15 % to 25 % (v/v). The results, as shown in **Figure 4.19**, indicated that increasing in ACN concentration led to significant decrease in % recovery, which may be due to the loss

of THC-COOH from the sorbent. Thus, 15 % (v/v) ACN was the optimum concentration for the washing solvent.
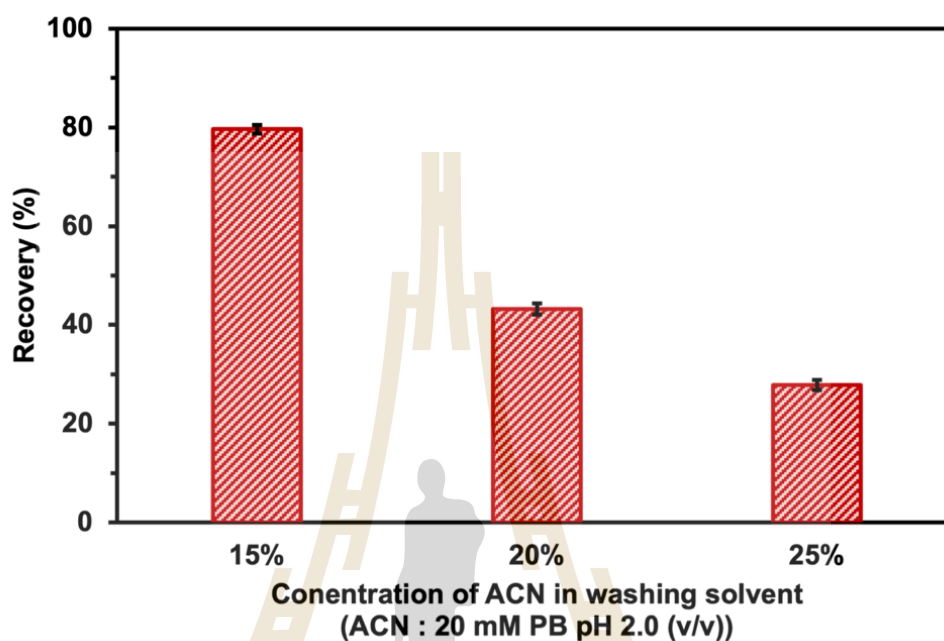
Figure 4.19 Effect of ACN concentration in washing solvent on recovery (%) of THC-COOH using the IT SMA-co-EDMA monolithic μ-SPE. IT monolith μ-SPE condition; Conditioning: 200 μL MeOH and 20 μL DI water, loading: 2.00 mL spiked urine sample containing 1 mg L^{-1} THC-COOH, washing: 400 μL, ACN : 20 mM PB pH 2.0, eluting: 100 μL 70 % (v/v) ACN : 20 mM tris buffer pH 10.0. HPLC-UV condition are shown in **Figure 4.18**.

4.2.3.3 Optimization of eluting solvent

In order to obtain an appropriate eluting solvent, ACN concentration and volume of eluting solvent were evaluated.

4.2.3.3.1 Effect of ACN concentration in eluting solvent

A buffer containing pH higher than THC-COOH's pKa was utilized for desorbing THC-COOH from the C18-monolith. A mixture of ACN and 20 mM tris buffer pH 10.0 was initially employed as the eluting solvent. The results in **Figure 4.20 (a)**, demonstrates that using 50 % (v/v) ACN in 20 mM tris buffer pH 10.0 presented % recovery of 66. Increasing ACN concentration of 70 % led to improving % recovery of ~90 %. A high recovery of 95 % was achieved by utilizing pure ACN (100 %ACN). These results clearly confirmed the reversed-phase mode of the extracting THC-COOH using the SMA-co-EDMA monolith.

However, % extraction efficiency was also investigated, as shown the result in **Figure 4.20(b)**.
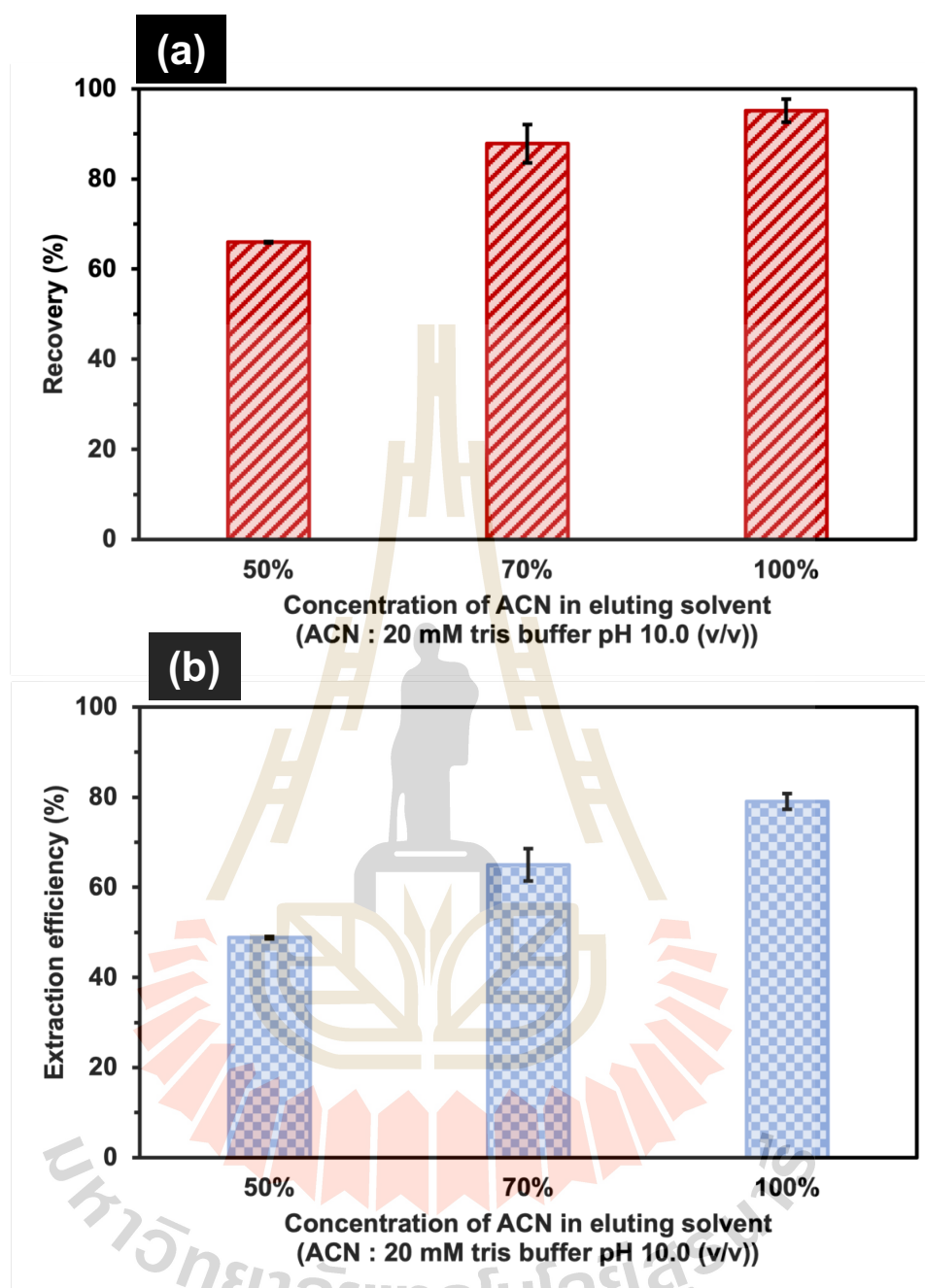
Figure 4.20 Effect of ACN concentration in eluting solvent on (a) recovery (%) and (b) extraction efficiency (%) of THC-COOH using the IT SMA-co-EDMA monolithic μ-SPE. IT monolith μ-SPE condition; Conditioning: 200 μL MeOH and 20 μL DI water, loading: 2.00 mL spiked urine sample containing 1 mg L^{-1} THC-COOH, washing: 400 μL, ACN : 20 mM PB pH 2.0, eluting: 100 μL ACN : 20 mM tris buffer pH 10.0. HPLC-UV condition are shown in **Figure 4.18**.

4.2.3.3.2 Effect of eluting volume

In order to improve the extraction efficiency, the volume of the ACN was investigated. The results presented in **Figure 4.21(a)**, exhibits that increasing the ACN volume did not significantly affect % recovery of THC-COOH. Acceptable % recovery of 95 could be obtained from eluting volumes of 100, 150, and 200 μL. However, increasing the ACN volume from 100 μL to 150 μL and 200 μL, increased the extraction efficiency from 80 % to >95 % (see **Figure 4.21(b)**).

To reach the highest pre-concentration and % extraction efficiency, a 150 μL aliquot of pure ACN was the optimum eluting solvent for the desorption of THC-COOH from the SMA-co-EDMA monolith.
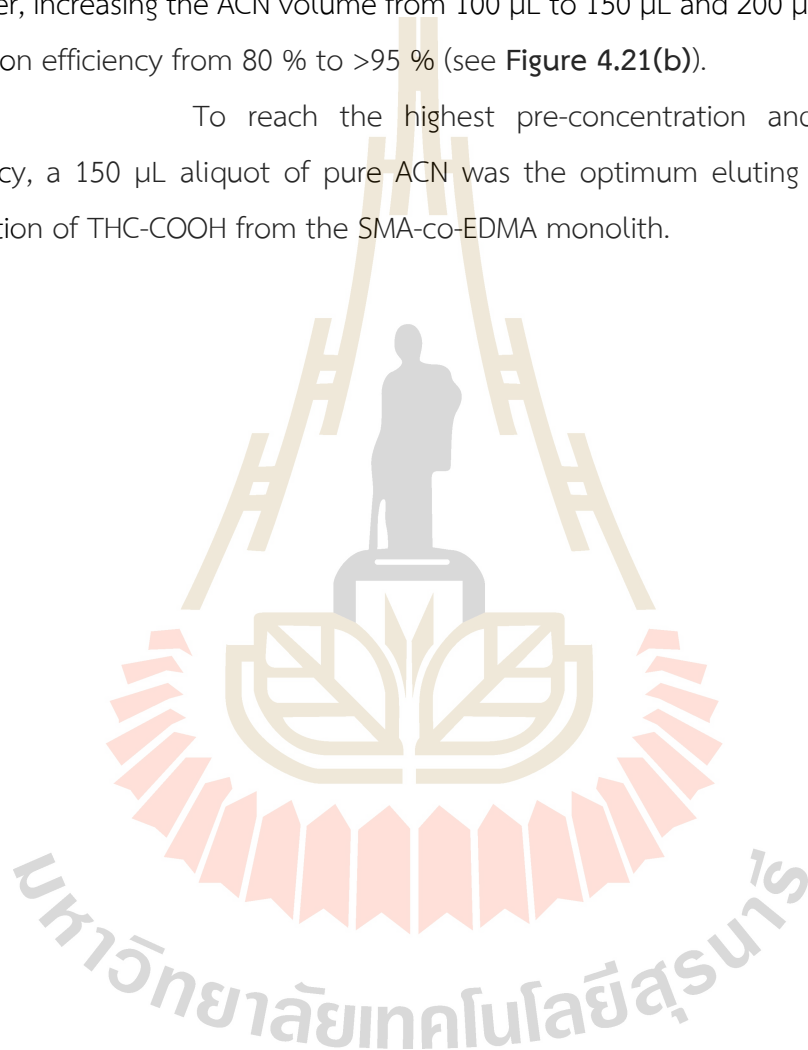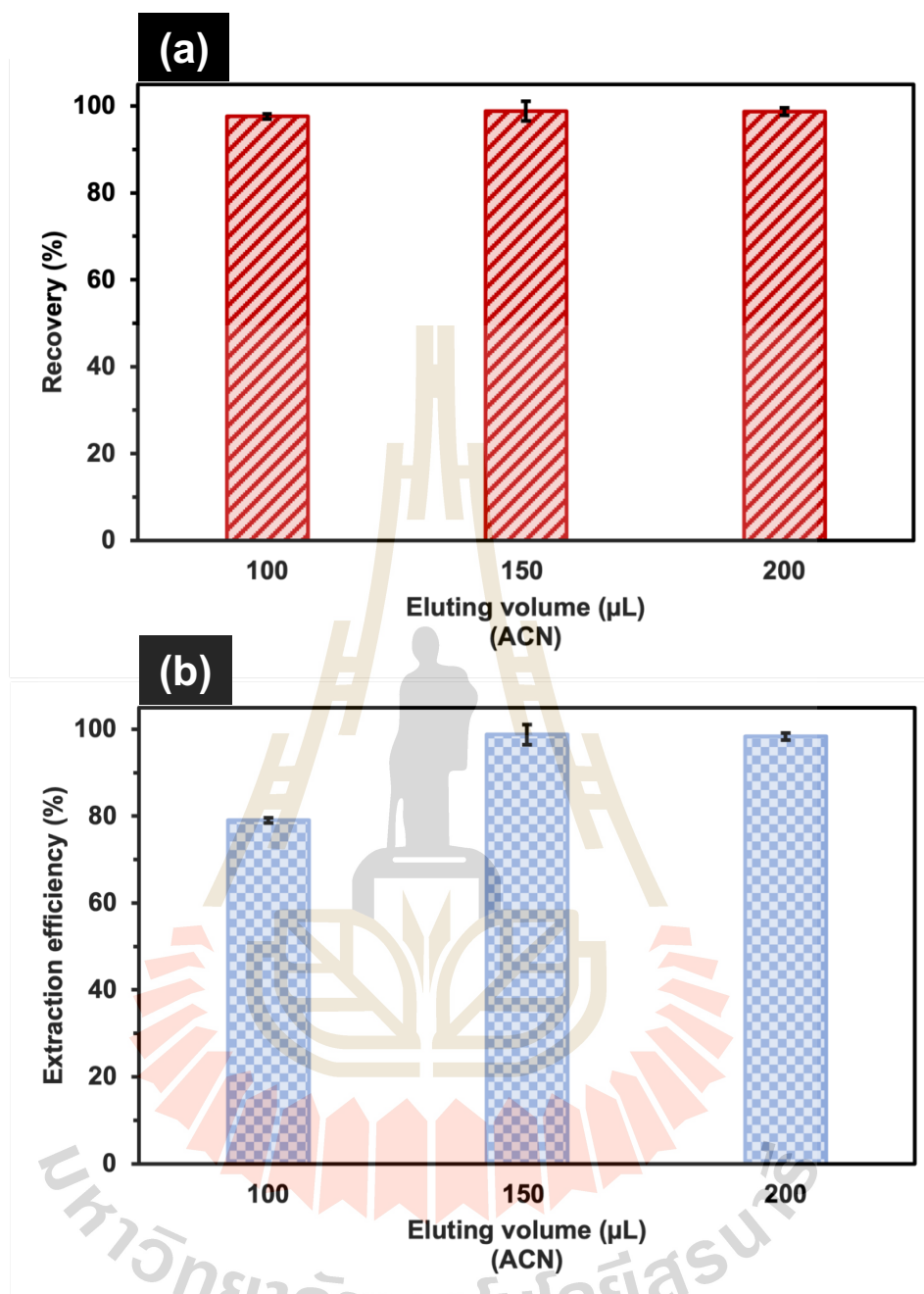
**Figure 4.21** Effect of ACN volume of eluting solvent on (a) recovery (%) and (b) extraction efficiency (%) of THC-COOH using the IT SMA-co-EDMA monolithic μ-SPE. IT monolith μ-SPE condition; Conditioning: 200 μL MeOH and 20 μL DI water, loading: 2.00 mL spiked urine sample containing 1 mg L^{-1} THC-COOH, washing: 400 μL, 15 % (v/v) ACN : 20 mM PB pH 2.0, eluting: pure ACN. HPLC-UV condition is shown in **Figure 4.18**.

4.2.4 Optimization of SPGE sensor

4.2.4.1 Effect of supporting electrolyte on electrochemical behavior of THC-COOH

Type and pH of the supporting electrolyte are commonly parameters affecting electrochemical behavior of the analyte. Four common supporting electrolytes, including 0.01 M phosphate buffer saline pH 7.4, 0.03 M borate buffer pH 10.0, 0.04 M Britton-Robinsin buffer pH 10.0 and 0.40 M carbonate buffer pH 10.3 were studied for electrochemical measurement of THC-COOH in cyclic voltammetry mode. Cyclic voltammograms of THC-COOH are presented in **Figure 4.22**. THC-COOH peak could not be seen when using 0.03 M borate buffer pH 10.0 as supporting electrolyte (see **Figure 4.22(a)**), which may be due to the high CV background of the supporting electrolyte. Meanwhile, anodic peak current of THC-COOH could be observed from the cyclic voltammogram using 0.01 M phosphate buffer saline pH 7.4, 0.04 Britton-Robinson buffer pH 10.0, and 0.40 M carbonate buffer pH 10.3 (see **Figure 4.22(b)-(d)**).
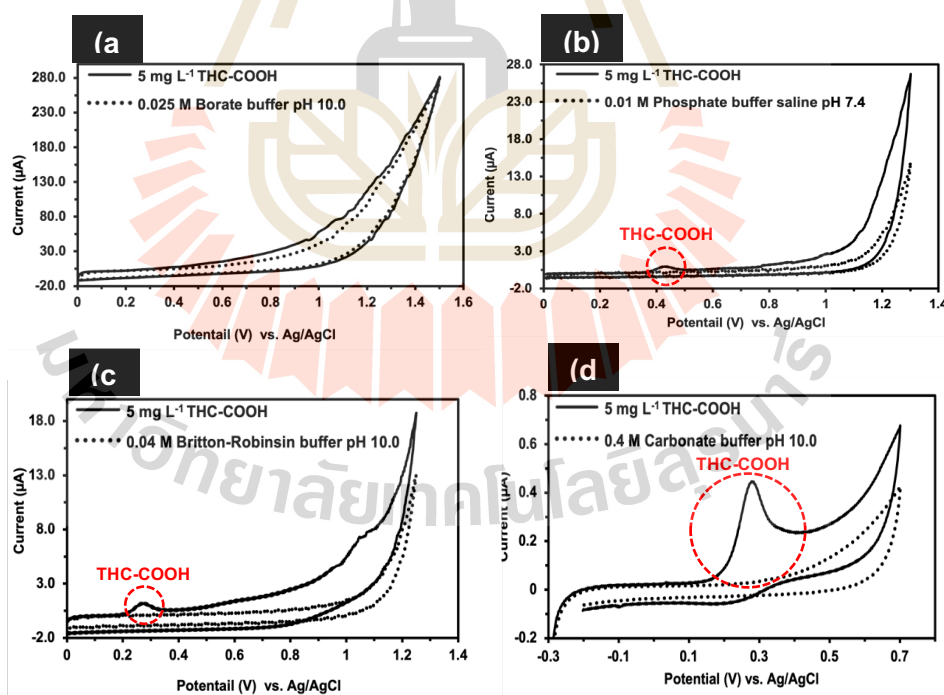
Figure 4.22 Cyclic voltammograms of 5 µg mL^{-1} THC-COOH in (a) 0.03 M borate buffer pH 10.0, (b) 0.01 M phosphate buffer saline pH 7.4, (c) 0.04 M Britton-Robinsin buffer pH 10.0, and (d) 0.40 M carbonate buffer pH 10.3 with a scan rate of 50 mV s^{-1}.

The anodic peak was predicted from the oxidation reaction of THC-COOH on the phenolic group (Renaud-Young et al., 2019). The possible oxidation reaction of THC-COOH is shown in **Figure 4.23**.
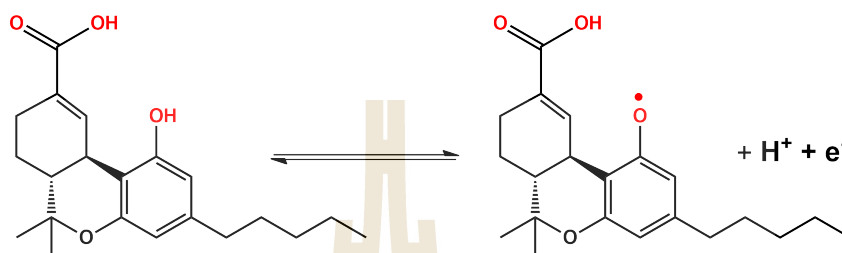
Figure 4.23 Predicted oxidation reaction of THC-COOH occurred on the SPEG.

To obtain the highly sensitive sensor method, 0.40 M carbonate buffer pH 10.3 was selected as the supporting electrolyte for the electrochemical sensor of THC-COOH using SPGE.

To enhance the sensitivity of the SPGE sensor method, square wave voltammetry (SWV) mode was employed and optimized. Important parameters, including step potential, amplitude and frequency were investigated. The highest peak currents were attained by applying step potential, amplitude, and frequency at 20 mV, 100 mV, and 45 Hz, respectively (see **Figure 4.14**).
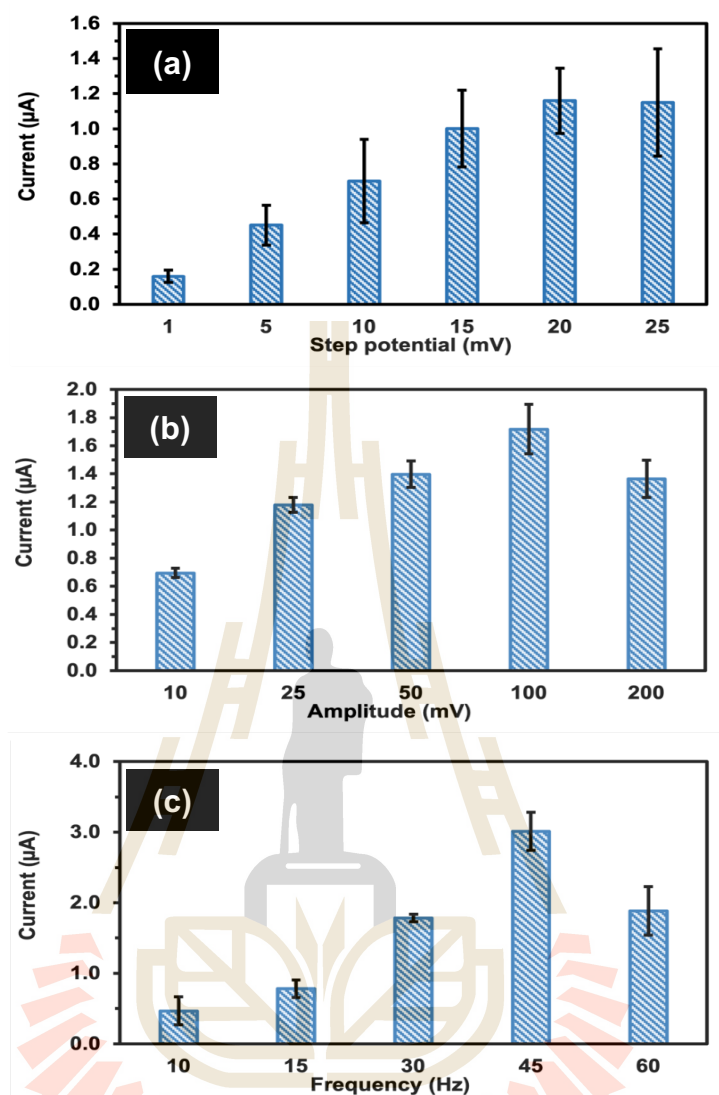
Figure 4.24 SWV optimization of (a) step potential, (b) amplitude, and (d) frequency for the detection of THC-COOH using SPGE.

4.2.4.2 Direct detection of THC-COOH using the developed SPGE sensor

The developed SPGE sensor was utilized for the detection of THC-COOH. Good linearity was observed with an R^2 of 0.9995, as shown in **Figure 4.25**. LOD and LOQ of 34.09 and 113.64 ng mL^{-1} were observed. Although the detection of THC-COOH can be performed directly by the developed SPGE sensor method, its sensitivity was not adequate for identifying cannabis users, as the cutoff concentration was

defined at 50 ng mL^{-1}. In order to improve the sensitivity and selectivity of the SPGE sensor, the developed SPGE and IT monolithic μ-SPE method were coupled.
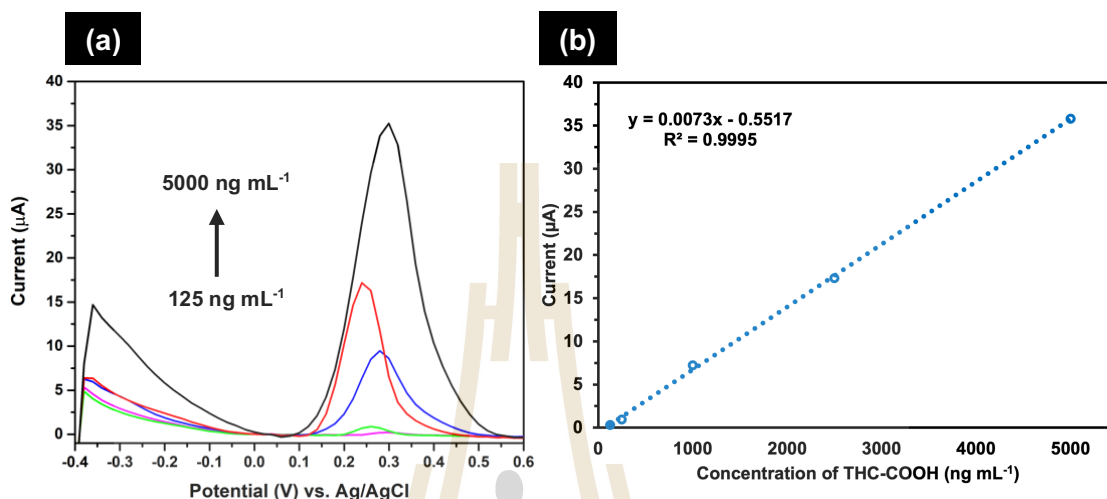
Figure 4.25 (a) SWVs and (b) calibration curve of THC-COOH detected by the developed SPGE sensor. SWV condition; THC-COOH in 0.40 M carbonate buffer pH 10.3, step potential: 20 mV, amplitude: 100 mV, and frequency: 45 Hz.

4.2.5 Coupling IT monolithic μ-SPE and SPGE sensor for the determination of THC-COOH

The interface between the two methods, μ-SPE and electrochemical sensor, is a critical consideration due to the eluant often demonstrating unsuitability as a supporting electrolyte. Fortunately, reconstitution can be achieved in this work, by blowing the extracted sample with N$_2$ gas until completely dry, then introducing to the appropriate supporting electrolyte. It should be noted here that, during the reconstitution process, glass container is recommended to prevent adsorbing THC-COOH on the container. The workflow diagram illustrating the coupling of IT monolithic μ-SPE and SPGE sensor is presented in **Figure 4.13**. Coupling the developed IT monolithic μ-SPE with SPGE method provided good THC-COOH peak potential at +0.28 V, as shown in **Figure 4.26**.
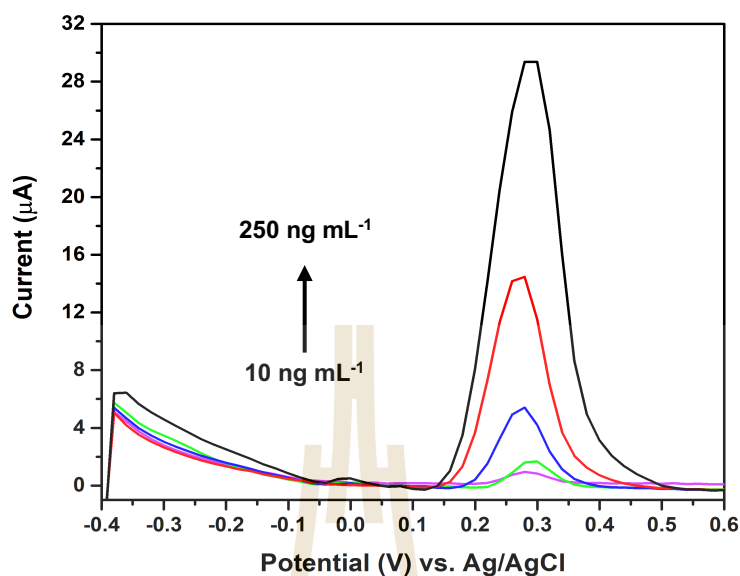
Figure 4.26 SWVs of the detection of THC-COOH using SPGE sensor coupled IT monolithic μ-SPE method.

The sensitivity of the method was significantly enhanced by the coupling, as shown in **Figure 4.27**. The IT monolithic μ-SPE coupled with SPGE sensor procedure is summarized in **Table 4.5**.
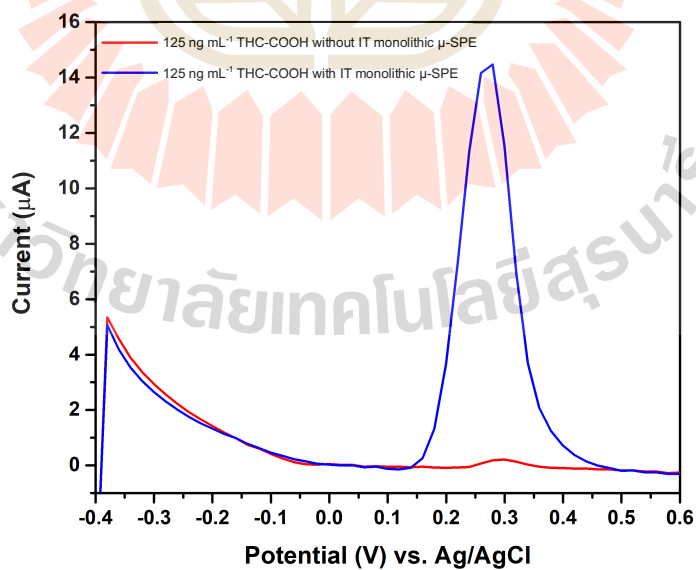
Figure 4.27 SWVs of the detection of 125 ng mL^{-1} THC-COOH using the developed SPGE sensor with and without IT monolithic μ-SPE.

Table 4.5 The IT monolithic μ-SPE coupled with SPGE sensor procedure for the determination of THC-COOH.

- **IT monolithic μ-SPE condition**

Step	Solvent	Volume
Conditioning	MeOH	200 μL
	DI water	20 μL
Loading	Urine sample	2000 μL
Washing	15 % (v/v) ACN : DI water	400 μL
Eluting	ACN	150 μL

- **Coupling with the SPGE sensor**

Method	Volume
1. Blowing with N_2 until complete dry	-
2. Reconstitution with 0.40 M carbonate buffer pH 10.3	100 μL

- **SPGE sensor condition (SWV mode)**

Supporting electrolyte	0.40 M carbonate buffer pH 10.3
Step potential	20 mV
Amplitude	100 mV
Frequency	45 Hz

4.2.6 Method validation

To evaluate the capability of the developed IT monolithic μ-SPE coupled with SPGE sensor, the method was fully validated according to the SWGTOX guidelines (SWGTOX, 2013).

Good linearity could be obtained from the developed IT monolithic μ-SPE coupled with SPGE sensor, as shown in **Figure 4.28.**
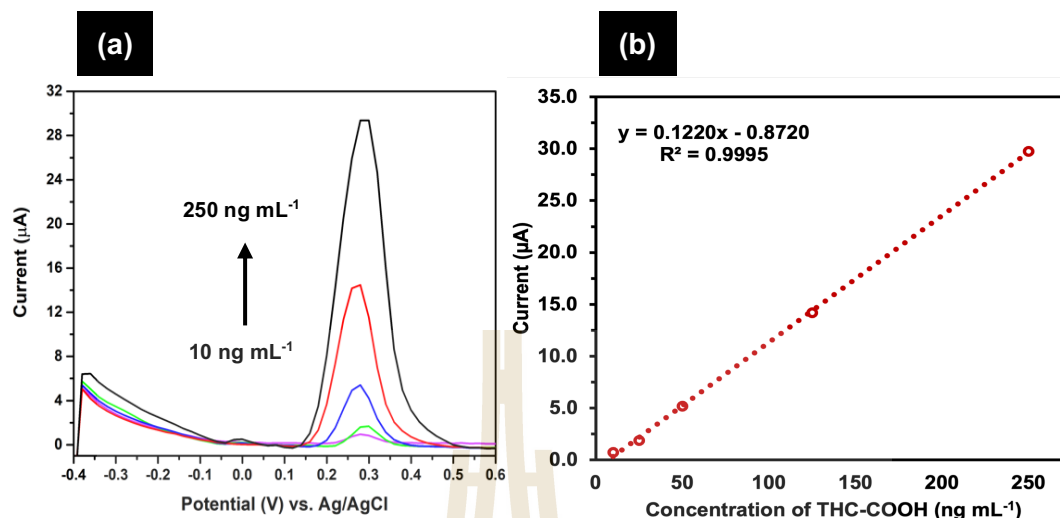
Figure 4.28 (a) SWVs and (b) calibration curve of THC-COOH determined by the developed IT monolithic µ-SPE coupled with SPGE sensor.

Comparing with the direct detection of THC-COOH by the developed SPGE, the sensitivity could be impressively enhanced when the sensor was coupled with the IT monolithic µ-SPE. The performances of the SPGE sensor with and without IT monolithic µ-SPE for the determination of THC-COOH are compared in **Table 4.6**.

Table 4.6 Comparison of concentration range, slope, intercept, correlation coefficient (R^2), LOD, and LOQ of SPGE sensor with and without IT-monolithic µ-SPE for the detection of THC-COOH.

	With µ-SPE	Without µ-SPE
Concentration range (ng mL^{-1})	10 - 250	125 - 5000
Slope	0.1220	0.0073
Intercept	- 0.8720	- 0.5517
Correlation coefficient (R^2)	0.9995	0.9995
LOD (ng mL^{-1})	2.68	34.09
LOQ (ng mL^{-1})	8.93	113.64

The LOD and LOQ could be reduced to 2.68 and 8.93 ng mL^{-1}, which are sufficient for the analysis of urinary THC-COOH, based on the cutoff concentration defined by the Substance Abuse and Mental Health Services Administration (50 µg L^{-1} for screening and 15 µg L^{-1} for confirming). The method performances of our developed method and the previous works are compared in **Table 4.7**. It demonstrates that our method is comparable with the sensitive gold methods, LC-MS/MS and GC-MS.

Table 4.7 Analytical method performances comparison of the developed method for the determination of THC-COOH in biological samples.

Sample	Analysis method	Sample preparation	Concentration range (ng mL^{-1})	LOD (ng mL^{-1})	Recovery (%)	Ref
Blood	LC-MS/MS	DPX (WAX-S)	0.5 – 100	0.3	71	(Andersson et al., 2016)
Serum	GC-MS	LLE	-	0.3	101 – 121	(Purschke et al., 2016)
Oral fluid/ urine/blood	LC-MS/MS	SPE	2 – 2000	0.5	83 – 96	(Teixeira et al., 2007)
Urine	GC-MS	LLE	1 – 100	0.5	-	(Chericoni et al., 2011)
Urine	LC-MS/MS	DPX (WAX-S)	0.5 – 100	0.5	69 – 74	(Andersson et al., 2016)
Urine	GC-MS	MIP-SPE	2 – 150	1.0	74 – 76	(Nestić et al., 2013)
Urine	LC-MS/MS	DPX (WAX-S)	1 – 500	1.0	86 – 89	(Sempio et al., 2018)
Urine	LC-MS/MS	MIP-SPE	5 – 170	1.0	12 – 15	(Sartore et al., 2020)
Blood urine	GC-MS/MS	Automated on-line SPE	3 – 200	1.0	79	(Frei et al., 2022)

Table 4.7 Analytical method performances comparison of the developed method for the determination of THC-COOH in biological samples (Continued).

Sample	Analysis method	Sample preparation	Concentration range (ng mL^{-1})	LOD (ng mL^{-1})	Recovery (%)	Ref
Blood	LC-MS/MS	LLE	2 – 160	2.0	105	(del Mar Ramirez Fernandez et al., 2008)
Urine	LC-MS/MS	Commercial C18 tip	6 – 250	2.0	71 – 75	(Montesano et al., 2014)
Urine	SPGE sensor	IT monolithic μ-SPE (C18)	15 – 125	2.7	85 – 108	This work
Urine	GC-MS	DPX (Divinyl benzene)	-	3.3	57	(Ellison et al., 2009)
Urine	GC-MS	Monolithic silica spin column	10 – 1000	5.0	95 – 103	(Namera and Saito, 2013)
Urine	GC-MS	Microextraction by packed sorbent (MEPS)	10 – 400	5.0	26 – 85	(Rosendo et al., 2022)
Urine	LC-MS/MS	Diluton	25 – 8000	25.0	>90	(Renaud-Young et al., 2019)
Blood	GC-MS	LLE	50 – 1500	40.0	80	(Álvarez-Freire et al., 2023)

DPX=Disposable pipette extraction, WAX-S=weak anionic extraction with salt.

In addition, good precisions were observed with % CV lower than 2.65 %. The IT monolithic μ-SPE could be reused at least 10 times (% RSD=3.0 %, n=10), which is superior to conventional disposable SPE cartridges and DPX.

An 18-fold pre-concentration factor was achieved with 91 % extraction efficiency. High-throughput analysis method could be achieved with extraction of 12 samples in 30 min (2.5 min/sample).

4.2.7. Selectivity and specificity

To study the selectivity and specificity of the developed method, pooled negative urine sample (No. 1) and positive drug-containing samples (No. 2 to No. 4) were analyzed. The effect of endogenous components such as urea, uric acid, organic/inorganic salts, or amino acid were evaluated from the pooled negative urine sample, while possible exogenous interferences were examined through the analysis of positive drug-containing samples (the samples are listed in **Table 3.4**).

The results in **Figure 4.29,** demonstrates that there was no significant interference peak at the THC-COOH potential (+0.28 V).
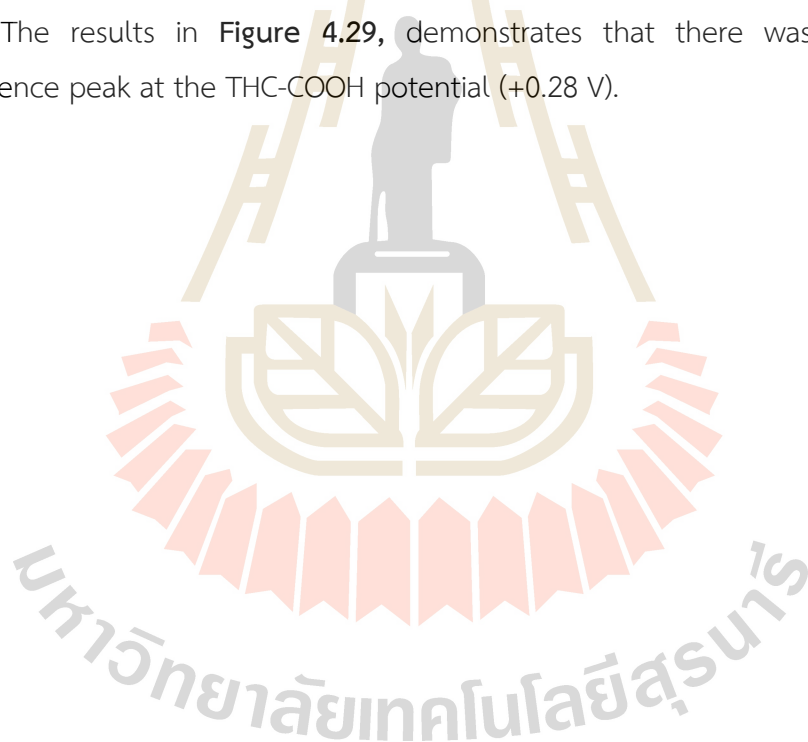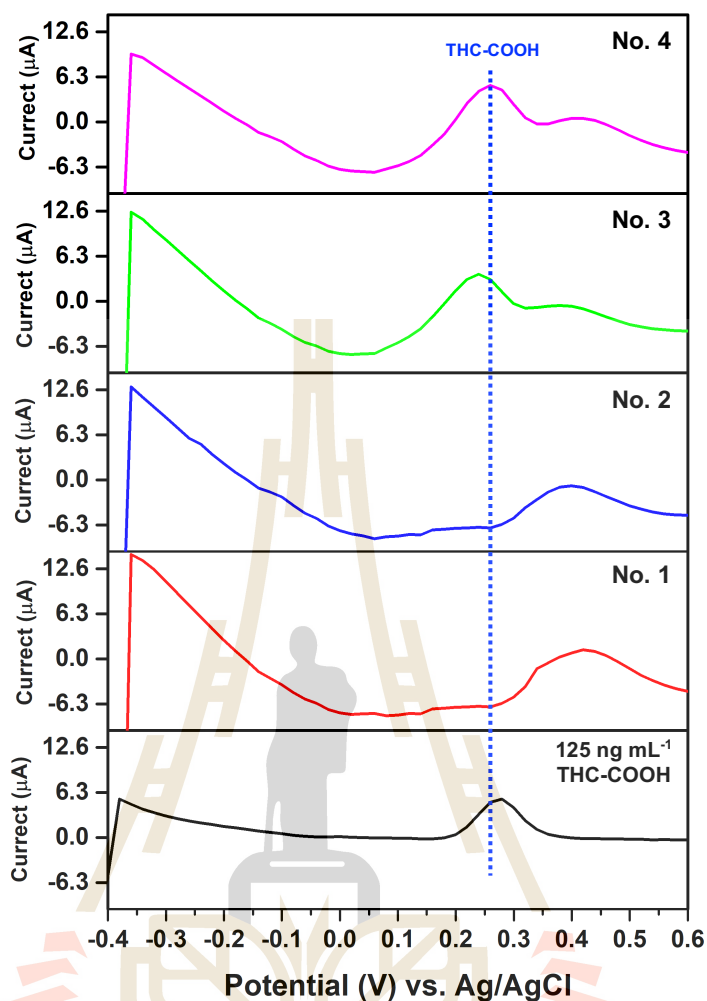
Figure 4.29 SWVs of the determination of THC-COOH in authentic human urine samples using the developed IT monolithic μ-SPE coupled with SPGE sensor.

4.2.8 Matrix effect and recovery

Matrix effect was evaluated by comparing the slope ratio of the THC-COOH, constructed from the external calibration curve and standard addition calibration curve. The results indicated good linearity of the standard addition curves (R^2 between 0.9990 - 0.9997), as summarized in **Table 4.8**. Slope ratios between 0.88 - 0.96 were observed, indicating no matrix effect from the analysis in real urine samples. The standard addition calibration curves are detailed in **Table 4.8**.

Table 4.8 Concentration range, equation, R^2 and matrix effect of the external and standard addition calibration curves.

Matrix	Concentration range (ng mL^{-1})	Equation	R^2	ME
DI water	25-125	Y = 0.1223X - 1.0545	0.9996	-
No. 1	25-125	Y = 0.1173X - 0.2314	0.9993	0.96
No. 2	25-125	Y = 0.1117X - 0.1931	0.9991	0.91
No. 3	25-125	Y = 0.1074X + 6.5995	0.9990	0.88
No. 4	25-125	Y = 0.1110X + 9.3242	0.9997	0.91

Accuracy was examined from evaluating % recovery. The recoveries were investigated at three different THC-COOH concentration levels of 25, 50 and 125 ng mL^{-1}. High recovery in the range of 85 - 108% was observed, as shown in **Table 4.9**, indicating high accuracy of the developed method.

Table 4.9 THC-COOH concentration and recovery of the determination of THC-COOH in authentic human urine samples using the developed IT monolithic µ-SPE coupled with SPGE sensor.

Sample	Urinary THC-COOH concentration ng mL^{-1} (Mean ± SD, n=2)		Recovery (%)
	Spiked	Found*	
No. 1	0	N.D.	
	25	27.05 ± 0.01	108
	50	51.16 ± 0.34	102
	125	123.17 ± 0.46	99
No. 2	0	N.D.	
	25	27.14 ± 0.08	109
	50	48.84 ± 0.24	98
	125	118.36 ± 0.28	95
No. 3	0	60.25 ± 0.11	
	25	82.75 ± 1.77	90
	50	107.48 ± 0.05	94
	125	170.42 ± 0.58	88
No. 4	0	81.34 ± 0.01	
	25	107.40 ± 6.18	104
	50	131.20 ± 3.66	100
	125	196.12 ± 0.30	92

N.D.=Not detected

* The urine samples were diluted 2 times.

4.2.9 Determination of urinary THC-COOH in forensic application

To evaluate the feasibility of the developed method for the determination of THC-COOH in forensic applications, the method was applied to authentic human urine samples. Urinary THC-COOH concentrations were found to be 120.50 (No. 3) and 162.68 ng mL^{-1} (No.4). SWVs of the real samples are shown in **Figure 4.29**.

The analysis results were validated with the standard addition method. The paired t-Test method indicated no significant different between the results at a 95 % confidence level (t-stat and t-critical two-tails were -2.58 and 12.71, respectively). Therefore, an ultra-sensitive and high-throughput analytical method for the determination of urinary THC-COOH in forensic applications was successfully developed using the IT monolithic μ-SPE coupled with SPGE sensor.
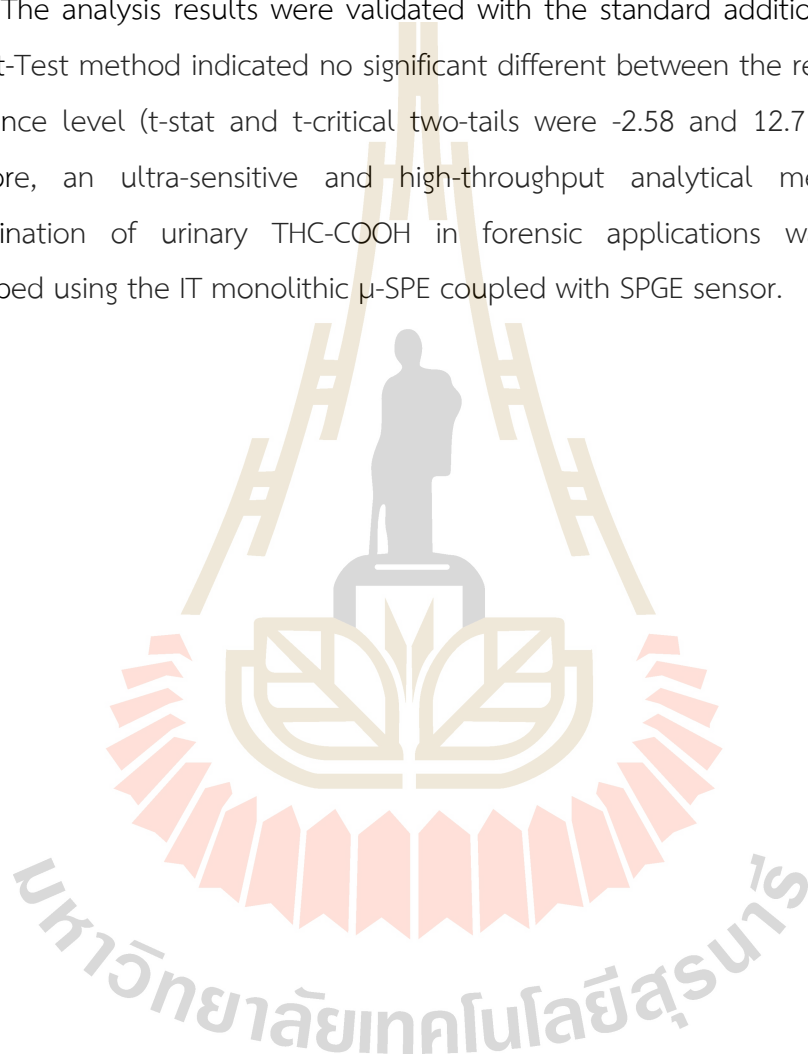
CHAPTER V

CONCLUSIONS

The preparation and application of monolithic materials in the field of µ-SPE have garnered increasing interest due to the superior features of the materials, such as facile preparation, high surface area with high permeability, tunable composition, and fast mass transfer. *In situ* synthesis of monoliths in polypropylene (PP) pipette tips is a convenient and versatile route for micro-scale extraction. However, the fabrication is complicated as detachment and shrinkage of the monolith are commonly found. Surface modification of PP pipette tips to anchor the monoliths against the tip wall was therefore developed.

This thesis investigated monolith shrinkage and surface modification of PP pipette tips for anchoring methacrylate and activated charcoal (AC) composite monoliths for µ-SPE. Monolith shrinkage was identified as the main problem leading to void space and monolith detachment. Type of monomer and degree of the crosslinker (ethylene dimethacrylate (EDMA)) were found to be critical factors affecting the shrinkage and detachment. Decreasing the EDMA content dramatically decreased the preparation success rate. The developed surface modification method consisted of 3 steps as follows:

(I) Creating an initiator surface of 2,2-dimethoxy-2-phenylacetophenone

(II) Forming a polymeric linking thin layer of EDMA

(III) Anchoring of monolith with the linking thin layer modified tip wall

The anchoring of the monolith against the modified tips was achieved through covalent bonding and/or physical intertwining between the linking layer and the polymeric monolith.

The modified PP tips could be applied for all common tip sizes available in the laboratory and for fabricating of AC composite monoliths. The capabilities of the fabricated IT monoliths were compared with those of commercial C18 SPE cartridge. Superior capacity breakthrough was observed from the continuously based monolith compared to those of SPE cartridges.

A portable and on-site analysis method is required for the determination of urinary THC-COOH. In pipette tip monolithic µ-SPE coupled with SPGE sensor was therefore proposed. The in tip monolithic µ-SPE was developed to improve sensitivity and selectivity of the optimized SPGE sensor. The developed method provided good linearity and precision with LOD and LOQ of 2.68 and 8.93 $\mu g\ L^{-1}$, respectively. An 18-fold pre-concentration factor was achieved with 91 % extraction efficiency. Good accuracy was observed with high % recovery between 85 - 108 %. The developed method was applied for forensic applications. THC-COOH concentrations of 120.50 and 162.68 $ng\ mL^{-1}$ was determined in authentic human urine samples. The results validated with standard addition and pair t-test methods indicate no significant sample matrix effect on the analysis.

REFERENCES

REFFERENCES

Akamine, L. A., Vargas Medina, D. A., and Lanças, F. M. (2021). Magnetic solid-phase extraction of gingerols in ginger containing products. *Talanta*, *222*, 121683. https://doi.org/10.1016/j.talanta.2020.121683

Altun, Z., Hjelmström, A., Abdel-Rehim, M., and Blomberg, L. G. (2007). Surface modified polypropylene pipette tips packed with a monolithic plug of adsorbent for high-throughput sample preparation. *Journal of Separation Science*, *30*, 1964–1972. https://doi.org/10.1002/jssc.200600523

Álvarez-Freire, I., Valeiras-Fernández, A., Cabarcos-Fernández, P., Bermejo-Barrera, A. M., and Tabernero-Duque, M. J. (2023). Simple Method for the Determination of THC and THC-COOH in Human Postmortem Blood Samples by Gas Chromatography-Mass Spectrometry. *Molecules*, *28*(8), 3586. https://doi.org/10.3390/molecules28083586

Alwael, H., Connolly, D., Clarke, P., Thompson, R., Twamley, B., O'Connor, B., and Paull, B. (2011). Pipette-tip selective extraction of glycoproteins with lectin modified gold nano-particles on a polymer monolithic phase. *Analyst*, *136*(12), 2619–2628. https://doi.org/10.1039/C1AN15137A

Andersson, M., Scheidweiler, K. B., Sempio, C., Barnes, A., and Huestis, M. A. (2016). Simultaneous quantification of eleven cannabinoids and metabolites in human urine by liquid chromatography tandem mass spectrometry using WAX-S tips. *Analytical and Bioanalytical Chemistry*, *408*(23), 6461–6471. https://doi.org/10.1007/s00216-016-9765-8

Antunes, M., Barroso, M., and Gallardo, E. (2023). Analysis of Cannabinoids in Biological Specimens: An Update. *International Journal of Environmental Research and Public Health*, *20*(3), 2312. https://doi.org/10.3390/ijerph20032312

Apul, O. G., Rowles, L. S., Khalid, A., Karanfil, T., Richardson, S. D., and Saleh, N. B. (2020). Transformation potential of cannabinoids during their passage through engineered water treatment systems: A perspective. *Environment International*, *137*, 105586. https://doi.org/10.1016/j.envint.2020.105586

Arrua, R. D., Strumia, M. C., and Alvarez Igarzabal, C. I. (2009). Macroporous Monolithic Polymers: Preparation and Applications. *Materials*, *2*(4), 2429–2466. https://doi.org/10.3390/ma2042429

Ar-sanork, K. (2018). *In-pipette tip monolithic micro-solid phase extraction coupled with high performance liquid chromatography for simultaneous determination of ractopamine and clenbuterol in animal urine and meat samples* (Thesis, School of Chemistry Institute of Science Suranaree University of Technology). School of Chemistry Institute of Science Suranaree University of Technology. Retrieved from http://sutir.sut.ac.th:8080/jspui/handle/123456789/8462

Ar-sanork, K., Karuwan, C., Surapanich, N., Wilairat, P., Nacapricha, D., and Chaisuwan, P. (2021). Mixed mode monolithic sorbent in pipette tip for extraction of ractopamine and clenbuterol prior to analysis by HPLC-UV and UHPLC-Q ExactiveTM Plus Orbitrap MS. *Journal of Analytical Science and Technology*, *12*, 23. https://doi.org/10.1186/s40543-021-00275-5

Bach, A., Fleischer, H., Wijayawardena, B., and Thurow, K. (2022). Automation System for the Flexible Sample Preparation for Quantification of Δ9-THC-D3, THC-OH and THC-COOH from Serum, Saliva and Urine. *Applied Sciences*, *12*(6), 2838. https://doi.org/10.3390/app12062838

Badawy, M. E. I., El-Nouby, M. A. M., Kimani, P. K., Lim, L. W., and Rabea, E. I. (2022). A review of the modern principles and applications of solid-phase extraction techniques in chromatographic analysis. *Analytical Sciences*, *38*(12), 1457–1487. https://doi.org/10.1007/s44211-022-00190-8

Burke, J. M., and Smela, E. (2012). A novel surface modification technique for forming porous polymer monoliths in poly(dimethylsiloxane). *Biomicrofluidics*, *6*(1), 016506. https://doi.org/10.1063/1.3693589

Buszewski, B., and Szultka, M. (2012). Past, Present, and Future of Solid Phase Extraction: A Review. *Critical Reviews in Analytical Chemistry*, *42*(3), 198–213. https://doi.org/10.1080/07373937.2011.645413

Castell, P., Wouters, M., de With, G., Fischer, H., and Huijs, F. (2004). Surface modification of poly(propylene) by photoinitiators: Improvement of adhesion and

wettability. *Journal of Applied Polymer Science*, *92*(4), 2341–2350. https://doi.org/10.1002/app.20276

Chericoni, S., Battistini, I., Dugheri, S., Pacenti, M., and Giusiani, M. (2011). Novel Method for Simultaneous Aqueous in Situ Derivatization of THC and THC-COOH in Human Urine Samples: Validation and Application to Real Samples. *Journal of Analytical Toxicology*, *35*(4), 193–198. https://doi.org/10.1093/anatox/35.4.193

Chiper, A., and Borcia, G. (2013). Argon versus helium dielectric barrier discharge for surface modification of polypropylene and poly(methyl methacrylate) films. *Plasma Chemistry and Plasma Processing*, *33*, 553–568. https://doi.org/10.1007/s11090-013-9442-z

Choi, H. S., Rybkin, V. V., Titov, V. A., Shikova, T. G., and Ageeva, T. A. (2006). Comparative actions of a low pressure oxygen plasma and an atmospheric pressure glow discharge on the surface modification of polypropylene. *Surface and Coatings Technology*, *200*(14), 4479–4488. https://doi.org/10.1016/j.surfcoat.2005.03.037

Crime, U. O. on D. and. (2021). *World drug report 2021*. UN, Office on Drugs and Crime,. Retrieved from https://digitallibrary.un.org/record/3931425

del Mar Ramirez Fernandez, M., De Boeck, G., Wood, M., Lopez-Rivadulla, M., and Samyn, N. (2008). Simultaneous analysis of THC and its metabolites in blood using liquid chromatography–tandem mass spectrometry. *Journal of Chromatography B*, *875*(2), 465–470. https://doi.org/10.1016/j.jchromb.2008.09.032

Ellison, S. T., Brewer, W. E., and Morgan, S. L. (2009). Comprehensive Analysis of Drugs of Abuse in Urine Using Disposable Pipette Extraction. *Journal of Analytical Toxicology*, *33*(7), 356–365. https://doi.org/10.1093/jat/33.7.356

Eom, H., Kang, J., Jang, S., Kwon, O., Choi, S., Shin, J., and Nam, I. (2022). Evaluating the Electrochemical Properties of Supercapacitors using the Three-Electrode System. *JoVE (Journal of Visualized Experiments)*, (179), e63319. https://doi.org/10.3791/63319

Frei, P., Frauchiger, S., Scheurer, E., and Mercer-Chalmers-Bender, K. (2022). Quantitative determination of five cannabinoids in blood and urine by gas chromatography

tandem mass spectrometry applying automated on-line solid phase extraction. *Drug Testing and Analysis, 14*(7), 1223–1233. https://doi.org/10.1002/dta.3241

Fresco-Cala, B., Cárdenas, S., and Herrero-Martínez, J. M. (2017). Preparation of porous methacrylate monoliths with oxidized single-walled carbon nanohorns for the extraction of nonsteroidal anti-inflammatory drugs from urine samples. *Microchimica Acta, 184*(6), 1863–1871. https://doi.org/10.1007/s00604-017-2203-6

Fresco-Cala, B., Mompó-Roselló, Ó., Simó-Alfonso, E. F., Cárdenas, S., and Manuel Herrero-Martínez, J. (2018). Carbon nanotube-modified monolithic polymethacrylate pipette tips for (micro)solid-phase extraction of antidepressants from urine samples. *Microchimica Acta, 185,* 127. https://doi.org/10.1007/s00604-017-2659-4

Gama, M. R., Rocha, F. R. P., and Bottoli, C. B. G. (2019). Monoliths: Synthetic routes, functionalization and innovative analytical applications. *TrAC Trends in Analytical Chemistry, 115,* 39–51. https://doi.org/10.1016/j.trac.2019.03.020

Gasse, A., Pfeiffer, H., Köhler, H., and Schürenkamp, J. (2016). Development and validation of a solid-phase extraction method using anion exchange sorbent for the analysis of cannabinoids in plasma and serum by gas chromatography-mass spectrometry. *International Journal of Legal Medicine, 130*(4), 967–974. https://doi.org/10.1007/s00414-016-1368-6

Gopanna, A., Mandapati, R. N., Thomas, S. P., Rajan, K., and Chavali, M. (2019). Fourier transform infrared spectroscopy (FTIR), Raman spectroscopy and wide-angle X-ray scattering (WAXS) of polypropylene (PP)/cyclic olefin copolymer (COC) blends for qualitative and quantitative analysis. *Polymer Bulletin, 76*(8), 4259–4274. https://doi.org/10.1007/s00289-018-2599-0

Gusev, I., Huang, X., and Horváth, C. (1999). Capillary columns with in situ formed porous monolithic packing for micro high-performance liquid chromatography and capillary electrochromatography. *Journal of Chromatography A, 855*(1), 273–290. https://doi.org/10.1016/S0021-9673(99)00697-4

Hefnawy, M., El-Gendy, M., Al-Salem, H., Marenga, H., El-Azab, A., Abdel-Aziz, A., … Hefnawy, A. (2023). Trends in monoliths: Packings, stationary phases and

nanoparticles. *Journal of Chromatography A, 1691,* 463819. https://doi.org/10.1016/j.chroma.2023.463819

Hjertén, S., Liao, J.-L., and Zhang, R. (1989). High-performance liquid chromatography on continuous polymer beds. *Journal of Chromatography A, 473,* 273–275. https://doi.org/10.1016/S0021-9673(00)91309-8

Hu, S., Ren, X., Bachman, M., Sims, C. E., Li, G. P., and Allbritton, N. L. (2004). Surface-directed, graft polymerization within microfluidic channels. *Analytical Chemistry, 76*(7), 1865–1870. https://doi.org/10.1021/ac049937z

Iacono, M., Connolly, D., and Heise, A. (2016). Fabrication of a GMA-co-EDMA monolith in a 2.0 mm i.d. Polypropylene housing. *Materials, 9,* 263. https://doi.org/10.3390/ma9040263

Jiang, Z., Smith, N. W., David Ferguson, P., and Robert Taylor, M. (2007). Preparation and characterization of long alkyl chain methacrylate-based monolithic column for capillary chromatography. *Journal of Biochemical and Biophysical Methods, 70*(1), 39–45. https://doi.org/10.1016/j.jbbm.2006.08.009

Kaczmarek, H., Gałka, P., and Kowalonek, J. (2010). Influence of a photoinitiator on the photochemical stability of poly(methyl methacrylate) studied with fourier transform infrared spectroscopy. *Journal of Applied Polymer Science, 115*(3), 1598–1607. https://doi.org/10.1002/app.31166

Karschner, E. L., Swortwood-Gates, M. J., and Huestis, M. A. (2020). Identifying and Quantifying Cannabinoids in Biological Matrices in the Medical and Legal Cannabis Era. *Clinical Chemistry, 66*(7), 888–914. https://doi.org/10.1093/clinchem/hvaa113

Klimuntowski, M., Alam, M. M., Singh, G., and Howlader, M. M. R. (2020). Electrochemical Sensing of Cannabinoids in Biofluids: A Noninvasive Tool for Drug Detection. *ACS Sensors, 5*(3), 620–636. https://doi.org/10.1021/acssensors.9b02390

Krenkova, J., and Foret, F. (2013). Nanoparticle-modified monolithic pipette tips for phosphopeptide enrichment. *Analytical and Bioanalytical Chemistry, 405*(7), 2175–2183. https://doi.org/10.1007/s00216-012-6358-z

Kubín, M., Špaček, P., and Chromeček, R. (1967). Gel permeation chromatography on porous poly(ethylene glycol methacrylate). *Collection of Czechoslovak*

Chemical Communications, *32*(11), 3881–3887. https://doi.org/10.1135/cccc19673881

Lirio, S., Fu, C.-W., Lin, J.-Y., Hsu, M.-J., and Huang, H.-Y. (2016). Solid-phase microextraction of phthalate esters in water sample using different activated carbon-polymer monoliths as adsorbents. *Analytica Chimica Acta*, *927*, 55–63. https://doi.org/10.1016/j.aca.2016.05.006

Ma, H., Davis, R. H., and Bowman, C. N. (2000). A Novel Sequential Photoinduced Living Graft Polymerization. *Macromolecules*, *33*(2), 331–335. https://doi.org/10.1021/ma990821s

Montesano, C., Sergi, M., Odoardi, S., Simeoni, M. C., Compagnone, D., and Curini, R. (2014). A μ-SPE procedure for the determination of cannabinoids and their metabolites in urine by LC–MS/MS. *Journal of Pharmaceutical and Biomedical Analysis*, *91*, 169–175. https://doi.org/10.1016/j.jpba.2013.12.035

Morisue Sartore, D., Costa, J. L., Lanças, F. M., and Santos-Neto, Á. J. (2022). Packed in-tube SPME–LC–MS/MS for fast and straightforward analysis of cannabinoids and metabolites in human urine. *ELECTROPHORESIS*, *43*(15), 1555–1566. https://doi.org/10.1002/elps.202100389

Namera, A., and Saito, T. (2013). Advances in monolithic materials for sample preparation in drug and pharmaceutical analysis. *TrAC Trends in Analytical Chemistry*, *45*, 182–196. https://doi.org/10.1016/j.trac.2012.10.017

Nestić, M., Babić, S., Pavlović, D. M., and Sutlović, D. (2013). Molecularly imprinted solid phase extraction for simultaneous determination of Δ9-tetrahydrocannabinol and its main metabolites by gas chromatography–mass spectrometry in urine samples. *Forensic Science International*, *231*(1), 317–324. https://doi.org/10.1016/j.forsciint.2013.06.009

Nicolaou, A. G., Christodoulou, M. C., Stavrou, I. J., and Kapnissi-Christodoulou, C. P. (2021). Analysis of cannabinoids in conventional and alternative biological matrices by liquid chromatography: Applications and challenges. *Journal of Chromatography A*, *1651*, 462277. https://doi.org/10.1016/j.chroma.2021.462277

Ohyama, K., Horiguchi, D., Kishikawa, N., and Kuroda, N. (2011). Monolithic poly(butyl methacrylate–ethylene dimethacrylate–methacrylic acid) column for capillary electrochromatography. *Journal of Separation Science*, *34*(16–17), 2279–2283. https://doi.org/10.1002/jssc.201100198

Okanda, F. M., and El Rassi, Z. (2005). Capillary electrochromatography with monolithic stationary phases. 4. Preparation of neutral stearyl – acrylate monoliths and their evaluation in capillary electrochromatography of neutral and charged small species as well as peptides and proteins. *Electrophoresis*, *26*(10), 1988–1995. https://doi.org/10.1002/elps.200500073

Oster, G., and Shibata, O. (1957). Graft copolymer of polyacrylamide and natural rubber produced by means of ultraviolet light. *Journal of Polymer Science*, *26*(113), 233–234. https://doi.org/10.1002/pol.1957.1202611311

Paimard, G., Ghasali, E., and Baeza, M. (2023). Screen-Printed Electrodes: Fabrication, Modification, and Biosensing Applications. *Chemosensors*, *11*(2), 113. https://doi.org/10.3390/chemosensors11020113

Płotka-Wasylka, J., Szczepańska, N., de la Guardia, M., and Namieśnik, J. (2015). Miniaturized solid-phase extraction techniques. *TrAC Trends in Analytical Chemistry*, *73*, 19–38. https://doi.org/10.1016/j.trac.2015.04.026

Purschke, K., Heinl, S., Lerch, O., Erdmann, F., and Veit, F. (2016). Development and validation of an automated liquid-liquid extraction GC/MS method for the determination of THC, 11-OH-THC, and free THC-carboxylic acid (THC-COOH) from blood serum. *Analytical and Bioanalytical Chemistry*, *408*(16), 4379–4388. https://doi.org/10.1007/s00216-016-9537-5

Rånby, B., Yang, W. T., and Tretinnikov, O. (1999). Surface photografting of polymer fibers, films and sheets. *Nuclear Instruments and Methods in Physics Research Section B: Beam Interactions with Materials and Atoms*, *151*(1), 301–305. https://doi.org/10.1016/S0168-583X(99)00158-5

Rånby, Bengt. (1992). Surface modification of polymers by photoinitiated graft polymerization. *Makromolekulare Chemie. Macromolecular Symposia*, *63*(1), 55–67. https://doi.org/10.1002/masy.19920630107

Renaud-Young, M., Mayall, R. M., Salehi, V., Goledzinowski, M., Comeau, F. J. E., MacCallum, J. L., and Birss, V. I. (2019). Development of an ultra-sensitive electrochemical sensor for Δ9-tetrahydrocannabinol (THC) and its metabolites using carbon paper electrodes. *Electrochimica Acta*, *307*, 351–359. https://doi.org/10.1016/j.electacta.2019.02.117

Rohr, T., Ogletree, D. f., Svec, F., and Fréchet, J. m. j. (2003). Surface functionalization of thermoplastic polymers for the fabrication of microfluidic devices by photoinitiated grafting. *Advanced Functional Materials*, *13*(4), 264–270. https://doi.org/10.1002/adfm.200304229

Rosendo, L. M., Rosado, T., Oliveira, P., Simão, A. Y., Margalho, C., Costa, S., ... Gallardo, E. (2022). The Determination of Cannabinoids in Urine Samples Using Microextraction by Packed Sorbent and Gas Chromatography-Mass Spectrometry. *Molecules*, *27*(17), 5503. https://doi.org/10.3390/molecules27175503

Rouquerol, J., Avnir, D., Fairbridge, C. W., Everett, D. H., Haynes, J. M., Pernicone, N., ... Unger, K. K. (1994). Recommendations for the characterization of porous solids (Technical Report). *Pure and Applied Chemistry*, *66*(8), 1739–1758. https://doi.org/10.1351/pac199466081739

Sartore, D. M., Vargas Medina, D. A., Costa, J. L., Lanças, F. M., and Santos-Neto, Á. J. (2020). Automated microextraction by packed sorbent of cannabinoids from human urine using a lab-made device packed with molecularly imprinted polymer. *Talanta*, *219*, 121185. https://doi.org/10.1016/j.talanta.2020.121185

Sempio, C., Scheidweiler, K. B., Barnes, A. J., and Huestis, M. A. (2018). Optimization of recombinant β-glucuronidase hydrolysis and quantification of eight urinary cannabinoids and metabolites by liquid chromatography tandem mass spectrometry. *Drug Testing and Analysis*, *10*(3), 518–529. https://doi.org/10.1002/dta.2230

Sorribes-Soriano, A., Valencia, A., Esteve-Turrillas, F. A., Armenta, S., and Herrero-Martínez, J. M. (2019). Development of pipette tip-based poly(methacrylic acid-co-ethylene glycol dimethacrylate) monolith for the extraction of drugs of

abuse from oral fluid samples. *Talanta*, *205*, 120158. https://doi.org/10.1016/j.talanta.2019.120158

Stachowiak, T. B., Rohr, T., Hilder, E. F., Peterson, D. S., Yi, M., Svec, F., and Fréchet, J. M. J. (2003). Fabrication of porous polymer monoliths covalently attached to the walls of channels in plastic microdevices. *Electrophoresis*, *24*, 3689–3693. https://doi.org/10.1002/elps.200305536

Stout, P. R., Horn, C. K., and Klette, K. L. (2001). Solid-Phase Extraction and GC-MS Analysis of THC-COOH Method Optimized for a High-Throughput Forensic Drug-Testing Laboratory*. *Journal of Analytical Toxicology*, *25*(7), 550–554. https://doi.org/10.1093/jat/25.7.550

SWGTOX. (2013). Scientific Working Group for Forensic Toxicology (SWGTOX) Standard Practices for Method Validation in Forensic Toxicology. *Journal of Analytical Toxicology*, *37*(7), 452–474. https://doi.org/10.1093/jat/bkt054

Teixeira, H., Verstraete, A., Proença, P., Corte-Real, F., Monsanto, P., and Vieira, D. N. (2007). Validated method for the simultaneous determination of **Δ**9-THC and **Δ**9-THC-COOH in oral fluid, urine and whole blood using solid-phase extraction and liquid chromatography–mass spectrometry with electrospray ionization. *Forensic Science International*, *170*(2), 148–155. https://doi.org/10.1016/j.forsciint.2007.03.026

Tian, Y., Yang, F., Yang, X., Fu, E., Xu, Y., and Zeng, Z. (2008). Macrocyclic polyamine-modified poly(glycidyl methacrylate-co-ethylene dimethacrylate) monolith for capillary electrochromatography. *Electrophoresis*, *29*(11), 2293–2300. https://doi.org/10.1002/elps.200700766

Wang, Hongxia, Zhang, H., Lv, Y., Svec, F., and Tan, T. (2014). Polymer monoliths with chelating functionalities for solid phase extraction of metal ions from water. *Journal of Chromatography A*, *1343*, 128–134. https://doi.org/10.1016/j.chroma.2014.03.072

Wang, Huiqi, Li, Z., Niu, Q., Ma, J., and Jia, Q. (2015). Preparation of a zeolite-modified polymer monolith for identification of synthetic colorants in lipsticks. *Applied Surface Science*, *353*, 1326–1333. https://doi.org/10.1016/j.apsusc.2015.07.002

Wanklyn, C., Burton, D., Enston, E., Bartlett, C.-A., Taylor, S., Raniczkowska, A., … Murphy, L. (2016). Disposable screen printed sensor for the electrochemical detection of delta-9-tetrahydrocannabinol in undiluted saliva. *Chemistry Central Journal*, *10*, 1. https://doi.org/10.1186/s13065-016-0148-1

Weinmann, W., Vogt, S., Goerke, R., Müller, C., and Bromberger, A. (2000). Simultaneous determination of THC-COOH and THC-COOH-glucuronide in urine samples by LC/MS/MS. *Forensic Science International*, *113*(1), 381–387. https://doi.org/10.1016/S0379-0738(00)00210-3

Williams, D. F., Abel, M.-L., Grant, E., Hrachova, J., and Watts, J. F. (2015). Flame treatment of polypropylene: A study by electron and ion spectroscopies. *International Journal of Adhesion and Adhesives*, *63*, 26–33. https://doi.org/10.1016/j.ijadhadh.2015.07.009

Yaman, N., Özdoğan, E., Seventekin, N., and Ayhan, H. (2009). Plasma treatment of polypropylene fabric for improved dyeability with soluble textile dyestuff. *Applied Surface Science*, *255*(15), 6764–6770. https://doi.org/10.1016/j.apsusc.2008.10.121

Yang, W. T., and Rånby, B. (1996). The role of far UV radiation in the photografting process. *Polymer Bulletin, 37*(1), 89–96. https://doi.org/10.1007/BF00313823

Young, B. L., and Victoria Zhang, Y. (2022). A rapid Dilute-and-Shoot LC-MS/MS method for quantifying THC-COOH and THC-COO(Gluc) in urine. *Journal of Chromatography B*, *1211*, 123495. https://doi.org/10.1016/j.jchromb.2022.123495

CURRICULUM VITAE

Name: Kesara Ar-sanork   **Date of Birth:** 30 July 1994

Place of Birth: Samutprakarn

Education: 2013-2016 B. Sc. Chemistry, Science, Suranaree University of technology

2017-2018 M. Sc. Chemistry, Science, Suranaree University of technology

2019-present Ph.D. Chemistry, Science, Suranaree University of technology

Publications:

1. **Ar-sanork K.**, Karuwan C., Surapanich N., Wilairat P., Nacapricha D., Chaisuwan P, Mixed mode monolithic sorbent in pipette tip for extraction of ractopamine and clenbuterol prior to analysis by HPLC-UV and UHPLC-Q Exactive™ Plus Orbitrap MS. Anal. Sci. Technol. 2021, 12:23. https://doi.org/10.1186/s40543-021-00275-5.

2. **Ar-sanork K.**, Wongbuth L., Surapanich N., Wilairat P., Nacapricha D., Chaisuwan P, rapid analysis of caffeine and paracetamol using micro-liquid chromatography with mixed mode monolithic column, Suranaree J. Sci. Technol. 2020, 28(2):030041.

3. **Ar-sanork K.**, Muekhunthod A., Chetsurakul A., Karuwan C., Surapanich N., Chaisuwan P, Characterization of methacrylate-based monolithic materials synthesized in pipette tip for micro-solid phase extraction, Pure and Applied Chemistry International Conference (PACCON), 2020, 207-212. (Proceeding)

Patents:

Thai patent: กระบวนการปรับสภาพพื้นผิวพอลิโพรพิลีนปิเปต (Process for polypropylene pipette tip surface pretreatment), Patent application no: 2101005113 (applied in August 2021)

Awards and other achievement:

1. Outstanding poster presentation award winners, Pure and Applied Chemistry International Conference (PACCON), 2020.

2. NSTDA Outstanding Student Award 2019